Complete suspension culture of human induced pluripotent stem cells supplemented with suppressors of spontaneous differentiation

Mami Matsuo-Takasaki[1], Sho Kambayashi[2], Yasuko Hemmi[1], Tamami Wakabayashi[1], Tomoya Shimizu[1], Yuri An[1], Hidenori Ito[1], Kazuhiro Takeuchi[2], Masato Ibuki[2], Terasu Kawashima[2], Rio Masayasu[2], Manami Suzuki[2], Naoki Nishishita[2], Yoshikazu Kawai[2], Masafumi Umekage[3], Tomoaki M Kato[3], Michiya Noguchi[4], Koji Nakade[5], Yukio Nakamura[4], Tomoyuki Nakaishi[2], Masayoshi Tsukahara[3], Yohei Hayashi[1,6]*.

[1]iPS Cell Advanced Characterization and Development Team, RIKEN BioResource Research Center, Ibaraki, 305-0074, Japan; [2]Regenerative Medicine and Cell Therapy Laboratories, KANEKA CORPORATION, Kobe, 650-0047, Japan; [3]Research and Development Center, CiRA Foundation, Kyoto, 606-8507, Japan; [4]Cell Engineering Division, RIKEN BioResource Research Center, Ibaraki, 305-0074, Japan; [5]Gene Engineering Division, RIKEN BioResource Research Center, Ibaraki, 305-0074, Japan; [6]Faculty of Medicine and School of Integrative and Global Majors, University of Tsukuba, Ibaraki, 305-8575, Japan.

*For corresponding: yohei.hayashi@riken.jp (YHa)

Abstract

Human induced pluripotent stem cells (hiPSCs) are promising resources for producing various types of tissues in regenerative medicine; however, the improvement in a scalable culture system that can precisely control the cellular status of hiPSCs is needed. Utilizing suspension culture without microcarriers or special materials allows for massive production, automation, cost-effectiveness, and safety assurance in industrialized regenerative medicine. Here, we found that hiPSCs cultured in suspension conditions with continuous agitation without any microcarriers or extracellular matrix components were more prone to spontaneous differentiation than those cultured in conventional adherent conditions. Adding PKCβ and Wnt signaling pathway inhibitors in the suspension conditions suppressed the spontaneous differentiation of hiPSCs into ectoderm and mesendoderm, respectively. In these conditions, we successfully completed the culture processes of hiPSCs including the generation of hiPSCs from peripheral blood mononuclear cells with the expansion of bulk population and single-cell sorted clones, long-term culture with robust self-renewal characteristics, single-cell cloning, direct cryopreservation from suspension culture and their successful recovery, and efficient mass production of a clinical-grade hiPSC line. Our results demonstrate that precise control of the cellular status in suspension culture conditions paves the way for their stable and automated clinical application.

Introduction

Human induced pluripotent stem cells (hiPSCs) are promising resources for various types of tissues in regenerative medicine (Takahashi *et al*, 2007; Yu *et al*, 2007). To enable cell therapy from hiPSCs, the development of a large-scale manufacturing system is essential because massive cell numbers are required to compose transplantable cells which are enough to rescue the desired physiological function (Chen *et al*, 2014; Kim & Kino-Oka, 2020; Tannenbaum & Reubinoff, 2022). In general, hiPSCs are believed to possess their scaffold dependency and are cultured under adhesion and monolayer culture conditions (Hayashi & Furue, 2016; Xu *et al*, 2001). However, utilizing suspension culture without microcarriers or special materials allows for massive production, automation, cost-effectiveness, and safety assurance in industrialized regenerative medicine.

Several attempts have been made to develop suspension culture technologies enabling rapid and large-scale preparation of hiPSCs (Amit *et al*, 2010; Amit *et al*, 2011; Dang *et al*, 2004; Elanzew *et al*, 2015; Horiguchi & Sakai, 2016; Hunt *et al*, 2014; Ibuki *et al*, 2019; Kehoe *et al*, 2010; Kim *et al*, 2019; Krawetz *et al*, 2010; Kwok *et al*, 2018; Lam *et al*, 2016; Lipsitz *et al*, 2018; Nath *et al*, 2017; Oh *et al*, 2009; Olmer *et al*, 2012; Rohani *et al*, 2020; Shafa *et al*, 2012; Singh *et al*, 2010; Steiner *et al*, 2010; Wang *et al*, 2013; Zweigerdt *et al*, 2011) (Summarized in Table 1). These studies have achieved long-term culture and/or mass expansion of hiPSCs and/or human embryonic stem cells (hESCs) in suspension conditions. However, completed processes from clonal hiPSC generation to mass production of hiPSCs based on the precise control of cell status have not yet been achieved.

In this study, we have investigated what hampers the stable maintenance of undifferentiated cell states in suspension conditions. HiPSCs cultured in suspension conditions with continuous agitation without any microcarriers or extracellular matrix (ECM) components were more prone to spontaneous differentiation than those cultured in conventional adherent conditions. From screening of candidate molecules to suppress the spontaneous differentiation of hiPSCs, we have identified that inhibitors of PKCβ and Wnt signaling pathways suppress their differentiation into ectoderm and mesendoderm, respectively. In these conditions, we aimed to complete the processes of handling hiPSCs including the generation of hiPSCs with the expansion of bulk population and single-cell sorted clones, long-term culture with robust self-renewal characteristics, single-cell cloning, direct cryopreservation from suspension culture and their successful recovery, and efficient mass production of a clinical-grade hiPSC line.

Results

Suspension cultured hiPSCs are prone to spontaneous differentiation.

First, we investigated whether the quality of hiPSCs in suspension and adherent conditions are

equivalent or not. A hiPSC line, WTC11, was cultured in a conventional medium, StemFit AK02N (Ajinomoto, Tokyo, Japan), with continuous agitation (90 rpm) in non-adhesive cell culture plates for 2 passages (5 days during passages) were examined (Figure 1A). In suspension culture on days 5 and 10, hiPSCs formed round cell assemblies with slightly uneven surfaces (Figure 1B). Gene expression analysis with RT-qPCR revealed that the expression of differentiation markers, such as *PAX6* (ectoderm), *SOX17* (endoderm), and *T* (mesoderm) increased in suspension-cultured hiPSCs for 10 days (Figure 1C). To monitor the spontaneous differentiation at single-cell resolution, we established knock-in reporter hiPSC lines of PAX6-tdTomato and SOX17-tdTomato to visualize and quantify the expression of PAX6 and SOX17 at the protein level, respectively (Figure 1—figure supplement 1A–H). tdTomato-positive cells were clearly observed in day 10 samples in suspension-cultured hiPSCs, whereas no fluorescent positive cells were observed in adherent culture conditions (Figure 1D). Flow cytometric analysis revealed that hiPSCs in suspension-culture conditions contained non-negligible percentages of PAX6-tdTomato-positive and SOX17-tdTomato-positive cells (Figure 1E and 1F). Western blot analysis revealed that protein expression of PAX6 and SOX17 in suspension conditions was significantly increased (Figure 2—figure supplement 1A–D). The ratio of positive cells for a cell surface marker for undifferentiated hiPSCs, TRA1-60, was significantly lower in suspension-culture conditions (Figure 2—figure supplement 1E and F). These results suggest that a portion of hiPSCs are spontaneously differentiated in suspension conditions when cultured in conventional media. To examine global changes in gene expression patterns between suspension and adherent conditions, whole-transcriptomic RNA-seq experiments with statistical tests were performed. Gene Set Enrichment Analysis (GSEA) of all the genes and Gene Ontology Enrichment Analysis (GOEA) on differentially-regulated genes revealed that, in suspension conditions, many genes involved in differentiation toward various tissues and cell-cell adhesions were significantly up-regulated. In contrast, genes involved in nucleotide metabolism, hypoxic responses, and extracellular matrix organization were down-regulated significantly (Figure 1G–J). These results suggest that hiPSCs in suspension conditions are in the process of spontaneous differentiation into various cell lineages and are characterized by specific signatures of gene expression patterns.

Wnt signaling inhibitors suppress spontaneous mesendodermal differentiation in suspension culture condition.

We next investigated the factors having an inhibitory effect on hiPSCs spontaneous differentiation in suspension conditions (Figure 2A). Exogenous Wnt signaling induces the differentiation of human pluripotent stem cells into mesendoderm lineages (Nakanishi *et al*, 2009; Sumi *et al*, 2008; Tran *et al*, 2009; Vijayaragavan *et al*, 2009; Woll *et al*, 2008). Also, endogenous expression and activation of Wnt signaling in pluripotent stem cells are involved in the regulation of mesendoderm differentiation potentials (Dziedzicka *et al*, 2021). Thus, we hypothesized that adding Wnt signaling inhibitors/activators may alter the spontaneous differentiation of hiPSCs into mesendoderm. Therefore, Wnt signaling inhibitors, IWP2 or IWR-

1-endo (Chen *et al*, 2009), or an activator, CHIR99021 (Ring *et al*, 2003), were added to the culture medium under suspension conditions. HiPSC aggregates treated with and without Wnt inhibitors showed similar round shapes (Figure 2B). In contrast, hiPSC aggregates treated with CHIR99021 formed heterogeneously shaped cyst-like structures, suggesting that they were largely differentiated. In samples treated with inhibitors, both T and SOX17 expression levels were significantly reduced to the level of adherent-cultured hiPSCs; however, there was only a small reduction in *PAX6* expression in the IWR-1-endo-treated condition and no reduction in the IWP2-treated condition (Figure 2C). In contrast, CHIR99021-treated cell aggregates showed markedly decreased *OCT4* and increased *T* and *SOX17* expression. Additionally, SOX17 protein expression was suppressed in hiPSCs treated with IWR-1-endo in suspension-culture conditions, although its expression increased in hiPSCs in suspension conditions with conventional culture medium compared to adherent conditions (Figure 2—figure supplement 1A and B). These results indicate that Wnt signaling inhibitors effectively suppress mesendodermal differentiation in suspension-culture, but are insufficient to suppress ectodermal differentiation.

PKC signal inhibitors suppress spontaneous neuroectododermal differentiation in suspension conditions.

To identify molecules with inhibitory activity on neuroectodermal differentiation, hiPSCs were treated with candidate molecules in suspension conditions. We selected these candidate molecules based on previous studies related to signaling pathways or epigenetic regulations in neuroectodermal development (reviewed in (Giacoman-Lozano *et al*, 2022; Imaizumi & Okano, 2021; Sasai *et al*, 2021; Stern, 2024)) or in pluripotency safeguards (reviewed in (Hackett & Surani, 2014; Li & Belmonte, 2017; Takahashi & Yamanaka, 2016; Yagi *et al*, 2017)) (Figure 2A; listed in Supplementary Table 1). Out of the candidate molecules tested, Gö6983, a pan-PKC inhibitor (Gschwendt *et al*, 1996), and BMP4 showed strong inhibition effect on *PAX6* expression (Figure 2D). Further, simultaneous treatment with Gö6983 and IWR-1-endo decreased *PAX6*, *T*, and *SOX17* expression, while maintaining *OCT4* expression. To confirm these screening test results, the dose-dependent effect of Gö6983 or another PKCα, β, γ inhibitor GF109203X (GFX) (Toullec *et al*, 1991) on the inhibition of *PAX6* expression was observed at constant concentrations of IWR-1-endo (Figure 2E and F). These results demonstrate that the inhibition of PKC signaling pathway effectively suppresses neuroectoderm differentiation and maintain self-renewal in hiPSCs cultured in suspension conditions.

Next, we tested various PKC inhibitors to suppress neuroectodermal differentiation from hiPSCs in suspension culture using another hiPSC line, 201B7 (Figure 2—figure supplement 2A). The suppression of *PAX6* expression in hiPSCs cultured in suspension conditions was observed with PKC inhibitors, enzastaurin (Ly317615), sotrastaurin (AEB071), Ro-32-0432, Gö6983, GF109203X, and LY333531, all of which possessed PKCβ inhibition activity (Figure 2—figure supplement 2B-D); however, sotrastaurin and Ro-32-0432 also showed growth inhibition of hiPSCs.

147 Further, we examined the expression pattern changes in specific isoforms of PKCs in hiPSCs
148 cultured in adherent/suspension conditions. RNA expression of PKCα (PRKCA) and PKCβ
149 (PRKCB) was significantly up-regulated under suspension-culture conditions compared to
150 adhesion conditions (Figure 3—figure supplement 1A). Moreover, phosphorylated PKCβ protein
151 expression was significantly elevated (Figure 3—figure supplement 1B and C). These results
152 suggest that elevated expression and activation of PKCβ in suspension-cultured hiPSCs could
153 affect the spontaneous differentiation.

154 **Combination of inhibitors of PKCβ and Wnt signaling pathways efficiently maintains self-**
155 **renewal of hiPSCs in suspension conditions**

156 To further explore the possibility that the inhibition of PKCβ is critical for the maintenance of
157 self-renewal of hiPSCs in the suspension culture, we evaluated the effect of LY333531, a PKCβ
158 specific inhibitor (Jirousek *et al*, 1996). As compared to controls, a hiPSC line, WTC11, cultured
159 in suspension conditions treated with IWR-1-endo and LY333531 formed homogenous, round,
160 smooth-surfaced aggregates (Figure 3A). *PAX6* expression was strongly suppressed by the
161 addition of LY333531 (Figure 3B). Furthermore, after adding IWR-1-endo, the inhibitory effect
162 of *PAX6* expression was further enhanced, and simultaneously, *OCT4* expression was restored to
163 the same level as in the adherent-culture. PAX6 protein expression was also suppressed in hiPSCs
164 treated with IWR-1-endo and LY333531 in suspension-culture conditions while its expression
165 increased in suspension conditions with conventional culture medium compared to adherent-
166 conditions (Figure 2—figure supplement 1C and D). The ratio of TRA-1-60-positive cells was
167 higher in suspension-culture conditions supplemented with IWR-1-endo and LY333531 than in
168 control conditions without these inhibitors (Figure 2—figure supplement 1E and F). These results
169 indicate that the maintenance of suspension-cultured hiPSCs is specifically facilitated by the
170 combination of PKCβ and Wnt signaling inhibition.

171 To examine the reproducibility of the effect of the inhibition of PKCβ and Wnt signaling
172 pathways on the maintenance of self-renewal of hiPSCs in the suspension culture among various
173 hiPSCs, we evaluated the expression of self-renewal and differentiation markers among 5
174 different hiPSC lines, 1231A3, 1383D6, 201B7, HiPS-NB1RGB, and WTC11, simultaneously.
175 Compared to adherent culture conditions, hiPSCs cultured in suspension conditions without
176 chemical treatment decreased the positive ratio of TRA-1-60/SSEA4 and OCT4 and increased the
177 expression levels of differentiation markers, *SOX17*, *T*, and *PAX6* (Figure 3C-E). These results
178 indicated that suspension culture conditions without chemical treatment are unstable to maintain
179 self-renewal and contain spontaneous differentiated cells. The addition of PKCβ and Wnt signal
180 inhibitors increased the positive ratio of TRA-1-60/SSEA4 and OCT4 and decreased the
181 expression levels of *SOX17*, *T*, and *PAX6* to the comparable level of adherent conditions.
182 Interestingly, the expression of KLF2 and KLF5, which are also known as naïve pluripotency
183 markers, were up-regulated in the suspension conditions treated with PKCβ and Wnt signal
184 inhibitors.

185 We also examined whether the combination of PKCβ and Wnt signaling inhibition affects
186 cell survival in suspension conditions. In this experiment, we used another PKC inhibitor,
187 Staurosporine (Omura *et al*, 1977), which has a strong cytotoxic effect as a positive control of cell
188 death in suspension conditions. The addition of IWR-1-endo and LY333531 for 10 days had no
189 effects on the apoptosis while the addition of Staurosporine for 2 hours induced Annexin-V-
190 positive apoptotic cells (Figure 3—figure supplement 2A-D). These results indicate that the
191 combination of PKCβ and Wnt signaling inhibition has no or little effects on the cell survival in
192 suspension conditions.
193 We next performed long-term culture for 10 passages in suspension conditions and
194 compared hiPSC growth in presence of LY333531 or Gö6983. When hiPSCs were seeded at 4 ×
195 10^5 cells/well, the average cell number reached approximately 12-fold after 5 days under both
196 conditions (Figure 4A and B). After 10 passages, aggregates of hiPSCs cultured in the presence
197 of LY333531 showed a uniform spherical shape, whereas aggregates cultured in the presence of
198 Gö6983 were heterogeneously spherical (Figure 4C). Notably, in LY333531-treated cells, OCT4-
199 positive cell numbers were significantly higher than in Gö6983-treated samples, as determined by
200 immunostaining (Figure 4D and E). To evaluate whether hiPSCs cultured in suspension
201 conditions with PKCβ and Wnt signaling inhibitors for 10 passages maintain pluripotency, we
202 performed embryoid body (EB) formation assay. These EBs contained positive cells for TUJ1,
203 SMA, and AFP as ectodermal, mesodermal, and endodermal marker, respectively (Figure 4F).
204 Copy number variation (CNV) array analysis showed that hiPSCs cultured long-term in the
205 presence of PKCβ and Wnt inhibitors retained their normal human karyotype (Figure 4G). These
206 results indicate that, for long-term culture, the inhibition of Wnt signaling and PKCβ in
207 suspension conditions is sufficient to maintain the self-renewal, pluripotency, and genomic
208 integrity of hiPSCs. Thus, we used the combination of IWR-1-endo and LY333531 for the rest of
209 this study.
210 We further investigated whether the effects of PKCβ and Wnt inhibitors on suppressing
211 hiPSCs spontaneous differentiation in suspension-culture conditions are applicable to other
212 culture media. First, morphologies and gene expression profile of hiPSCs cultured in suspension
213 conditions with another commercially available maintenance medium, StemScale (ThermoFisher
214 Scientific, MA, USA), were examined (Figure 4—figure supplement 1A). A hiPSC line, WTC11,
215 cultured in suspension treated with IWR-1-endo and LY333531 formed homogenously round and
216 smooth-surfaced aggregates compared to controls (Figure 4—figure supplement 1B). The
217 differentiation markers expression, which was elevated under suspension conditions, was
218 suppressed by the simultaneous addition of PKCβ and Wnt signal inhibitors, as observed with
219 StemFit medium (Figure 4—figure supplement 1C and D). Second, morphologies and gene
220 expression profile of hiPSCs, cultured in suspension conditions with another commercially
221 available maintenance medium, mTeSR1 (Stem Cell Technologies, Vancouver, Canada), were
222 examined in 4 different hiPSC lines (1231A3, 201B7, HiPS-NB1RGB, and WTC11)
223 simultaneously (Figure 4—figure supplement 2A). Compared to adherent culture conditions,

224 hiPSCs cultured in suspension conditions without chemical treatment significantly decreased the
225 positive ratio of TRA-1-60/SSEA4 and OCT4 and increased the expression levels of
226 differentiation markers, *SOX17*, *T*, and *PAX6* (Figure 4—figure supplement 2B-D). These results
227 indicated that suspension culture conditions using mTeSR1 medium contain spontaneous
228 differentiated cells. The addition of PKCβ and Wnt signal inhibitors increased the positive ratio
229 of TRA-1-60/SSEA4 and OCT4 and decreased the expression levels of SOX17, T, and PAX6 to
230 the comparable level of adherent conditions. Together, these results suggest that conventional
231 suspension culture methods contain spontaneous differentiating cells and that the addition of
232 inhibitors of PKCβ and Wnt signaling pathways to conventional culture media generally
233 suppresses spontaneous differentiation and maintains self-renewal.

234 **Global gene expression signatures in hPSCs supplemented inhibitors of PKCβ and Wnt**
235 **signaling pathways in suspension conditions.**

236 We next examined the effect of PKCβ and Wnt inhibitors on global gene expression of hiPSCs
237 under suspension conditions. Bulk RNA-seq data were obtained from suspension conditions in
238 absence of inhibitors (Sus), supplemented with IWR-1-endo (IWR), LY333531 (LY), IWR-1-
239 endo and LY333531 (IWRLY), and adherent conditions (Ad). Hierarchical clustering obtained
240 from these data showed that LY and IWRLY were grouped closely with Ad (Figure 5A). In
241 contrast, Sus and IWR were both grouped as discrete populations from Ad. Additionally,
242 hierarchical clustering in gene expression among these conditions was supported by principal
243 component 1 (PC1) in the principal component analysis (PCA) (Figure 5B). In contrast, PC2
244 represented genes related to the effects of specific inhibitors under these conditions. Next, we
245 investigated the effect of LY333531 and IWR-1-endo in suspension culture. Many genes
246 involved in pluripotency: *KLF4* and *ID1*, and epithelial cell-cell interactions: *CDH1* (E-cadherin),
247 were significantly up-regulated in IWRLY, while many transcription factors involved in
248 differentiation: *PAX2*, *PAX3, PAX5, PAX8*, *SP5*, *DBX1*, and *TFAP2B*, were down-regulated in
249 IWRLY (Figure 5C). GSEA and GOEA on down-regulated genes in IWRLY showed that the
250 expression of developmentally associated genes, whose expression was elevated in Sus, was
251 generally reduced in IWRLY (Figure 5D and E). GOEA on up-regulated genes revealed gene sets
252 involved in epithelial cell types (Figure 5F). As compared to Ad, genes involved in sensory
253 system development, cell-cell adhesion, and Wnt and PI3K signaling pathways were up-regulated
254 in IWRLY, and genes involved in nucleotide metabolism and hypoxic responses were down-
255 regulated under IWRLY conditions (Figure 5—figure supplement 1A-D). These results suggest
256 that PKCβ and Wnt signaling inhibitors in suspension conditions regulate global gene expression
257 patterns to suppress spontaneous differentiation, albeit remaining expression signatures of
258 suspension culture, possibly due to the microenvironment within the formed aggregates and
259 physiological differences. We also extracted and analyzed individual gene expression data of
260 pluripotency markers from RNA-seq results. Compared to adherent condition, the expression of
261 naïve pluripotency markers, *KLF2*, *KLF4*, *KLF5*, and *DPPA3*, were up-regulated in IWRLY
262 conditions while *OCT4* and *NANOG* were at the similar levels (Figure 5—figure supplement 2).

263 Combined with RT-qPCR analysis data on 5 different hiPSC lines (Figure 3E), these results
264 suggest that IWRLY conditions may drive hiPSCs in suspension conditions to shift toward naïve
265 pluripotent states.

266 **Mass expansion of hiPSCs in suspension conditions supplemented with inhibitors of PKCβ**
267 **and Wnt signaling pathways.**

268 For the clinical applications of hiPSCs, its homogenous mass production is required to obtain
269 sufficient quantities. To test the feasibility of mass production under suspension-culture
270 conditions supplemented with PKCβ and Wnt signal inhibitors, we first performed suspension-
271 culture using a healthy-donor derived hiPSC line, 1383D6, in a 30 mL bioreactor with stirring
272 conditions (Matsumoto *et al*, 2022) at different cell seeding densities and different stirring speeds
273 (Figure 6—figure supplement 1A). HiPSCs steadily proliferated at 0.5 x 10^5 - 2 x 10^5 cells/mL of
274 the cell seeding density, but cells hardly proliferated at 8 x 10^5 cells/mL (Figure 6—figure
275 supplement 1B). Since the number of total collected cells was the lowest at a seeding density of
276 0.5 x 10^5 cells/mL, the seeding density of 1 x 10^5 - 2 x 10^5 cells/mL is considered suitable. Also,
277 hiPSCs steadily proliferated at 50 - 150 rpm of the stirring speed, but not at 250 rpm (Figure 6—
278 figure supplement 1C). Then, we analyzed protein expression of PAX6 and SOX17 in these cells
279 after 3 passages with these conditions at 50 - 150 rpm of stirring speed. Suspension culture in the
280 presence of PKCβ and Wnt inhibitors decreased the positive ratio of PAX6 and SOX17 in these
281 reactor stirring speeds (Figure 6—figure supplement 1D). These results suggest that PKCβ and
282 Wnt inhibitors suppressed spontaneous differentiation in bioreactor conditions at suitable stirring
283 speeds.

284 Next, we examined that undifferentiated hiPSCs were efficiently maintained in these
285 bioreactor conditions with 5 serial passages using two hiPSC lines, 1383D6 and 1231A3 (Figure
286 6—figure supplement 2A). These cell lines showed higher cell density in the bioreactor at each
287 passage after 3 days (Figure 6—figure supplement 2B). Under these conditions, the concentration
288 of glucose decreased daily (Figure 6—figure supplement 2C), whereas that of L-lactic acid
289 increased (Figure 6—figure supplement 2D). These results indicate that the cell lines proliferated
290 with active energy consumption. Further, RT-qPCR analysis showed no marked differences in the
291 undifferentiated and differentiation markers expression between hiPSCs cultured in adhesion vs.
292 suspension with PKCβ and Wnt inhibitors (Figure 6—figure supplement 2E and F). Flow
293 cytometric analysis showed that more than 90% of these cells were positive for pluripotency
294 marker proteins: NANOG, OCT4, and SOX2 (Figure 6—figure supplement 2G). G-band analysis
295 of suspension-cultured hiPSCs after five passages revealed normal karyotype (Figure 6—figure
296 supplement 2H). These results demonstrate that undifferentiated hiPSCs were efficiently
297 maintained in the bioreactor using the culture medium supplemented with inhibitors of PKCβ and
298 Wnt signaling pathways.

299 Then, we expanded hiPSCs in a large-scale culture system under perfusion conditions in the
300 presence of IWR-1-endo and LY333531. In this experiment, clinical-grade hiPSC line, Ff-l14s04,

301 which is derived from PBMCs of a donor carrying homozygous alleles for major HLA loci
302 (HLA-A, HLA-B, and HLA-DR) was used (Kitano *et al*, 2022). Large-scale hiPSCs preparation
303 using a perfusion-culture system with 320 mL bioreactor having stirred-wing (Kropp *et al*, 2016)
304 was performed in GMP-compliant, clinical grade StemFit AK03N medium containing IWR-1-
305 endo and LY333531 (Figure 6A). When the culture was started at 1×10^5 cells/mL in 320 mL
306 medium, hiPSCs proliferated nearly 10-fold after 3 - 4 days to produce ~300 stock vials (1×10^6
307 cells/vial). This large-scale culture was repeated three times (Passages 1, 2, and 3). Since the
308 population doubling time (PDT) of this hiPSC line in adherent culture conditions is 21.8 - 32.9
309 hours determined at its production, this proliferation rate in this large scale suspension culture is
310 comparable to adherent culture conditions. The frozen vials of this hiPSC lines obtained at each
311 passage in large-scale suspension culture conditions were characterized. Cells obtained from
312 large-scale suspension cultures formed typical hiPSC-like colonies after vials were thawed and
313 seeded in adherent-culture conditions (Figure 6B).These samples from suspension culture
314 conditions showed similar or higher viability (>90%) to that of adherent-culture derived vials
315 (Figure 6C). When compared to adherent conditions, these samples from suspension culture
316 conditions showed a similar or higher proliferation rate after thawing (Figure 6D). Flow
317 cytometric analysis showed that over 90% of cells were positive for pluripotent cell markers
318 expression: TRA-1-60, SSEA4, and OCT4 (Figure 6E and F). Further, G-band analysis revealed
319 that hiPSCs retained their normal karyotype even after three passages under large-scale
320 suspension conditions (Figure 6G). When large-scale suspension-culture derived hiPSCs were
321 incubated in each germ layer-specific differentiation medium for 4 - 7 days, the expression of
322 early differentiation markers for ectoderm (*PAX6* and *SOX1*), mesoderm (*T* and *PDGFRA*) and
323 endoderm (*SOX17* and *CXCR4*) was significantly induced (Figure 6H). These cells were then
324 directly differentiated into dopaminergic neural progenitors, cardiomyocytes, and hepatocytes to
325 evaluate their differentiation capacity and propensity. There were no differences in the
326 differentiation efficiency toward these lineages (Figure 6I-M). These results indicate that the
327 characteristics and quality of clinical-grade hiPSCs cultured in large-scale suspension conditions
328 in the presence of PKCβ and Wnt inhibitors are equivalent to those of hiPSCs maintained under
329 adherent conditions. Taken together, we made successful in mass suspension-culture conditions
330 of hiPSCs supplemented with Wnt and PKCβ inhibitors.

331 **Single-cell sorting and expansion of hiPSC subclones cultured in suspension conditions.**
332 To test the feasibility of our suspension culture method to single cell sorting, we sorted a hiPSC
333 line, 201B7, with TRA-1-60 antibody into individual wells of a 96-well plate and attempted to
334 establish subclones by expanding them with serial passages using StemFit AK02N medium
335 (Figure 7A). On day 7 after single cell sorting, we counted the number of colonies to calculate the
336 cloning efficiency (Figure 7B). The cloning efficiency in adherent culture conditions was around
337 30%. While the cloning efficiency in suspension culture conditions without any chemical
338 treatment was less than 10%. The treatment of IWR-1-endo in the suspension culture conditions

339 increased the efficiency more than 20% although the treatment of LY333531 decreased the
340 efficiency. These results indicated that the IWR-1-endo treatment is beneficial in single-cell
341 cloning in suspension culture conditions. On day 14, we performed passages of formed colonies
342 and cultured in suspension conditions supplemented with IWR-1-endo LY333531. By day 28
343 after this single-cell sorting, we expanded single-cell-sorted hiPSC subclones in suspension
344 culture supplemented with IWR1-endo and LY3333531. On day 28, we examined seven
345 subclones for their cell growth and expression of OCT4 and TRA-1-60. The subclones showed
346 round-shaped aggregates with more than three million cells and high ratios of OCT4- and TRA1-
347 60-positive cells (Figure 7C-F). These results indicate that we have successfully derived single-
348 cell-cloned sublines in suspension culture.

349 **Direct freeze and thaw of hiPSCs cultured in suspension conditions.**
350 To test the feasibility of our suspension culture method to direct freeze and thaw processes, we
351 froze a hiPSC line, 201B7, in suspension culture conditions using StemFit AK02N medium
352 supplemented with IWR1-endo and LY3333531. Then, we thawed these frozen vials and directly
353 reseeded the cells in suspension conditions supplemented with IWR1-endo and LY3333531
354 (Figure 8A). By day 10 after reseeding, we expanded the hiPSCs in suspension culture
355 supplemented with IWR1-endo and LY3333531 (Figure 8B). On day 10, we examined three vials
356 for their cell growth and expression of OCT4 and TRA-1-60. The subclones showed more than
357 three million cells and high ratios of OCT4- and TRA1-60-positive cells (Figure 8C-E). We also
358 tested mTeSR1 medium for this process. Three different hiPSC lines, WTC11, 1231A3, and
359 HiPS-NB1RGB, cultured in mTeSR1 supplemented with IWR1-endo and LY3333531
360 successfully recovered from frozen vials (Figure 8—figure supplement 1A-D). These results
361 indicate that we have successfully frozen and thawed hiPSCs in suspension culture conditions
362 directly.

363 **Establishment of hiPSC lines in complete suspension-culture conditions supplemented with**
364 **inhibitors of PKCβ and Wnt signaling pathways.**
365 For the clinical use of hiPSCs, more secure and efficient establishment of hiPSCs in closed
366 systems is strongly desired. To achieve this, we aimed to establish hiPSCs in suspension culture
367 conditions. Using PBMCs as a starting material, we generated hiPSCs using a novel replication-
368 defective and persistent Sendai virus vector (SeVdp) infection or episomal vector electroporation,
369 as these methods are well-known for producing transgene-free, clinical-grade hiPSCs (Fusaki *et*
370 *al*, 2009; Nishimura *et al*, 2011) (Figure 9A). PBMCs were infected with SeVdp carrying *OCT4*,
371 *SOX2*, *KLF4*, and *L-MYC* genes. Infected cells were kept cultured by repeating passages every 5 -
372 6 days. Cell aggregates cultured with IWR1-endo and LY333531 showed uniform spherical
373 structure (Figure 9B), and most of the cells were positive for OCT4 (Figure 9C) and TRA-1-60
374 (Figure 9D) on day 56. These bulk cells were able to differentiate into three germ layers in an in
375 vitro EB formation assay (Figure 9E) and in teratomas that were transplanted into

376 immunodeficient NOD.Cg-Prkdcscid Il2rgtm1Wjl/SzJ (NSG) mice (Figure 9F). These bulk-
377 hiPSCs maintained normal karyotype (Figure 9G). By single cell sorting with fluorescent labeled
378 TRA-1-60 antibody, we expanded single-cell-derived clones in suspension-culture conditions. A
379 clone (F-10) showed OCT4 and TRA1-60 expressions (Figure 9H-J). In addition, the established
380 clone showed potency to differentiate into derivatives of three germ layers *in vitro* as EBs (Figure
381 7K) and *in vivo* as teratoma transplanted into NSG mice (Figure. 9L). A normal karyotype was
382 observed in this clone (Figure 9M). SeVdp was nearly extinct in these bulk populations and F-10
383 clone (Figure 7N). These results demonstrate that, we were successful in establishing transgene-
384 free hiPSC lines using SeVdp infection in suspension-culture conditions in the presence of PKCβ
385 and Wnt inhibitors.

386 Furthermore, we were successful in establishing single-cell-derived hiPSC lines using the
387 transfection of episomal plasmid vectors in suspension-culture conditions in the presence of
388 PKCβ and Wnt signaling inhibitors. PMBCs were transfected with episomal plasmid vector mix
389 carrying *OCT4*, *SOX2*, *KLF4*, *L-MYC*, *LIN28*, and *mp53DD* and cultured in suspension
390 conditions in the presence or absence of IWR-1-endo and LY33351 with repeated passages to
391 reach enough cell numbers to make cell stocks and characterization (Figure 9—figure supplement
392 1A). After 36 days of culture, 59% double positive cells for TRA-1-60 and SSEA4 were observed
393 in control, whereas 78% were seen in the presence of IWR-1-endo and LY333531 (Figure 9—
394 figure supplement 1B and C). We performed cell sorting of TRA-1-60 and SSEA4 double
395 positive cells and further repeated 5 more passages in the absence or presence of IWR-1-endo and
396 LY333531. Cell aggregates cultured in culture medium supplemented with IWR-1-endo and
397 LY333531 showed uniform spherical structures (Figure 9—figure supplement 1D), and the most
398 of these cells were TRA-1-60 and SSEA4 double positive (Figure 9—figure supplement 1E). In
399 contrast, cell aggregates cultured without these inhibitors showed lumpy, heterogeneous shapes,
400 and decreased undifferentiated population. Immunostaining of OCT4 on dissociated cell
401 aggregates resulted in higher OCT4 positive cells in IWR-1-endo and LY333531 treated cells
402 (Figure 9—figure supplement 1F and G). We further performed single cell sorting of TRA-1-60-
403 positive cells from bulk-cultured populations at 10 passages (Figure 9—figure supplement 1H
404 and I). We selected 3 clones to be characterized further. These clones showed round spherical
405 shapes in their aggregates and expression of OCT4, NANOG, and TRA-1-60 proteins (Figure 9—
406 figure supplement 1J-L). Pluripotency into three germ layers was confirmed in vitro with EB
407 formation assay (Figure 9—figure supplement 1M) and teratoma formation analysis (Figure.
408 Figure 9—figure supplement 1N). These clones retained a normal karyotype even after a long-
409 culture (Figure 9—figure supplement 1O). These results demonstrate that single-cell-derived
410 hiPSC lines were established using the transfection of episomal plasmid vectors in suspension
411 culture conditions in the presence of PKCβ and Wnt signaling inhibitors.
412

413 **Discussion**

414 In this study, we have developed a series of methods to generate and maintain hiPSCs in
415 suspension conditions. First, we have identified compounds that suppress the spontaneous
416 differentiation of hiPSCs in suspension cultures. Based on these findings, we have newly
417 achieved a complete series of culture processes including hiPSC establishment, long-term culture,
418 mass culture, single-cell cloning, and direct freeze and thaw. Our methods are validated in several
419 conventional culture media and many hiPSC lines. Thus, our findings show that suspension
420 culture conditions with Wnt and PKCβ inhibitors (IWRLY suspension conditions) can precisely
421 control cell conditions and are comparable to conventional adhesion cultures regarding cellular
422 function and proliferation. Many previous 3D culture methods intended for mass expansion used
423 hydrogel-based encapsulation or microcarrier-based methods to provide scaffolds and biophysical
424 modulation (Chan *et al*, 2020). These methods are useful in that they enable mass culture while
425 maintaining scaffold dependence. However, the need for special materials and equipment and the
426 labor and cost involved are concerns toward industrial mass culture. On the other hand, our
427 IWRLY suspension conditions do not require special materials such as hydrogels, microcarriers,
428 or dialysis bags, and have the advantage that common bioreactors can be used. Furthermore, we
429 have observed some differences in conventional media used for suspension culture conditions for
430 maintaining self-renewal characteristics, preventing spontaneous differentiation into specific
431 lineages, and performing stability among different experimental times. Overcoming these
432 heterogeneity caused by conventional media, the IWRLY suspension conditions robustly
433 maintain hiPSC self-renewal and pluripotency. Therefore, this IWRLY suspension culture of
434 hiPSCs is advantageous in terms of mass culture, automation, safety assurance, and is expected to
435 have novel industrial applications that could not be achieved by conventional methods.

436 HiPSCs have been generally considered to be scaffold-dependent and are cultured under
437 adherent monolayer culture conditions (Hayashi & Furue, 2016; Xu *et al.*, 2001). On the other
438 hand, some studies reported that floating cultures without external ECM addition or scaffolds
439 have been successfully performed on hiPSCs for their long-term and/or mass expansion
440 (summarized in Table 1). However, dissociation into single cells and amplification from these
441 single cells in suspension culture conditions have never been achieved. Thus, it remains arguable
442 whether culturing human pluripotent stem cells without providing a scaffold is possible. In this
443 study, we demonstrated that many existing hiPSCs quickly acclimatized to the IWRLY
444 suspension culture conditions and that they could be successfully cultured even under harsh
445 conditions such as colony formation from single cells or direct freeze-thaw processes. These
446 findings suggest that hiPSCs can be sufficiently cultured even without scaffolds or exogenous
447 ECM proteins. However, as previous studies have shown, hiPSCs themselves secrete scaffold
448 substances such as ECM proteins, which may affect the status of suspension culture conditions
449 (Kim *et al.*, 2019).

450 On the other hand, it is interesting to see whether and how the properties of hiPSCs
451 cultured in IWRLY suspension culture conditions are altered from the adherent conditions. Our
452 transcriptome results in comparison to adherent conditions show that gene expression associated
453 with cell-to-cell attachment, including E-cadherin (CDH1), is more activated. This may be due to
454 the status that these hiPSCs are more dependent on cell-to-cell adhesion where there is no
455 exogenous cell-to-substrate attachment in the three-dimensional culture. Previous studies have
456 shown that cell-to-cell adhesion by E-cadherin positively regulates the survival, proliferation, and
457 self-renewal of human pluripotent stem cells (Aban *et al*, 2021; Li *et al*, 2012; Ohgushi *et al*,
458 2010). Furthermore, studies have shown that human pluripotent stem cells can be cultured using
459 an artificial substrate consisting of recombinant E-cadherin protein alone without any ECM
460 proteins (Nagaoka *et al*, 2010). Also, cell-to-cell adhesion through gap junctions regulates the
461 survival and proliferation of human pluripotent stem cells (Wong *et al*, 2006; Wong *et al*, 2004).
462 These findings raise the possibility that the cell-to-cell adhesion, such as E-cadherin and gap
463 junctions, are compensatory activated and support hiPSC self-renewal in situations where there
464 are no exogenous ECM components and its downstream integrin and focal adhesion signals are
465 not forcedly activated in suspension culture conditions. It will be interesting to elucidate these
466 molecular mechanisms related to E-cadherin in the hiPSC survival and self-renewal in IWRLY
467 suspension conditions in the future.

468 We have identified two compounds as factors that ameliorate the disadvantages of the
469 suspension culture of hiPSCs. Wnt signaling inhibitors specifically inhibited differentiation
470 toward mesendoderm, whereas, the PKCβ inhibitor, LY333531, inhibited ectodermal
471 differentiation and, when combined with IWR-1-endo, maintained the undifferentiated nature of
472 hiPSCs with high efficiency. As for Wnt activation in human pluripotent stem cells, previous
473 studies reported some WNT agonists were expressed in undifferentiated human pluripotent stem
474 cells (Dziedzicka *et al.*, 2021; Jiang *et al*, 2013; Konze *et al*, 2014). In suspension culture, cell
475 aggregation causes tight cell-cell interaction. The paracrine effect of WNT agonists in the cell
476 aggregation may strongly affect neighbor cells to induce spontaneous differentiation into
477 mesendodermal cells. Thus, the inhibition of WNT signaling should be effective to suppress the
478 spontaneous differentiation into mesendodermal lineages in suspension culture. Gö6983, a pan-
479 PKC inhibitor, has been used to promote the self-renewal of mammalian PSCs (Dutta *et al*, 2011;
480 Kinehara *et al*, 2013; Rajendran *et al*, 2013; Takashima *et al*, 2014); however, in these cases, the
481 role of specific isoforms in PSC self-renewal and differentiation are not fully elucidated yet. Also,
482 PKC signaling is involved in neural induction conserved in animals shown in sea urchin (Range
483 *et al*, 2013), Xenopus (Otte *et al*, 1988; Otte *et al*, 1989), mouse (Stumpo *et al*, 1995). Our
484 findings suggested the involvement of PKCβ in human neuroectodermal differentiation using
485 hiPSCs. It will be interesting to elucidate the molecular mechanisms of how PKC signaling is
486 involved in neuroectoderm differentiation in the future.

487 Interestingly, these combinations of chemical inhibitors against WNT and PKC signaling
488 pathways are also being used in the induction and maintenance of naïve human pluripotent stem
489 cells (Bayerl *et al*, 2021; Bredenkamp *et al*, 2019; Guo *et al*, 2017; Khan *et al*, 2021). Previous
490 studies suggested that cell state transition toward naïve state in hPSCs had beneficial effects in
491 the suspension culture of hiPSCs (Lipsitz *et al.*, 2018; Rohani *et al.*, 2020). While, in suspension-
492 culture, we did not aim to drive hiPSCs to a naïve state by the use of these combinations of
493 chemical inhibitors conditions, we found that naïve pluripotency marker genes were up-regulated
494 in the IWRLY suspension conditions consistently. The question of why the transition to the naïve
495 PSCs type facilitates suspension culture adaptation remains elusive; however, considering early
496 development, the inner cell mass in blastocysts in the earlier stages that maintains pluripotency
497 forms a three-dimensional morphology, whereas epiblasts, where the development is more
498 proceeded, form a flattened epithelial morphology (Sheng, 2015). The same is true for pluripotent
499 stem cells in mice, where naïve mouse embryonic stem cells derived from blastocysts form three-
500 dimensional colonies, whereas epiblast stem cells derived from the later developmental stages
501 form flattened epithelial colonies (Brons *et al*, 2007; Tesar *et al*, 2007). We showed that these
502 differences in the morphology of mouse pluripotent stem cells could be regulated by the
503 activation state of ECM and integrin signaling and that the situation where these signals are not
504 active is suited to the naïve state (Hayashi *et al*, 2007). The same characteristics may be applied
505 to human pluripotent stem cells, although no direct results have yet been shown in human
506 pluripotent stem cells (Hayashi & Furue, 2016). Thus, hiPSCs can be adapted to form three-
507 dimensional colony morphology in IWRLY suspension cultures by shifting their state to a naïve
508 PSCs type, which may facilitate self-renewal in suspension culture.

509 Last but not least, we successfully generated hiPSC lines from PBMCs in suspension
510 conditions for the first time by adding the abovementioned compounds to the culture medium.
511 Both transduction methods with SeVdp and episomal plasmid vectors enabled the establishment
512 of hiPSCs under suspension conditions in the presence of IWR-1-endo and LY333531. Clonal
513 expansion of hiPSCs was also performed by single-cell sorting with flow cytometry, and the
514 established hiPSCs were successfully characterized for their self-renewal, pluripotency, and
515 genomic integrity. These results indicate that hiPSC lines generated in suspension conditions
516 have the same quality in terms of their pluripotency, self-renewal, and genomic integrity as those
517 generated with conventional adherent conditions. This consistent process from establishing
518 hiPSCs from somatic cells to their mass expansion with precise control of cellular status in
519 suspension culture may pave the way for their stable and automated clinical application toward
520 autologous cell therapy of hiPSCs.
521

522 **Methods**
523
524 **Human subjects**
525 The generation and use of hiPSCs were approved by the Ethics Committee of RIKEN
526 BioResource Research Center, Graduate School of Medicine of Kyoto University, and KANEKA
527 CORPORATION.
528
529 **Animal experiments**
530 All animal experiments were approved by the Animal Experimentation Committee of the RIKEN
531 Tsukuba branch and were performed according to the committee's guiding principles and the
532 "Guide for the Care and Use of Laboratory Animals" published by the National Institute of
533 Health.
534
535 **Data availability**
536 All data are available in the main text or the supplementary materials. RNA-seq data are available
537 in the Gene Expression Omnibus as GSE222833. All the data supporting the findings of this
538 study are available from the lead contact upon reasonable request. Source data is provided with
539 this paper. This paper does not report original code.
540
541 **HiPSCs cultured in adherent conditions**
542 WTC11 (GM25256 from Coriell Institute) (Hayashi *et al*, 2016), 201B7 (HPS0063 from RIKEN
543 Cell Bank) (Takahashi *et al.*, 2007), 454E2 (HPS0077 from RIKEN Cell Bank) (Okita *et al*,
544 2011), 1383D6 (HPS1006 from RIKEN Cell Bank) (Okita *et al.*, 2011), 1231A3 (HPS0381 from
545 RIKEN Cell Bank) (Okita *et al.*, 2011), Ff-I14s04 (CiRA foundation, Kyoto University) (Kitano
546 *et al.*, 2022), and HiPS-NB1RGB (HPS5067 from RIKEN Cell Bank), which were generated
547 from human neonatal skin fibroblast (RCB0222) (Borisova *et al*, 2022; Shimizu *et al*, 2022),
548 were used as healthy-donor hiPSC lines. With tdTomato-reporter hiPSC lines, we generated
549 knock-in hiPSC lines for PAX6-TEZ (constructed from 454E2 line) and SOX17-TEZ
550 (constructed from 1383D6 line) using CRISPR-Cas9 genome editing (Tsukamoto *et al*, 2021)
551 (Figure. S1A). These hiPSCs were cultured in StemFit AK02N medium (Cat#AK02N,
552 Ajinomoto, Co., Ltd., Tokyo, Japan). Medium change was performed every day and passaged at
553 80%–90% confluency after 6-7 days of culture. At passage, PBS/EDTA solution (0.5 mM,
554 Cat#06894-14, Nacalai Tesque) was used to dissociate hiPSC colonies, and these cells were
555 seeded at a density of 2,500 cells/cm^2. 10 μM Y-27632 (Cat#HY-10071, FUJIFILM Wako Pure
556 Chemical Corporation, Osaka, Japan) and 0.25 μg/cm^2 iMatrix-511 silk (Cat#892021, Matrixome
557 Inc, Osaka, Japan) were added to the culture dish on seeding day. These hiPSC cells were
558 cultured in a CO_2 incubator (Forma Steri-Cycle i160, Thermo Fisher Scientific) with a gas
559 conditions at 5% CO_2, 21% O_2, >95% humidity, and 37 ºC.

560

561 **Suspension-culture of hiPSCs**

562 Suspension culture with rotation at 90 rpm was performed with a plate shaker (Cat#WB-101SRC,
563 WAKENBTECH, Kyoto, Japan or #0081704-000, TAITEC, Tokyo, Japan) installed in a CO_2
564 incubator (Cat#Steri-Cycle i160, Thermo Fisher Scientific, MA, USA) and operated under high
565 humidity continuously during the whole culture period. To start the culture hiPSCs in suspension
566 conditions, 4×10^5 cells were seeded in one well of a low-attachment 6-well plate (Cat#MS-
567 80060, Sumitomo Bakelite, Tokyo, Japan) with 4 mL of StemFit AK02N medium, StemScale
568 PSC suspension medium (A4965001, Thermo Fisher Scientific, MA, USA), or mTeSR medium
569 (Stem Cell Technologies, Vancouver, Canada) supplemented with 10 μM Y-27632. This plate
570 was placed onto the plate shaker in the CO_2 incubator (Forma Steri-Cycle i160, Thermo Fisher
571 Scientific). The medium without Y-27632 was changed every day unless otherwise specified. On
572 days 3 - 5, the hiPSC aggregates were dissociated with Accutase (Cat#12679-54, Nacalai Tesque)
573 at 37°C for 10 min. The dissociated cells were counted with an automatic cell counter (Model R1,
574 Olympus) with Trypan Blue staining to detect live/dead cells. These cell suspension was spun
575 down at 200 rpm for 3 minutes, and the supernatant was aspirated. The cell pellet was re-
576 suspended with a new culture medium at an appropriate cell concentration and used for the next
577 suspension culture. This passage was performed every 5 days unless otherwise specified. To
578 screen for factors that inhibit spontaneous differentiation of hiPSCs, chemicals or recombinant
579 proteins were added to the culture medium (listed in Supplementary Table S1). These hiPSC cells
580 were cultured in a CO_2 incubator with a gas conditions at 5% CO_2, 21% O_2, >95% humidity, and
581 37 ºC.

582

583 **Bioreactor culture of hiPSCs**

584 A frozen stock of hiPSCs was pre-cultured twice in adherent conditions to prepare enough cell
585 numbers. To prepare enough hiPSCs to start large-scale culture, hiPSCs were pre-cultured in
586 iMatrix-511MG (Cat#892 005, Matrixome, Inc, Osaka, Japan) or Vitronectin (VTN-N)
587 Recombinant Human Protein, Truncated (Cat#A14700, Thermo Fisher Scientific, MA, USA)-
588 coated cell culture flasks with StemFitAK03N (Cat#AK03N, Ajinomoto, Co., Ltd., Tokyo, Japan)
589 including 20 μM IWR-1-endo and 1 μM LY333531. A 30-mL stirred suspension bioreactor
590 (BWV-S03A, Able Co., Tokyo, Japan) was used according to a previous study (Matsumoto *et al.*,
591 2022). The medium change was manually performed every other days. After 3-4 days of culture,
592 the formed hiPSC aggregates were dissociated with TrypLE SELECT (Cat#A12859-01, Thermo
593 Fisher Scientific, MA, USA). As for large-scale hiPSCs culture, the reactor system BioFlo320
594 (Eppendorf, Hamburg, Germany) was used according to a previous study (Kropp *et al.*, 2016).
595 Perfusion-culture was started with $3.2 - 4.8 \times 10^7$ cells in 320 mL of StemFit AK03N medium
596 with IWR-1-endo and LY333531. To maintain the lactate concentration below a certain level and
597 to regulate the pH, the culture was carried out by increasing the amount of medium perfusion per
598 unit time in accordance with the cell proliferation transition. To prevent pH decrease, CO_2

599 concentration was regulated by feedback control in the reactor system. After 3-4 days of culture,
600 the formed hiPSC aggregates were dissociated with TrypLE SELECT (Cat#A12859-01, Thermo
601 Fisher Scientific, MA, USA) collected for making cell stocks (~300 tubes). This perfusion culture
602 was repeated three times (P1, P2, and P3) and the cells were prepared at each expansion step.
603
604 **HiPSC generation in suspension culture conditions**
605 HiPSCs were generated from healthy donor-derived PBMCs (Precision for Medicine). Thawed
606 PMBCs from a vial containing around 1×10^7 cells were pre-cultured in one well of low
607 attachment 6-well plate including 4 mL of StemSpan-AOF (Cat#ST100-0130, STEMCELL
608 Technologies, Vancouver, Canada) supplemented with recombinant human IL-6 (100 ng/mL),
609 IL-3 (10 ng/mL), SCF (300 ng/mL), TPO (300 ng/mL), and FLT3 ligand (300 ng/mL) (all from
610 FUJIFILM Wako Pure Chemical Corporation, Tokyo Japan). After 24 h of incubation with
611 continuous stirring at 37°C/5% CO_2/21% O_2, PBMCs were spun down with centrifugation at 200
612 × g for 10 min at low deceleration speed and resuspended in StemSpan ACF for cell counting.
613 For episomal vetor transduction, 2.5×10^6 cells of PMBCs were centrifuged at 200 × g for 10 min
614 with low deceleration speed and electroporated using Nucleofector 2b device (Lonza, Basel,
615 Switzerland) with iPS cell Generation Episomal vector Mix (Takara Bio, Shiga, Japan) and
616 Amaxa Human $CD34^+$ Cell Nucleofector kit (Lonza, Basel, Switzerland) according to
617 manufacturer's protocol. 5×10^5 of electroporated cells were seeded in one well of a low
618 attachment 6-well plate in 4 mL StemSpan ACF with the cytokines mentioned above.
619 Suspension-culture was performed with continuous agitation at 90 rpm. Stem span ACF medium
620 were gradually replaced with StemFit AK02N medium. Formed cell aggregates were passaged
621 with Accutase on day 16 in the presence of 10 μM Y27632, and suspension-culture was
622 continued until the cell numbers reached a sufficient amount for characterization. 10 μM IWR-1-
623 endo and 1 μM LY333531 were added from day 3.
624 SeVdp infection was performed with Sendai Reprogramming Kit (CytoTune EX-iPS of
625 virus solution, ID Pharma, Tsukuba, Japan) according to the manufacturer's protocol with some
626 modifications. Briefly, pre-cultured 1×10^6 PMBCs were centrifuged at 200 × g for 10 min, with
627 low deceleration speed, and resuspended in 2 mL of StemSpan ACF with cytokines. PMBCs were
628 gently mixed with 2 mL of virus solution prepared at MOI = 5 per 1×10^6 cells. 5×10^5 infected
629 cells were seeded in one well of low-attachment 6-well plate at a total volume of 4 mL with
630 StemSpan ACF plus cytokines. Suspension-culture was initiated with continuous agitation at 90
631 rpm. Stem span ACFs were gradually replaced with StemFit AK02N as mentioned above, and the
632 cell aggregates were passaged with Accutase on day 16 in the presence of 10 μM Y-27632.
633 Suspension-culture and passages continued until cell reached a sufficient number for
634 characterization. 10 μM IWR-1-endo and 1 μM LY333531 were added from day 23. These cells
635 were cultured in a CO_2 incubator (Forma Steri-Cycle i160, Thermo Fisher Scientific) with a gas
636 conditions at 5% CO_2, 21% O_2, >95% humidity, and 37 ºC.
637

638 **Three germ layer differentiation *in vitro***
639 For embryoid body (EB) formation assay, suspension-cultured hiPSC lines were dissociated with
640 Accutase, and 1.0 x 10^4 cells were seeded in each well of an EZ-BindShut 96-well-V plate
641 (Cat#4420-800SP AGC TECHNO GLASS CO., LTD, Shizuoka, Japan) with 100 µL Stem Fit
642 AK02N medium supplemented with 10 µM Y-27632. Before culture, the 96-well-V plate was
643 centrifuged at 200 x g for 3 min for efficient cell mass formation. The next day, the culture
644 medium was switched to DMEM high Glucose (Cat#08458-16, Nacalai tesque, Kyoto, Japan)
645 supplemented with 10% fetal bovine serum (here after referred as EB medium). On day 8, EBs
646 were transferred into 0.1% (w/v) Gelatin Solution (Cat#190–15805, FUJIFILM Wako Pure
647 Chemical Corporation, Tokyo Japan) -coated 12-well plate and further cultured in EB medium for
648 another 8 days. The medium was changed every day. EBs were fixed with 4% paraformaldehyde
649 in Dulbecco's Phosphate Buffered Saline (D-PBS) (Cat#14249-24, Nacalai tesque, Kyoto, Japan)
650 for 10 min at room temperature and used for immunostaining. The differentiation was validated
651 by immunostaining against each germ layer markers.
652 The differentiation potency of suspension-cultured hiPSCs toward three germ layers was
653 also evaluated by culturing in germ layer specific differentiation medium. As in the maintenance
654 conditions, 4×10^5 hiPSC were seeded in one well of a low-attachment 6-well plate with 4 mL of
655 StemFit AK02N medium supplemented with 10 µM Y-27632. This plate was placed onto the
656 plate shaker in the CO_2 incubator. Next day, the medium was changed to the germ layer specific
657 differentiation medium. For ectodermal differentiation, suspension-cultured hiPSCs spheroids
658 were cultured with Stem Fit AK02N without C medium supplemented with 10 µM SB431542
659 (Cat#198-16543, FUJIFILM Wako Pure Chemical Corporation, Tokyo, Japan) and 10 µM
660 DMH1 (Cat#041-33881FUJIFILM Wako Pure Chemical Corporation, Tokyo, Japan) for 7 days.
661 For mesodermal differentiation, suspension-cultured hiPSCs spheroids were cultured with
662 RPMI1640 medium (FUJIFILM Wako Pure Chemical Corporation, Tokyo, Japan) supplemented
663 with B-27 supplement, minus insulin (A1895601, Thermo Fisher Scientific, MO, USA) and 7.5
664 µM CHIR99021 (Cat#034-23103, FUJIFILM Wako Pure Chemical Corporation, Tokyo, Japan)
665 for 1 day, and continuously with RPMI1640 medium supplemented with B-27 supplement for 2
666 days. For endodermal differentiation, suspension-cultured hiPSCs spheroids were cultured with
667 RPMI1640 medium supplemented with 1 mM Sodium pyruvate (FUJIFILM Wako Pure
668 Chemical Corporation, Tokyo, Japan), 1 x NEAA (FUJIFILM Wako Pure Chemical Corporation,
669 Tokyo, Japan), 80 ng/mL Activin A (R&D Systems, MN, USA), 55 µM 2-mercaptethanol
670 (FUJIFILM Wako Pure Chemical Corporation, Tokyo, Japan), 50 ng/mL FGF2 (R&D Systems,
671 MN, USA), 20 ng/mL BMP4, and 3 µM CHIR99021 for 2 days, and continuously with
672 RPMI1640 medium supplemented with 1 mM Sodium pyruvate, 1× NEAA, 80 ng/mL Activin A,
673 55 µM 2-mercaptethanol, and 0.5% Knockout serum replacement (KSR; Thermo Fisher
674 Scientific, MO , USA) for 2 days.
675
676 **Neuroectoderm and endoderm differentiation of reporter hiPSC lines**

677 Reporter hiPSC lines, PAX6-TEZ and SOX17-TEZ were used as positive controls for in vitro
678 neuroectoderm and endoderm differentiation, respectively. PAX6-TEZ was seeded in each well
679 of a 24 well-plate coated with 0.25 μg/cm^2 iMatrix-511 silk with 1 mL StemFit AK02N medium
680 supplemented with 10 μM Y-27632. Next day, the culture medium was switched to Stem Fit
681 AK02N medium without supplement C, instead of containing 10 μM SB431542 and 10 μM
682 DMH1. SOX17-TEZ was seeded in each well of a 24 well-plate (same as above), and on the next
683 day, the culture medium was switched to StemFit AK02N medium without supplement C instead
684 of containing 3 μM CHIR99021 and 10 ng/mL Activin A (Cat#014-23961, FUJIFILM Wako
685 Pure Chemical Corporation, Tokyo, Japan). The medium was changed every day. On day 7,
686 tdTomato expression was observed under all-in-one fluorescent microscope (BZ-X800;
687 KEYENCE).
688
689 **Cardiomyocyte differentiation**
690 Cardiomyocyte differentiation was performed according to a modified method described
691 previously (Funakoshi *et al*, 2016). Both large-scale suspension cultured hiPSCs and typical
692 adherent-cultured hiPSC were collected by centrifugation after dissociation into single cell with
693 TrypLE Select. The cells were suspended in 1.5 mL cardiomyocyte differentiation media (CDM),
694 consisting of StemPro34 medium (Thermo Fisher Scientific) supplemented with 2 mM Glutamax
695 (Thermo Fisher Scientific), 50 μg/mL ascorbic acid, 4×10^{-4} M monothioglycerol (Sigma-
696 Aldrich), 150 μg/mL transferrin (Roche), and with Matrigel (Cat#354277, Corning, NY, USA)),
697 10 μM Y-27632 and 2 ng/mL human recombinant BMP4 (R&D Systems) and then cultured in
698 ultra-low attachment 6 well plate (Corning) in 5%CO_2/5% O_2. After 24 h, 1.5 mL CDM with
699 6 ng/mL human recombinant activin A (R&D Systems) and 5 ng/mL bFGF (R&D Systems) were
700 added into the wells. After 3 days, medium was changed to 3 mL CDM with 10 ng/mL VEGF
701 (R&D Systems), SB431542 (Sigma-Aldrich), Dorsomorphin (Sigma-Aldrich) and 1 μM IWP-3
702 (Stemgent). After 7 days, medium was changed to 3 mL CDM with 10 ng/mL VEGF (R&D
703 Systems). The medium was changed every 2 days. The cells were collected at 15 days after
704 differentiation and analyzed by flow cytometry.
705
706 **Dopaminergic progenitor cells differentiation**
707 Dopaminergic progenitor cells differentiation was performed according to a modified method
708 described previously (Doi *et al*, 2020). Both large-scale suspension cultured hiPSCs and typical
709 adherent-cultured hiPSC were collected by centrifugation after dissociation into single cell with
710 TrypLE Select. The cells were suspended in 1 mL dopaminergic progenitor cells differentiation
711 medium-1 (DPM-1), consisting of Glasgow's minimum essential medium (Thermo Fisher)
712 supplemented with 8% knockout serum replacement (Thermo Fisher Scientific), 1% MEM Non-
713 Essential Amino Acids Solution (Thermo Fisher Scientific), 1 mM sodium pyruvate (Sigma-
714 Aldrich), 0.1 mM 2-mercaptoethanol (FujiFilm Wako) and 100 nM LDN193189 (Stemgent), and
715 were then seeded in iMatrix-coated 24-well plates at a density of 1×10^6 cells/well with 10 μM

716 Y-27632 and 500 nM A-83-01 (FujiFilm Wako). After 1 and 2 days, medium was changed to
717 DPM-1 with 500 nM A-83-01, 100 ng/mL recombinant human FGF8 (FujiFilm Wako), and 2 μM
718 purmorphamine (FujiFilm Wako). After 3 to 6 days, medium was changed every day to DPM-1
719 with 500 nM A-83-01, 100 ng/mL recombinant human FGF8, 2 μM purmorphamine, and 3 μM
720 CHIR99021 (FujiFilm Wako). After 7 to 11 days, medium was changed every day to DPM-1
721 with 3 μM CHIR99021. On differentiation day 12, cells were dissociated using TrypLE select
722 and suspended in the dopaminergic progenitor cells differentiation medium-2 (DPM-2),
723 consisting Neurobasal medium (Thermo Fisher Scientific), 2% B27 supplement (without Vitamin
724 A, Thermo Fisher), 1% GlutaMAX (Thermo Fisher Scientific), 10 ng /mL human recombinant
725 glial cell-derived neurotrophic factor (FujiFilm Wako), 200 mM ascorbic acid, 20 ng / mL human
726 recombinant brain-derived neurotrophic factor (FujiFilm Wako), and 400 μM dibutyryl cAMP
727 (FujiFilm Wako), and were then plated on U-shaped 96-well plates (Thermo Fisher Scientific) at
728 a density of 2×10^4 cells/150 μL/well with 10 μM Y-27632. After 15 to 26 days, half of medium
729 was changed every 2 days to DPM-2. Dopaminergic progenitor cells differentiation efficiency
730 was analyzed by flow cytometry at 12 days after differentiation. On differentiation day 12, cells
731 were labeled with anti-CORIN antibody (Clone 5B6, Sigma-Aldrich) and secondary antibody
732 (A11001, Thermo Fisher).
733
734 **Hepatocyte differentiation**
735 Hepatocyte differentiation was performed according to a modified method described previously
736 (Si-Tayeb *et al*, 2010). Both large-scale suspension-cultured and typical adherent-cultured hiPSCs
737 were collected by centrifugation after dissociation into single cell with TrypLE Select. These
738 hiPSCs were cultured on Matrigel-coated 6-well plates until 80% confluency with StemFit
739 medium (Ajinomoto). To initiate differentiation, the medium was changed to 1 mL Hepatocyte
740 differentiation medium (HDM) consisting of RPMI1640 medium (Thermo Fisher) supplemented
741 with 1× GlutaMax (Thermo Fisher) and 1× B27 Supplement minus vitamin A, with the addition
742 of 100 ng/mL Activin A (R&D Systems). After 1 to 3 days, medium was changed every day to
743 HDM with 100 ng/mL Activin A. After 4 to 8 days, medium was changed every day to HDM
744 with 20 ng/mL human recombinant BMP-4 (R&D Systems) and 20 ng/mL human recombinant
745 FGF-4 (R&D Systems). After 9 to 13 days, medium was changed every day to HDM with 20
746 ng/mL human recombinant HGF (R&D Systems). After 14 to 24 days, medium was changed
747 every 2 days to Hepatocyte Culture Medium (HCM; Lonza) with 20 ng/mL human recombinant
748 Oncostatin M (R&D Systems). On differentiation day 25, the albumin concentration in the culture
749 supernatant was determined by ELISA using an anti-human albumin antibody (Betyl
750 Laboratories, Catalog # E88-129).
751
752 **Teratoma formation**
753 Suspension-cultured hiPSCs were dissociated with Accutase and then resuspended with 1 mL of
754 StemFit AK02N medium supplemented with 10 μM Y-27632. 1 x 10^6 cells were collected by

755 centrifugation at 200 × g for 3 m and suspended in ice-cold 50% Matrigel solution: StemFit
756 AK02N with 10 μM Y-27632 = 1:1). Cells were injected into testis or leg of NOD.Cg-Prkdcscid
757 Il2rgtm1Wjl/SzJ (NSG) mice (The Jackson Laboratory, Bar Harbor, ME, USA) using an 18-G
758 needle. Two to three months later, teratomas were collected and fixed with 4% paraformaldehyde
759 in D-PBS. Paraffin-embedded sectioning and hematoxylin-eosin (HE) staining was performed.
760 Three germ layer derivatives were observed under CKX53 microscope with a DP22 camera and
761 CellSens software (EVIDENT, Tokyo, Japan).
762
763 **Apoptosis assay of suspension-cultured iPSCs**
764 Suspension-cultured hiPSCs were dissociated with Accutase. The dissociated cells were aliquoted
765 into 1 x10^5 cells/100 μL with a binding buffer consisted of 10 mM HEPES, 140 mM NaCl, 2.5
766 mM $CaCl_2$, then added with 5 μL Annexin V (Alexa Fluor 680) conjugates (Cat# A35109,
767 Thermo Fisher scientific) and 1 μL DAPI solution (Cat# 340-07971, FUJIFILM Wako, Pure
768 Chemical Corporation, Tokyo, Japan). After incubation for 15 minutes at room temperature in
769 dark conditions, 400 μL of cold binding buffer was added. The apoptotic cells were immediately
770 analyzed with a flow cytometer (SH800S, SONY, Tokyo, Japan). As a positive control of
771 apoptosis, suspension-cultured hiPSCs were treated with Staurosporine (1 μM) (Cat#S1421,
772 Selleck Biotech, Tokyo, Japan), one of the apoptosis-inducing factors, for 2 hours before
773 collection.
774
775 **Karyotyping**
776 For virtual karyotyping, genomic DNA (gDNA) was extracted from hiPSCs using a DNeasy
777 Blood & Tissue Kit (Cat#69504, QIAGEN, Hulsterweg, Netherland) and was used for microarray
778 assay. Virtual karyotyping was performed with GeneChip Scanner System 3000 using Karyostat
779 Assay arrays (Cat#905403, both from Thermo Fisher Scientific, MA, US) according to the
780 manufacturer's protocol. Data were analyzed using the Chromosome Analysis Suite (ChAS) and
781 Affymetrix GeneChip Command Console software programs.
782 G-band analysis was performed using the common Giemsa staining method with hiPSCs
783 fixed by Carnoy's fixtative (3:1 ratio of methanol: glacial acetic acid).
784
785 **qRT-PCR**
786 Total RNA was extracted with a FastGene RNA premium kit (Cat#FG-81250, NIPPON Genetics,
787 Tokyo, Japan) and used for reverse transcription reaction. cDNA was synthesized by using a
788 ReverTra Ace qPCR RT kit (Cat#FSQ-101, TOYOBO, Osaka, Japan) with random primers.
789 Real-Time qPCR reactions were performed with a QuantStudio 3 System (Thermo Fisher
790 Scientific) using THUNDERBIRD Probe qPCR Mix (Cat#QPS-101, TOYOBO) with TaqMan
791 probes (listed in Supplementary Table 2) (Thermo Fisher Scientific) according to the
792 manufacturer's instructions. Gene expression was described as the fold change relative to the
793 control sample value (ΔΔCt method) after normalization to the corresponding GAPDH or β-Actin

794 values, unless otherwise specified. For the residual SeV detection, data were normalized to the
795 expression of GAPDH and displayed as a relative fold increase to hiPSC line established with
796 episomal vector (WTC11 line). SeVdp-infected fibroblasts on passage 1 (SeV-34 and -39) were
797 used as positive controls.
798
799 **Immunocytochemistry**
800 Immunocytochemistry was performed on adherent cells. Suspension-cultured hiPSCs were
801 dissociated with Accutase and transiently cultured as adherent in iMatrix-coated culture dishes for
802 3 h before immunocytochemistry. The cells were fixed with 4% paraformaldehyde in D-PBS for
803 10 min at room temperature, then permeabilized in D-PBS containing 0.1% Triton X-100 for
804 another 10 min. Cells were incubated with primary antibodies in D-PBS containing 0.1% Bovine
805 Serum Albumin (BSA; Cat#017-22231, FUJIFILM Wako Pure Chemical Corporation, Tokyo,
806 Japan) overnight at 4 °C. The secondary antibodies were incubated for 1 hour at room
807 temperature in D-PBS containing 0.1% BSA. Fluoro-KEEPER Antifade Reagent, Non-Hardening
808 Type with DAPI (Cat#12745-74, Nacalai tesque, Kyoto, Japan) was used for nuclear
809 counterstaining. Fluorescence images were taken with an all-in-one fluorescent microscope (BZ-
810 X800; KEYENCE, Osaka, Japan). The primary and secondary antibodies used in this study are
811 listed in Supplementary Tables 3 and 4, respectively.
812
813 **Automatic capillary Western blot (Simple Western Assays)**
814 To detect the expression of PAX6 or SOX17, adherent- or suspension-cultured PAX6-TEZ or
815 SOX17-TEZ hiPSCs were collected on day 10 (Passage 2). The cell lysate was prepared from 1 ×
816 10^6 cells with sodium dodecyl sulfate-polyacrylamide gel electrophoresis (SDS-PAGE) sample
817 buffer solution without 2-ME (2x) (Cat#30567-12, Nacalai Tesque) supplemented with 100 mM
818 Dithiothreitol (DTT) (Cat#14130-41, Nacalai Tesque). To detect phosphorylated PKCβ, cell
819 lysates were collected on day 5 of suspension-cultured hiPSCs with extraction buffer mentioned
820 above, containing 1% phosphatase inhibitor cocktail (Cat#07574-61, Nacalai Tesque). Samples
821 were denatured at 95°C for 5 min. Western blotting was performed with a capillary automatic
822 western blotting device (Simple Western, Wes; Bio-Techne, CA, USA). Jes/Wes 12- to 230-kDa
823 separation module for Wes, 8 × 25 capillary cartridges (Cat#SM-W004, ProteinSimple), and
824 Anti-Rabbit/Goat/Mouse Detection Module kit (Cat#DM-002/DM-001/DM/006, ProteinSimple)
825 were used. Preparation of reagents and sample loading were conducted according to the
826 manufacturer's instructions. The data were analyzed and quantified by compass for simple
827 Western software program (ProteinSimple). GAPDH was used as the reference for normalization.
828 The primary antibodies used in this study are listed in Supplementary Table 3.
829
830 **Flow cytometry**
831 Flow cytometry of self-renewal markers, TRA-1-60 and SSEA4 was performed as described in
832 our previous study. Briefly, adherent- or suspension-cultured hiPSCs were dissociated with 0.5

833 mM EDTA solution in D-PBS or Accutase, respectively. Dissociated cells (0.5 or 1 × 10^6 cells)
834 were collected and centrifuged at 200 × g for 3 minutes and resuspended in 500 or 1000 μL PBS
835 containing 0.1% BSA and 0.5 mM EDTA, then incubated with or without anti-TRA-60 antibody
836 or anti-SSEA4 antibody for 1 hour at 4 °C under oblique light conditions. After washing with
837 PBS, cells were resuspended in 500 mL D-PBS containing 0.1% BSA and 0.5 mM EDTA, and
838 filtrated with 35-mm cell strainer (Cat#352235, FALCON, Thermo Fisher Scientific). For PAX6-
839 TEZ and SOX17-TEZ hiPSC lines, adherent- or suspension-cultured hiPSCs were dissociated
840 into single cells and collected cells were resuspended in 500 mL PBS containing 0.1% BSA and
841 0.5 mM EDTA. After passing through the 35-mm cell strainer, cells were analyzed for tdTomato.
842 The primary and secondary antibodies used in this study are listed in Supplementary Table 3 and
843 4, respectively. Flow cytometry was performed with SH800 cell Sorter (SONY, Tokyo, Japan).
844
845 **RNA-Seq**
846 Total RNA was extracted using the FastGene RNA premium kit, and strand-specific library
847 preparation was performed. The prepared library was sequenced using a NovaSeq6000 (Illumina,
848 Inc, CA, USA). Sequencing was performed in a 150 bp × 2 paired-end conFigureuration with a
849 data output of about 6 Gb per sample (~ 20 million paired reads). Library preparation and
850 sequencing was performed in GENEWIZ (Azenta, MA, USA). To identify differentially
851 regulated genes, sequencing data was analyzed with a CLC Genomics Workbench (QIAGEN,
852 Hulsterweg, the Neterlands) and R package, edgeR (v3.30.3) in R language (v 4.1.0). An MA plot
853 (log2 fold change versus mean average expression) comparing transcriptomes between
854 suspension- and adherent-culture from RNA-seq data. Transcripts with log2 fold change ≧ 2 or ≦
855 -2 (FDR <0.01) are highlighted with red and blue dots, respectively. The extracted genes were
856 analyzed for gene ontology enrichment and biological pathways using the R package,
857 clusterProfiler (v3.16.1). GSEA was also performed using clusterProfiler. An enrichment map
858 was used to visualize the GSEA results with enrichment score (ES) and false discovery rate
859 (FDR) values. Software used for the analysis is listed in Supplementary Table 5.
860
861 **Statistical analysis**
862 Statistical analysis was performed using Student's t-test, Dunnett's test for multiple comparisons
863 with a single control condition, and one-way ANOVA and Tukey's tests for multiple comparisons
864 with all the conditions. P values < 0.05 were considered statistically significant. *, ** or *** in
865 the graphs indicate P<0.05, P<0.01 or P<0.001, respectively. No statistical methods were used to
866 predetermine sample size. The experiments were not randomized and the investigators were not
867 blinded to allocation during experiments and outcome assessment.
868

Acknowledgments
We thank Dr. Bruce Conklin for providing us with the WTC11 hiPSC line; Dr. Shinya Yamanaka, Dr. Kazutoshi Takahashi, Dr. Masato Nakagawa, and Dr. Keisuke Okita for providing us with 201B7, 454E2, 1231A3, 1383D6, and Ff-I14s04 hiPSC lines. We would like to express our sincere gratitude to Dr. Kaoru Saijo, Mr. Daiki Kondo and Mr. Masahiko Yamada for their technical assistance, and Ms. Kumiko Omori for her administrative support. This work was funded by a grant from AMED (23bm1423010h0001) to Y.Ha., a collaborative research grant from Kaneka corporation to Y.Ha., and an endowment to CiRA foundation. We would like to thank Editage [http://www.editage.com] for editing and reviewing this manuscript for English language.

Author Contributions: Conceptualization: YHA, Methodology: MMT, SK, CW, KT, MI, NN YHA, Investigation: MMT, SK, YHE, TW, TS, YA, KT, MI, MN, MU, TMK, MN, TK, RM, MS, NN, KN, YN, YHA, Visualization: MMT, SK, TS, YH, Funding acquisition: MMT, TN, YK, YHA, Project administration: MMT, NN, TN, YK, YHA, Supervision: MMT, TN, YN, NT, YK, YHA, Writing – original draft: MMT, KS, MT, YHA, Writing – review & editing: MMT, YHA

Competing Interest Statement: YHA received collaborative research grant from KANEKA corporation during this study. SK, KT, MI, YK, TN, TK, RM, MS, and NN were employed with KANEKA corporation during this study. MMT, SK, KT, MI, YK, and YHA. are inventors of patents arising from this work (WO/2021/162090 and PCT/JP2020/005255). The other authors declare no competing interests.

Classification: Applied Biological Sciences, Cell Biology, and Developmental Biology in BIOLOGICAL SCIENCES

Keywords: induced pluripotent stem cells (iPSCs), suspension culture, spontaneous differentiation, Protein Kinase C (PKC), WNT

895 **References**

896 Aban CE, Lombardi A, Neiman G, Biani MC, La Greca A, Waisman A, Moro LN, Sevlever G,
897 Miriuka S, Luzzani C (2021) Downregulation of E-cadherin in pluripotent stem cells triggers
898 partial EMT. *Sci Rep* 11: 2048
899 Amit M, Chebath J, Margulets V, Laevsky I, Miropolsky Y, Shariki K, Peri M, Blais I, Slutsky
900 G, Revel M *et al* (2010) Suspension culture of undifferentiated human embryonic and induced
901 pluripotent stem cells. *Stem Cell Rev Rep* 6: 248-259
902 Amit M, Laevsky I, Miropolsky Y, Shariki K, Peri M, Itskovitz-Eldor J (2011) Dynamic
903 suspension culture for scalable expansion of undifferentiated human pluripotent stem cells. *Nat*
904 *Protoc* 6: 572-579
905 Bayerl J, Ayyash M, Shani T, Manor YS, Gafni O, Massarwa R, Kalma Y, Aguilera-Castrejon A,
906 Zerbib M, Amir H *et al* (2021) Principles of signaling pathway modulation for enhancing human
907 naive pluripotency induction. *Cell Stem Cell* 28: 1549-1565 e1512
908 Borisova E, Nishimura K, An Y, Takami M, Li J, Song D, Matsuo-Takasaki M, Luijkx D,
909 Aizawa S, Kuno A *et al* (2022) Structurally-discovered KLF4 variants accelerate and stabilize
910 reprogramming to pluripotency. *iScience* 25: 103525
911 Bredenkamp N, Yang J, Clarke J, Stirparo GG, von Meyenn F, Dietmann S, Baker D, Drummond
912 R, Ren Y, Li D *et al* (2019) Wnt Inhibition Facilitates RNA-Mediated Reprogramming of Human
913 Somatic Cells to Naive Pluripotency. *Stem Cell Reports* 13: 1083-1098
914 Brons IG, Smithers LE, Trotter MW, Rugg-Gunn P, Sun B, Chuva de Sousa Lopes SM, Howlett
915 SK, Clarkson A, Ahrlund-Richter L, Pedersen RA *et al* (2007) Derivation of pluripotent epiblast
916 stem cells from mammalian embryos. *Nature* 448: 191-195
917 Chan SW, Rizwan M, Yim EKF (2020) Emerging Methods for Enhancing Pluripotent Stem Cell
918 Expansion. *Front Cell Dev Biol* 8: 70
919 Chen B, Dodge ME, Tang W, Lu J, Ma Z, Fan CW, Wei S, Hao W, Kilgore J, Williams NS *et al*
920 (2009) Small molecule-mediated disruption of Wnt-dependent signaling in tissue regeneration
921 and cancer. *Nat Chem Biol* 5: 100-107
922 Chen KG, Mallon BS, McKay RD, Robey PG (2014) Human pluripotent stem cell culture:
923 considerations for maintenance, expansion, and therapeutics. *Cell Stem Cell* 14: 13-26
924 Dang SM, Gerecht-Nir S, Chen J, Itskovitz-Eldor J, Zandstra PW (2004) Controlled, scalable
925 embryonic stem cell differentiation culture. *Stem Cells* 22: 275-282
926 Doi D, Magotani H, Kikuchi T, Ikeda M, Hiramatsu S, Yoshida K, Amano N, Nomura M,
927 Umekage M, Morizane A *et al* (2020) Pre-clinical study of induced pluripotent stem cell-derived
928 dopaminergic progenitor cells for Parkinson's disease. *Nat Commun* 11: 3369
929 Dutta D, Ray S, Home P, Larson M, Wolfe MW, Paul S (2011) Self-renewal versus lineage
930 commitment of embryonic stem cells: protein kinase C signaling shifts the balance. *Stem Cells*
931 29: 618-628
932 Dziedzicka D, Tewary M, Keller A, Tilleman L, Prochazka L, Ostblom J, Couvreu De
933 Deckersberg E, Markouli C, Franck S, Van Nieuwerburgh F *et al* (2021) Endogenous suppression
934 of WNT signalling in human embryonic stem cells leads to low differentiation propensity towards
935 definitive endoderm. *Sci Rep* 11: 6137
936 Elanzew A, Sommer A, Pusch-Klein A, Brustle O, Haupt S (2015) A reproducible and versatile
937 system for the dynamic expansion of human pluripotent stem cells in suspension. *Biotechnol J*
938 10: 1589-1599
939 Funakoshi S, Miki K, Takaki T, Okubo C, Hatani T, Chonabayashi K, Nishikawa M, Takei I,
940 Oishi A, Narita M *et al* (2016) Enhanced engraftment, proliferation, and therapeutic potential in
941 heart using optimized human iPSC-derived cardiomyocytes. *Sci Rep* 6: 19111

942 Fusaki N, Ban H, Nishiyama A, Saeki K, Hasegawa M (2009) Efficient induction of transgene-
943 free human pluripotent stem cells using a vector based on Sendai virus, an RNA virus that does
944 not integrate into the host genome. *Proc Jpn Acad Ser B Phys Biol Sci* 85: 348-362
945 Giacoman-Lozano M, Melendez-Ramirez C, Martinez-Ledesma E, Cuevas-Diaz Duran R,
946 Velasco I (2022) Epigenetics of neural differentiation: Spotlight on enhancers. *Front Cell Dev*
947 *Biol* 10: 1001701
948 Gschwendt M, Dieterich S, Rennecke J, Kittstein W, Mueller HJ, Johannes FJ (1996) Inhibition
949 of protein kinase C mu by various inhibitors. Differentiation from protein kinase c isoenzymes.
950 *FEBS Lett* 392: 77-80
951 Guo G, von Meyenn F, Rostovskaya M, Clarke J, Dietmann S, Baker D, Sahakyan A, Myers S,
952 Bertone P, Reik W *et al* (2017) Epigenetic resetting of human pluripotency. *Development* 144:
953 2748-2763
954 Hackett JA, Surani MA (2014) Regulatory principles of pluripotency: from the ground state up.
955 *Cell Stem Cell* 15: 416-430
956 Hayashi Y, Furue MK (2016) Biological Effects of Culture Substrates on Human Pluripotent
957 Stem Cells. *Stem Cells Int* 2016: 5380560
958 Hayashi Y, Furue MK, Okamoto T, Ohnuma K, Myoishi Y, Fukuhara Y, Abe T, Sato JD, Hata R,
959 Asashima M (2007) Integrins regulate mouse embryonic stem cell self-renewal. *Stem Cells* 25:
960 3005-3015
961 Hayashi Y, Hsiao EC, Sami S, Lancero M, Schlieve CR, Nguyen T, Yano K, Nagahashi A, Ikeya
962 M, Matsumoto Y *et al* (2016) BMP-SMAD-ID promotes reprogramming to pluripotency by
963 inhibiting p16/INK4A-dependent senescence. *Proc Natl Acad Sci U S A* 113: 13057-13062
964 Horiguchi I, Sakai Y (2016) Serum replacement with albumin-associated lipids prevents excess
965 aggregation and enhances growth of induced pluripotent stem cells in suspension culture.
966 *Biotechnol Prog* 32: 1009-1016
967 Hunt MM, Meng G, Rancourt DE, Gates ID, Kallos MS (2014) Factorial experimental design for
968 the culture of human embryonic stem cells as aggregates in stirred suspension bioreactors reveals
969 the potential for interaction effects between bioprocess parameters. *Tissue Eng Part C Methods*
970 20: 76-89
971 Ibuki M, Horiguchi I, Sakai Y (2019) A novel tool for suspension culture of human induced
972 pluripotent stem cells: Lysophospholipids as a cell aggregation regulator. *Regen Ther* 12: 74-82
973 Imaizumi K, Okano H (2021) Modeling neurodevelopment in a dish with pluripotent stem cells.
974 *Dev Growth Differ* 63: 18-25
975 Jiang W, Zhang D, Bursac N, Zhang Y (2013) WNT3 is a biomarker capable of predicting the
976 definitive endoderm differentiation potential of hESCs. *Stem Cell Reports* 1: 46-52
977 Jirousek MR, Gillig JR, Gonzalez CM, Heath WF, McDonald JH, 3rd, Neel DA, Rito CJ, Singh
978 U, Stramm LE, Melikian-Badalian A *et al* (1996) (S)-13-[(dimethylamino)methyl]-10,11,14,15-
979 tetrahydro-4,9:16, 21-dimetheno-1H, 13H-dibenzo[e,k]pyrrolo[3,4-
980 h][1,4,13]oxadiazacyclohexadecene-1,3(2H)-d ione (LY333531) and related analogues: isozyme
981 selective inhibitors of protein kinase C beta. *J Med Chem* 39: 2664-2671
982 Kehoe DE, Jing D, Lock LT, Tzanakakis ES (2010) Scalable stirred-suspension bioreactor culture
983 of human pluripotent stem cells. *Tissue Eng Part A* 16: 405-421
984 Khan SA, Park KM, Fischer LA, Dong C, Lungjangwa T, Jimenez M, Casalena D, Chew B,
985 Dietmann S, Auld DS *et al* (2021) Probing the signaling requirements for naive human
986 pluripotency by high-throughput chemical screening. *Cell Rep* 35: 109233
987 Kim MH, Kino-Oka M (2020) Bioengineering Considerations for a Nurturing Way to Enhance
988 Scalable Expansion of Human Pluripotent Stem Cells. *Biotechnol J* 15: e1900314

989 Kim MH, Takeuchi K, Kino-Oka M (2019) Role of cell-secreted extracellular matrix formation in
990 aggregate formation and stability of human induced pluripotent stem cells in suspension culture. *J*
991 *Biosci Bioeng* 127: 372-380
992 Kinehara M, Kawamura S, Tateyama D, Suga M, Matsumura H, Mimura S, Hirayama N, Hirata
993 M, Uchio-Yamada K, Kohara A *et al* (2013) Protein kinase C regulates human pluripotent stem
994 cell self-renewal. *PLoS One* 8: e54122
995 Kitano Y, Nishimura S, Kato TM, Ueda A, Takigawa K, Umekage M, Nomura M, Kawakami A,
996 Ogawa H, Xu H *et al* (2022) Generation of hypoimmunogenic induced pluripotent stem cells by
997 CRISPR-Cas9 system and detailed evaluation for clinical application. *Mol Ther Methods Clin*
998 *Dev* 26: 15-25
999 Konze SA, van Diepen L, Schroder A, Olmer R, Moller H, Pich A, Weissmann R, Kuss AW,
1000 Zweigerdt R, Buettner FF (2014) Cleavage of E-cadherin and beta-catenin by calpain affects Wnt
1001 signaling and spheroid formation in suspension cultures of human pluripotent stem cells. *Mol Cell*
1002 *Proteomics* 13: 990-1007
1003 Krawetz R, Taiani JT, Liu S, Meng G, Li X, Kallos MS, Rancourt DE (2010) Large-scale
1004 expansion of pluripotent human embryonic stem cells in stirred-suspension bioreactors. *Tissue*
1005 *Eng Part C Methods* 16: 573-582
1006 Kropp C, Kempf H, Halloin C, Robles-Diaz D, Franke A, Scheper T, Kinast K, Knorpp T, Joos
1007 TO, Haverich A *et al* (2016) Impact of Feeding Strategies on the Scalable Expansion of Human
1008 Pluripotent Stem Cells in Single-Use Stirred Tank Bioreactors. *Stem Cells Transl Med* 5: 1289-
1009 1301
1010 Kwok CK, Ueda Y, Kadari A, Gunther K, Ergun S, Heron A, Schnitzler AC, Rook M, Edenhofer
1011 F (2018) Scalable stirred suspension culture for the generation of billions of human induced
1012 pluripotent stem cells using single-use bioreactors. *J Tissue Eng Regen Med* 12: e1076-e1087
1013 Lam AT, Chen AK, Ting SQ, Reuveny S, Oh SK (2016) Integrated processes for expansion and
1014 differentiation of human pluripotent stem cells in suspended microcarriers cultures. *Biochem*
1015 *Biophys Res Commun* 473: 764-768
1016 Li L, Bennett SA, Wang L (2012) Role of E-cadherin and other cell adhesion molecules in
1017 survival and differentiation of human pluripotent stem cells. *Cell Adh Migr* 6: 59-70
1018 Li M, Belmonte JC (2017) Ground rules of the pluripotency gene regulatory network. *Nat Rev*
1019 *Genet* 18: 180-191
1020 Lipsitz YY, Woodford C, Yin T, Hanna JH, Zandstra PW (2018) Modulating cell state to enhance
1021 suspension expansion of human pluripotent stem cells. *Proc Natl Acad Sci U S A* 115: 6369-6374
1022 Matsumoto T, Kim MH, Kino-Oka M (2022) Effect of Rho-Associated Kinase Inhibitor on
1023 Growth Behaviors of Human Induced Pluripotent Stem Cells in Suspension Culture.
1024 *Bioengineering (Basel)* 9
1025 Nagaoka M, Si-Tayeb K, Akaike T, Duncan SA (2010) Culture of human pluripotent stem cells
1026 using completely defined conditions on a recombinant E-cadherin substratum. *BMC Dev Biol* 10:
1027 60
1028 Nakanishi M, Kurisaki A, Hayashi Y, Warashina M, Ishiura S, Kusuda-Furue M, Asashima M
1029 (2009) Directed induction of anterior and posterior primitive streak by Wnt from embryonic stem
1030 cells cultured in a chemically defined serum-free medium. *FASEB J* 23: 114-122
1031 Nath SC, Nagamori E, Horie M, Kino-Oka M (2017) Culture medium refinement by dialysis for
1032 the expansion of human induced pluripotent stem cells in suspension culture. *Bioprocess Biosyst*
1033 *Eng* 40: 123-131
1034 Nishimura K, Sano M, Ohtaka M, Furuta B, Umemura Y, Nakajima Y, Ikehara Y, Kobayashi T,
1035 Segawa H, Takayasu S *et al* (2011) Development of defective and persistent Sendai virus vector:
1036 a unique gene delivery/expression system ideal for cell reprogramming. *J Biol Chem* 286: 4760-
1037 4771

1038 Oh SK, Chen AK, Mok Y, Chen X, Lim UM, Chin A, Choo AB, Reuveny S (2009) Long-term
1039 microcarrier suspension cultures of human embryonic stem cells. *Stem Cell Res* 2: 219-230
1040 Ohgushi M, Matsumura M, Eiraku M, Murakami K, Aramaki T, Nishiyama A, Muguruma K,
1041 Nakano T, Suga H, Ueno M *et al* (2010) Molecular pathway and cell state responsible for
1042 dissociation-induced apoptosis in human pluripotent stem cells. *Cell Stem Cell* 7: 225-239
1043 Okita K, Matsumura Y, Sato Y, Okada A, Morizane A, Okamoto S, Hong H, Nakagawa M,
1044 Tanabe K, Tezuka K *et al* (2011) A more efficient method to generate integration-free human iPS
1045 cells. *Nat Methods* 8: 409-U452
1046 Olmer R, Lange A, Selzer S, Kasper C, Haverich A, Martin U, Zweigerdt R (2012) Suspension
1047 culture of human pluripotent stem cells in controlled, stirred bioreactors. *Tissue Eng Part C*
1048 *Methods* 18: 772-784
1049 Omura S, Iwai Y, Hirano A, Nakagawa A, Awaya J, Tsuchya H, Takahashi Y, Masuma R (1977)
1050 A new alkaloid AM-2282 OF Streptomyces origin. Taxonomy, fermentation, isolation and
1051 preliminary characterization. *J Antibiot (Tokyo)* 30: 275-282
1052 Otte AP, Koster CH, Snoek GT, Durston AJ (1988) Protein kinase C mediates neural induction in
1053 Xenopus laevis. *Nature* 334: 618-620
1054 Otte AP, van Run P, Heideveld M, van Driel R, Durston AJ (1989) Neural induction is mediated
1055 by cross-talk between the protein kinase C and cyclic AMP pathways. *Cell* 58: 641-648
1056 Rajendran G, Dutta D, Hong J, Paul A, Saha B, Mahato B, Ray S, Home P, Ganguly A, Weiss
1057 ML *et al* (2013) Inhibition of protein kinase C signaling maintains rat embryonic stem cell
1058 pluripotency. *J Biol Chem* 288: 24351-24362
1059 Range RC, Angerer RC, Angerer LM (2013) Integration of canonical and noncanonical Wnt
1060 signaling pathways patterns the neuroectoderm along the anterior-posterior axis of sea urchin
1061 embryos. *PLoS Biol* 11: e1001467
1062 Ring DB, Johnson KW, Henriksen EJ, Nuss JM, Goff D, Kinnick TR, Ma ST, Reeder JW,
1063 Samuels I, Slabiak T *et al* (2003) Selective glycogen synthase kinase 3 inhibitors potentiate
1064 insulin activation of glucose transport and utilization in vitro and in vivo. *Diabetes* 52: 588-595
1065 Rohani L, Borys BS, Razian G, Naghsh P, Liu S, Johnson AA, Machiraju P, Holland H, Lewis
1066 IA, Groves RA *et al* (2020) Stirred suspension bioreactors maintain naive pluripotency of human
1067 pluripotent stem cells. *Commun Biol* 3: 492
1068 Sasai N, Kadoya M, Ong Lee Chen A (2021) Neural induction: Historical views and application
1069 to pluripotent stem cells. *Dev Growth Differ* 63: 26-37
1070 Shafa M, Sjonnesen K, Yamashita A, Liu S, Michalak M, Kallos MS, Rancourt DE (2012)
1071 Expansion and long-term maintenance of induced pluripotent stem cells in stirred suspension
1072 bioreactors. *J Tissue Eng Regen Med* 6: 462-472
1073 Sheng G (2015) Epiblast morphogenesis before gastrulation. *Dev Biol* 401: 17-24
1074 Shimizu T, Matsuo-Takasaki M, Luijkx D, Takami M, Arai Y, Noguchi M, Nakamura Y, Hayata
1075 T, Saito MK, Hayashi Y (2022) Generation of human induced pluripotent stem cell lines derived
1076 from four DiGeorge syndrome patients with 22q11.2 deletion. *Stem Cell Res* 61: 102744
1077 Si-Tayeb K, Noto FK, Nagaoka M, Li J, Battle MA, Duris C, North PE, Dalton S, Duncan SA
1078 (2010) Highly efficient generation of human hepatocyte-like cells from induced pluripotent stem
1079 cells. *Hepatology* 51: 297-305
1080 Singh H, Mok P, Balakrishnan T, Rahmat SN, Zweigerdt R (2010) Up-scaling single cell-
1081 inoculated suspension culture of human embryonic stem cells. *Stem Cell Res* 4: 165-179
1082 Steiner D, Khaner H, Cohen M, Even-Ram S, Gil Y, Itsykson P, Turetsky T, Idelson M,
1083 Aizenman E, Ram R *et al* (2010) Derivation, propagation and controlled differentiation of human
1084 embryonic stem cells in suspension. *Nat Biotechnol* 28: 361-364
1085 Stern CD (2024) The organizer and neural induction in birds and mammals. *Curr Top Dev Biol*
1086 157: 43-65

1087 Stumpo DJ, Bock CB, Tuttle JS, Blackshear PJ (1995) MARCKS deficiency in mice leads to
1088 abnormal brain development and perinatal death. *Proc Natl Acad Sci U S A* 92: 944-948
1089 Sumi T, Tsuneyoshi N, Nakatsuji N, Suemori H (2008) Defining early lineage specification of
1090 human embryonic stem cells by the orchestrated balance of canonical Wnt/beta-catenin,
1091 Activin/Nodal and BMP signaling. *Development* 135: 2969-2979
1092 Takahashi K, Tanabe K, Ohnuki M, Narita M, Ichisaka T, Tomoda K, Yamanaka S (2007)
1093 Induction of pluripotent stem cells from adult human fibroblasts by defined factors. *Cell* 131:
1094 861-872
1095 Takahashi K, Yamanaka S (2016) A decade of transcription factor-mediated reprogramming to
1096 pluripotency. *Nat Rev Mol Cell Biol* 17: 183-193
1097 Takashima Y, Guo G, Loos R, Nichols J, Ficz G, Krueger F, Oxley D, Santos F, Clarke J,
1098 Mansfield W *et al* (2014) Resetting transcription factor control circuitry toward ground-state
1099 pluripotency in human. *Cell* 158: 1254-1269
1100 Tannenbaum SE, Reubinoff BE (2022) Advances in hPSC expansion towards therapeutic entities:
1101 A review. *Cell Prolif*: e13247
1102 Tesar PJ, Chenoweth JG, Brook FA, Davies TJ, Evans EP, Mack DL, Gardner RL, McKay RD
1103 (2007) New cell lines from mouse epiblast share defining features with human embryonic stem
1104 cells. *Nature* 448: 196-199
1105 Toullec D, Pianetti P, Coste H, Bellevergue P, Grand-Perret T, Ajakane M, Baudet V, Boissin P,
1106 Boursier E, Loriolle F *et al* (1991) The bisindolylmaleimide GF 109203X is a potent and
1107 selective inhibitor of protein kinase C. *J Biol Chem* 266: 15771-15781
1108 Tran TH, Wang X, Browne C, Zhang Y, Schinke M, Izumo S, Burcin M (2009) Wnt3a-induced
1109 mesoderm formation and cardiomyogenesis in human embryonic stem cells. *Stem Cells* 27: 1869-
1110 1878
1111 Tsukamoto S, Nakade K, Wakabayashi T, Nakashima K, Takami M, Hemmi Y, Kuramochi Y,
1112 Shimizu T, Arai Y, Matsuo-Takasaki M *et al* (2021) Generation of two ISL1-tdTomato reporter
1113 human induced pluripotent stem cell lines using CRISPR-Cas9 genome editing. *Stem Cell Res* 53:
1114 102363
1115 Vijayaragavan K, Szabo E, Bosse M, Ramos-Mejia V, Moon RT, Bhatia M (2009) Noncanonical
1116 Wnt signaling orchestrates early developmental events toward hematopoietic cell fate from
1117 human embryonic stem cells. *Cell Stem Cell* 4: 248-262
1118 Wang Y, Chou BK, Dowey S, He C, Gerecht S, Cheng L (2013) Scalable expansion of human
1119 induced pluripotent stem cells in the defined xeno-free E8 medium under adherent and
1120 suspension culture conditions. *Stem Cell Res* 11: 1103-1116
1121 Woll PS, Morris JK, Painschab MS, Marcus RK, Kohn AD, Biechele TL, Moon RT, Kaufman
1122 DS (2008) Wnt signaling promotes hematoendothelial cell development from human embryonic
1123 stem cells. *Blood* 111: 122-131
1124 Wong RC, Dottori M, Koh KL, Nguyen LT, Pera MF, Pebay A (2006) Gap junctions modulate
1125 apoptosis and colony growth of human embryonic stem cells maintained in a serum-free system.
1126 *Biochem Biophys Res Commun* 344: 181-188
1127 Wong RC, Pebay A, Nguyen LT, Koh KL, Pera MF (2004) Presence of functional gap junctions
1128 in human embryonic stem cells. *Stem Cells* 22: 883-889
1129 Xu C, Inokuma MS, Denham J, Golds K, Kundu P, Gold JD, Carpenter MK (2001) Feeder-free
1130 growth of undifferentiated human embryonic stem cells. *Nat Biotechnol* 19: 971-974
1131 Yagi M, Yamanaka S, Yamada Y (2017) Epigenetic foundations of pluripotent stem cells that
1132 recapitulate in vivo pluripotency. *Lab Invest* 97: 1133-1141
1133 Yu J, Vodyanik MA, Smuga-Otto K, Antosiewicz-Bourget J, Frane JL, Tian S, Nie J, Jonsdottir
1134 GA, Ruotti V, Stewart R *et al* (2007) Induced pluripotent stem cell lines derived from human
1135 somatic cells. *Science* 318: 1917-1920

1136 Zweigerdt R, Olmer R, Singh H, Haverich A, Martin U (2011) Scalable expansion of human
1137 pluripotent stem cells in suspension culture. *Nat Protoc* 6: 689-700

1138

1139 **Figures and Tables**

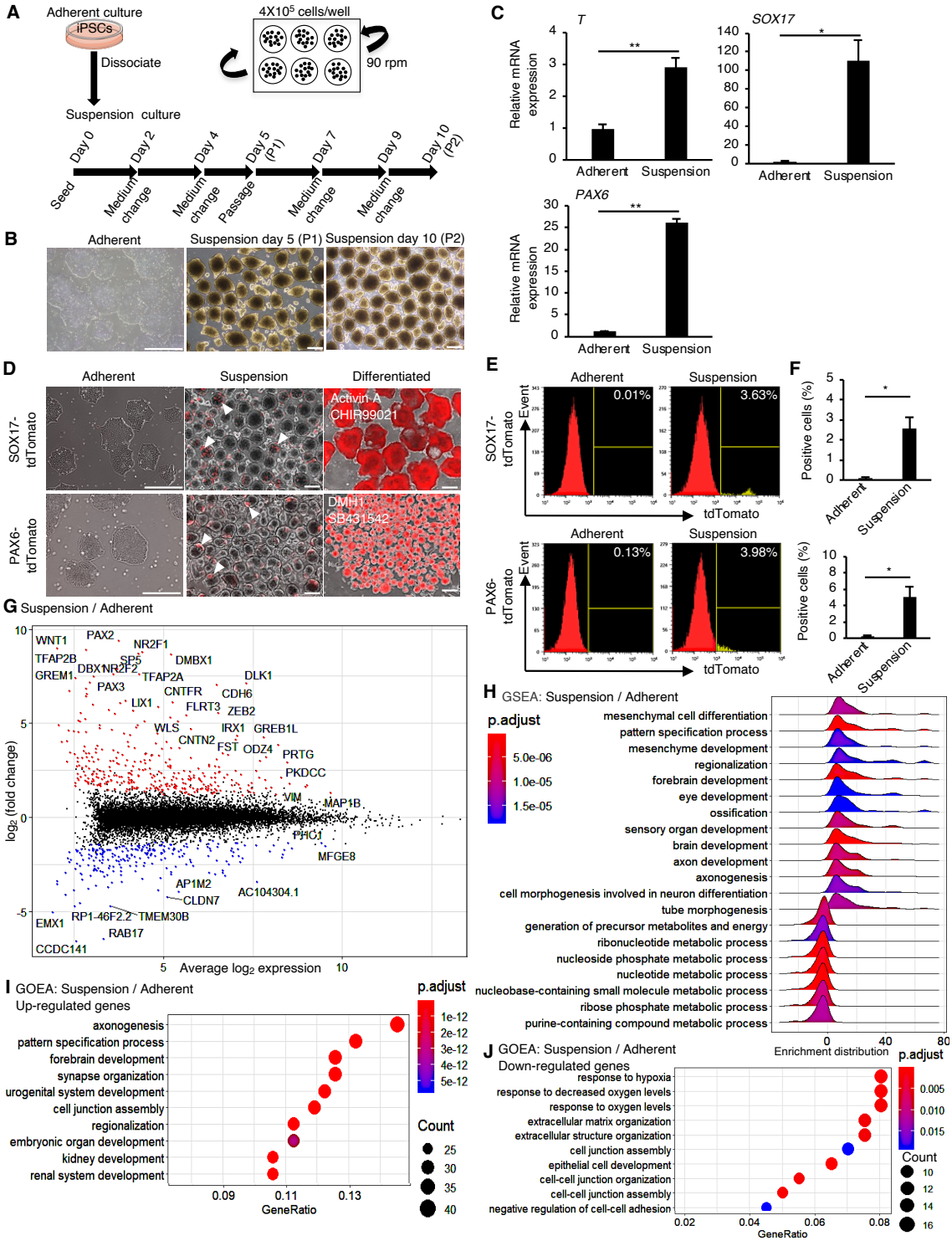

1140 **Figure 1. HiPSCs maintained under suspension-culture conditions undergo spontaneous**
1141 **differentiation.** (A) Schematics representing hiPSCs in suspension-culture conditions. (B) Phase-

1142 contrast images of adherent- or suspension-cultured hiPSCs on day 5 (Passage 1 (P1)) and day 10
1143 (Passage 2 (P2)). Scale bars: 400 µm. (C) Gene expression in hiPSCs cultured under adherent or
1144 suspension conditions on P2. Bar graphs show the mean ± SE (n=3). P-values were statistically
1145 analyzed by Student's t-test. (D) Phase-contrast and fluorescent images of adherent or suspension-
1146 cultured reporter hiPSCs on P2. White arrowheads indicate spontaneous expression of SOX17
1147 and PAX6 in suspension conditions. Scale bars: 400 µm. (E) Quantification of hiPSCs
1148 spontaneous differentiation with flow cytometry. (F) Averaged tdTomato-positive cell ratio (%)
1149 from flow cytometry data (mean ± SE from n=3). P-values were statistically analyzed by
1150 Student's t-test. (G) An MA plot comparing transcriptomes between suspension- and adherent-
1151 culture from RNA-seq data. The representative gene name is shown in the plot. (H) GSEA on the
1152 gene sets of suspension-cultured hiPSCs to adherent cultures. Adjusted P-values are shown as
1153 blue to red from low to high values. (I and J) GOEA on the gene sets of suspension-cultured
1154 hiPSCs to adherent culture. Results are ranked by significance (p-adjusted value) and/or counted
1155 gene numbers.

1156

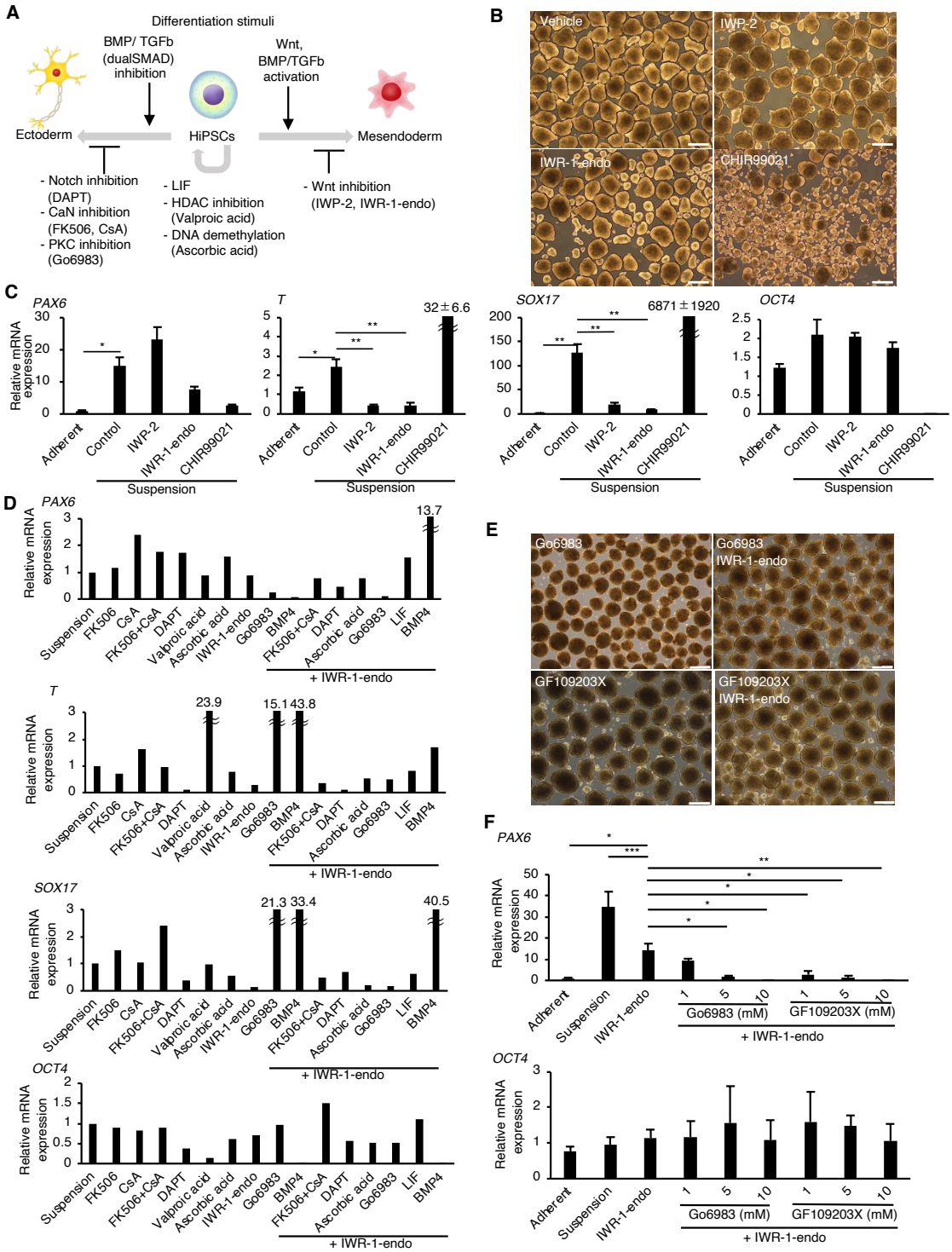

Figure 2. PKC inhibitors suppress spontaneous differentiation of hiPSCs into neural ectoderm in suspension-culture conditions. (A) Schematics. (B) Phase-contrast pictures of suspension-cultured hiPSCs in the presence of Wnt signaling inhibitors (IWP-2 and IWR-1-endo) or activator (CHIR99021). Scale bars: 400 μm. (C) Gene expression of hiPSCs in suspension-

1161 culture conditions with or without IWP2, IWR-1-endo or CHIR99021. RT-qPCR was performed
1162 on day 10 samples (P2). Gene expressions were normalized to GAPDH and displayed as relative
1163 fold increase to adherent-cultured samples. Bar graphs show the mean ± SE. P-values were
1164 statistically analyzed using Dunnett's multiple comparisons test. (D) Screening of inhibitory
1165 activity of candidate molecules on neuroectoderm differentiation in suspension-cultured hiPSCs.
1166 Candidate molecules were added in combination as shown. Results are displayed as relative fold
1167 increase to suspension-cultured samples without pharmacological treatment. n=1. (E) Phase-
1168 contrast images of suspension-cultured hiPSCs on P2 in the presence of PKC inhibitors (Gö6983
1169 or GF109203X) alone, or in combination with IWR-1-endo. Scale bars: 400 µm. (F) Suspension-
1170 cultured hiPSCs gene expression in the presence of IWR-1-endo or with combined IWR-1-endo
1171 and different doses of PKC inhibitors. Results are displayed as relative fold increase to adherent-
1172 culture. Data are presented as mean ± SE (n=3).
1173

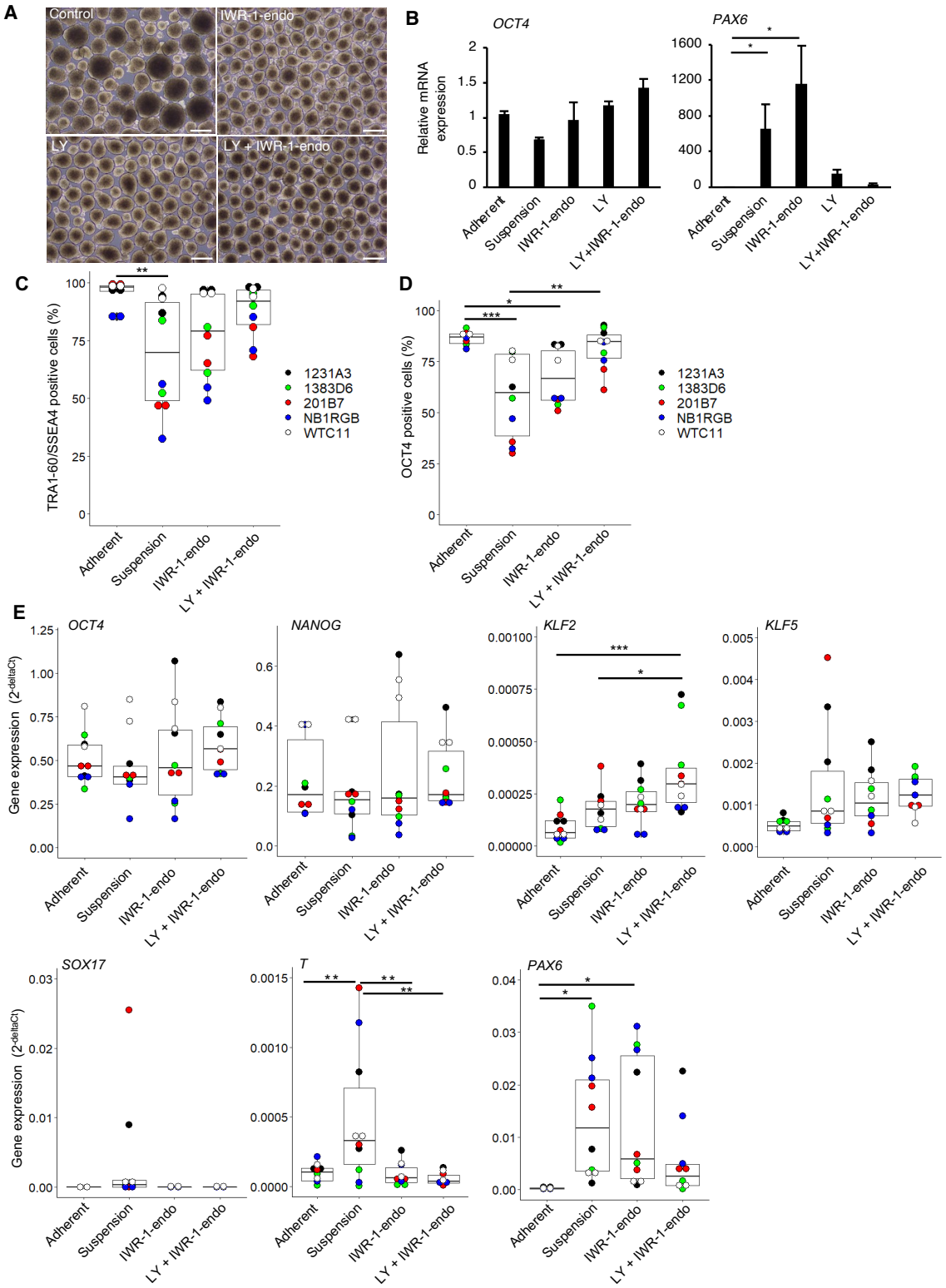

1174 **Figure 3. The inhibitors of WNT and PKCβ efficiently maintain the self-renewal of hiPSCs**
1175 **in suspension conditions.** (A) Phase-contrast images of suspension-cultured hiPSCs on day 10 (2

1176 passages) in the presence of IWR-1-endo, LY333531, or both. Scale bars: 400 µm. (B) Gene
1177 expression of suspension-cultured hiPSCs on P2 in the presence of IWR-1-endo, LY333531, or
1178 both. Data are presented as mean ± SE. P-values were statistically analyzed with Dunnett's test.
1179 (C) After suspension culture of 5 hiPSC lines for 10 days (2 passages), WTC11, 1231A3, HiPS-
1180 NB1RGB (NB1RGB), 1383D6 and 201B7, in StemFit AK02N medium with or without IWR-1-
1181 endo and LY333531, characteristic analysis was performed. Box plots of flow cytometry for
1182 TRA-1-60 and SSEA4 double positive cells (%) are shown. Used cell lines are indicated by the
1183 different colored circles shown on the right side of the graph (n=2 x 5 cell lines). (D) Box plots of
1184 OCT4 positive cells (%) are shown (n=2 x 5 cell lines) (E) Box plots of RT-qPCR data are
1185 shown. Differentiation markers (*SOX17*, *T*, *PAX6*), undifferentiated markers (*OCT4, NANOG*),
1186 and naïve markers (*KLF2*, *KLF5*) were assessed. Statistical analysis was performed using by one-
1187 way Anova and Tukey's test for all graphs. P values < 0.05 were considered statistically
1188 significant. *, ** or *** in the graphs indicate P<0.05, P<0.01 or P<0.001, respectively (n=2 x 5
1189 cell lines).
1190

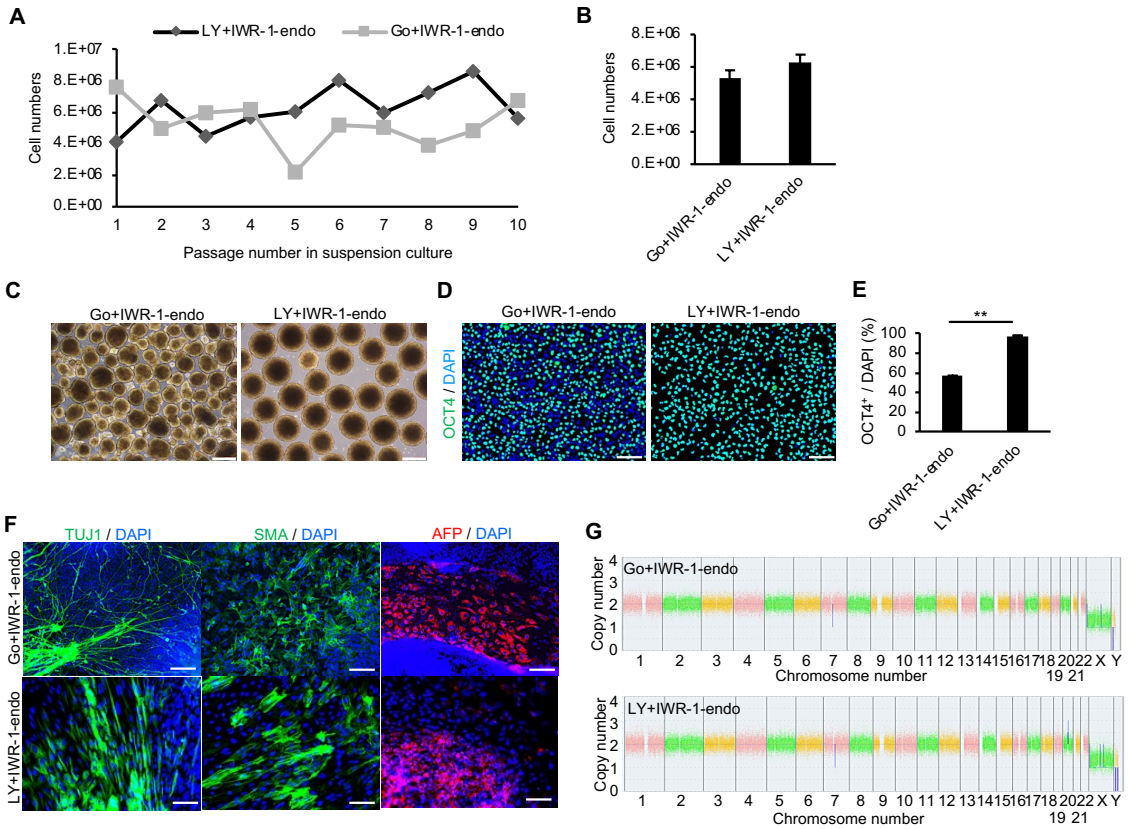

Figure 4. Long-term suspension culture of hiPSCs is maintained by simultaneous suppression of PKCβ and Wnt signals. (A) The number of hiPSCs at passage during long-term suspension-culture every 5 days. Cell culture was performed in the presence of IWR-1-endo plus Gö6983 or LY333531. (B) Bar graph indicating average cell numbers for 10 passages (mean ± SE). (C) Phase-contrast images of suspension-cultured hiPSCs on passage 10. Scale bars: 400 µm. (D) Immunocytochemistry of OCT4 on passage 10 samples. Scale bars: 100 µm. (E) Bar graph showing the percentages of OCT4 positive cells. Values were calculated from randomly selected three regions from immunofluorescence images. Data are presented as mean ± SE. P-value was statistically analyzed by Student's t-test. (F) Immunocytochemistry of differentiated cells in EBs from suspension-cultured hiPSCs in the presence of IWR-1-endo; and Gö6983 or LY333531. Anti-TUJ1, -SMA and -AFP antibodies were used to detect ectoderm, mesoderm and endoderm differentiation, respectively. Scale bars:100 µm. (G) Chromosomal copy numbers detected with CNV array analysis (Karyostat assay) of suspension-cultured hiPSCs in the presence of IWR-1-endo; and Gö6983 (Upper panel) or LY333531 (Lower panel) at passage 10.

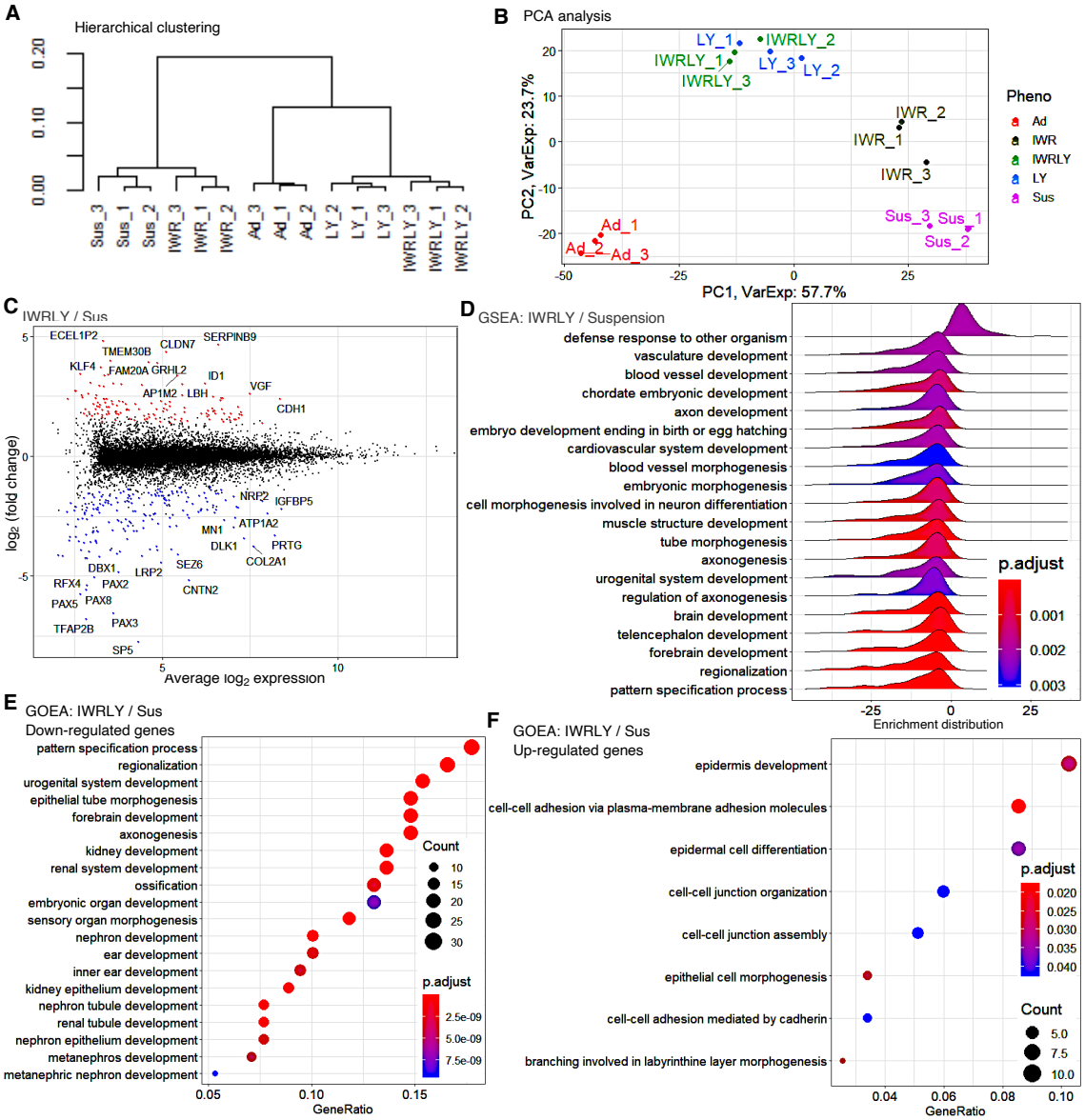

Figure 5. The inhibitors of WNT and PKCβ in suspension conditions efficiently suppress differentiated gene marker expression in transcriptome analysis. (A) Hierarchical clustering of adherent and suspension-cultured hiPSCs on P2 using Ward's method from RNA-seq data (n=3 in each condition). Ad, Adherent; Sus, Suspension; IWR, IWR-1-endo; LY, LY333531; IWRLY, IWR-1-endo and LY333531. (B) Principal component analysis (PCA) plot showing clusters of samples based on similarity. Gene expression variance are displayed as PC1 and PC2. (C) MA plot comparing transcriptomes between IWRLY and Sus. (D) GSEA on the gene sets of IWRLY to Sus from these RNA-seq data. Statistically significant enrichment is shown. P-values are represented in blue to red from low to high values. (E and F) GOEA for the gene sets of IWRLY

1215 to Sus from these RNA-seq data. Analysis was performed on down-regulated genes in (E) and up-
1216 regulated genes in (F).
1217

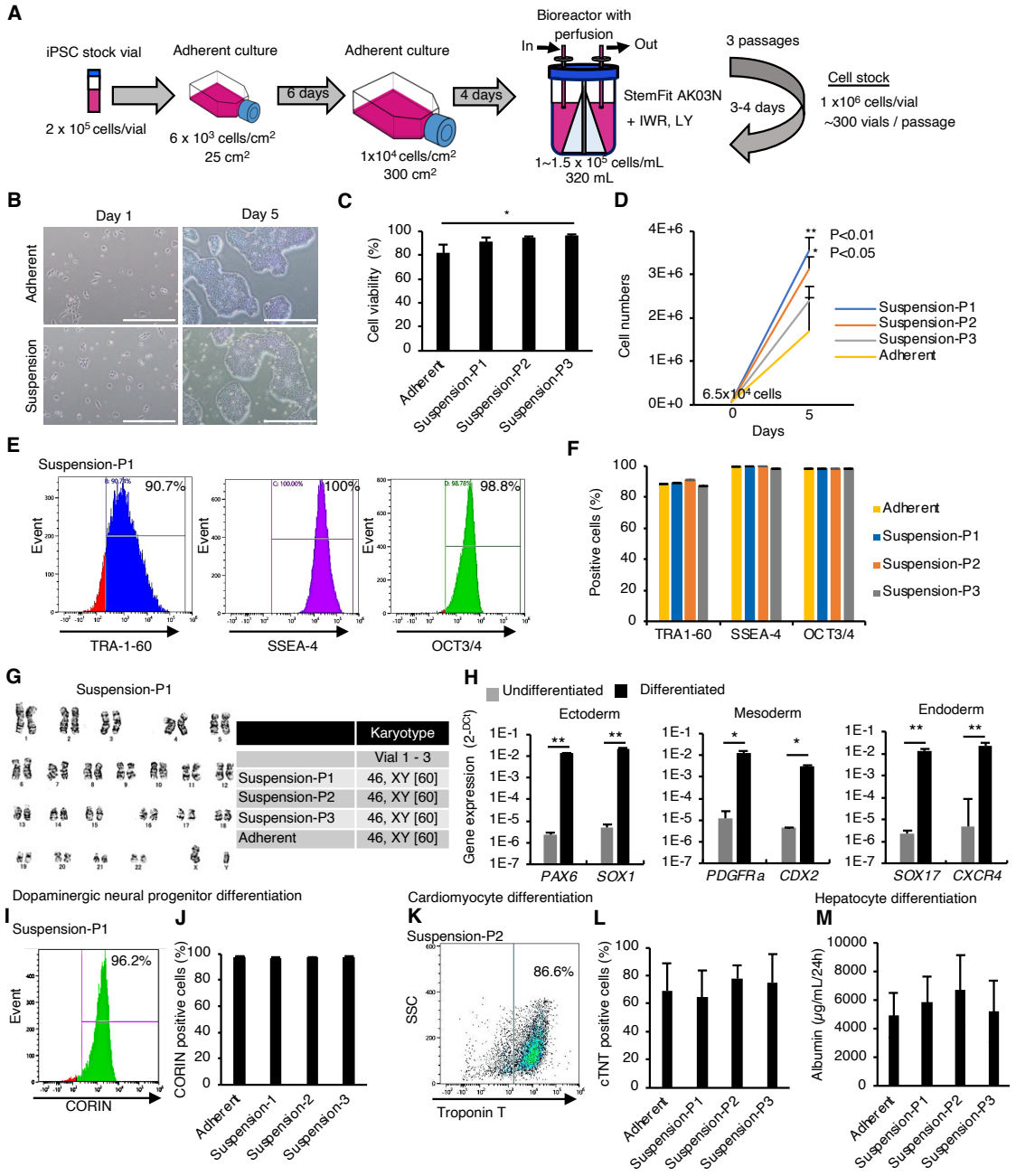

Figure 6. Mass suspension-culture of clinical-grade hiPSCs in the presence of PKCβ and Wnt signaling inhibitors. (A) Schematics. (B) Representative phase-contrast images of these hiPSCs. Scale bar: 1 mm. (C) Cell viability at seeding. Data are presented as mean ± SE (n=3). P-values were statistically analyzed with Dunnett's multiple comparisons test. (D) Total cell numbers were counted on day 5 after thawing. Data were presented as mean ± SE (n=3). P-values were statistically analyzed with Dunnett's test. (E) Representative flow cytometry data of pluripotent markers in these hiPSCs. (F) Quantification of flow cytometry data for the pluripotent

1225 markers. Data are presented as mean ± SE (n=3). (G) Karyotypes of these hiPSCs. Left:
1226 Representative pictures of G-band analysis. Right: Table of karyotype results (n=3). The numbers
1227 in brackets indicate the cell numbers examined. (H) *In vitro* differentiation from hiPSCs was
1228 assessed using RT-qPCR (mean ± SE) (n=3). P-value was statistically analyzed by Student's t-
1229 test. (I) Representative flow cytometry data for CORIN. (J) Quantification of CORIN-positive
1230 cells (mean ± SE, n=3). (K) Representative flow cytometry data for cardiac Troponin T (cTnT).
1231 (L) Quantification of cTnT-positive cells (mean ± SE, n=3). (M) Albumin secretion levels of
1232 hepatocytes differentiated from hiPSCs (mean ± SE, n=3).
1233

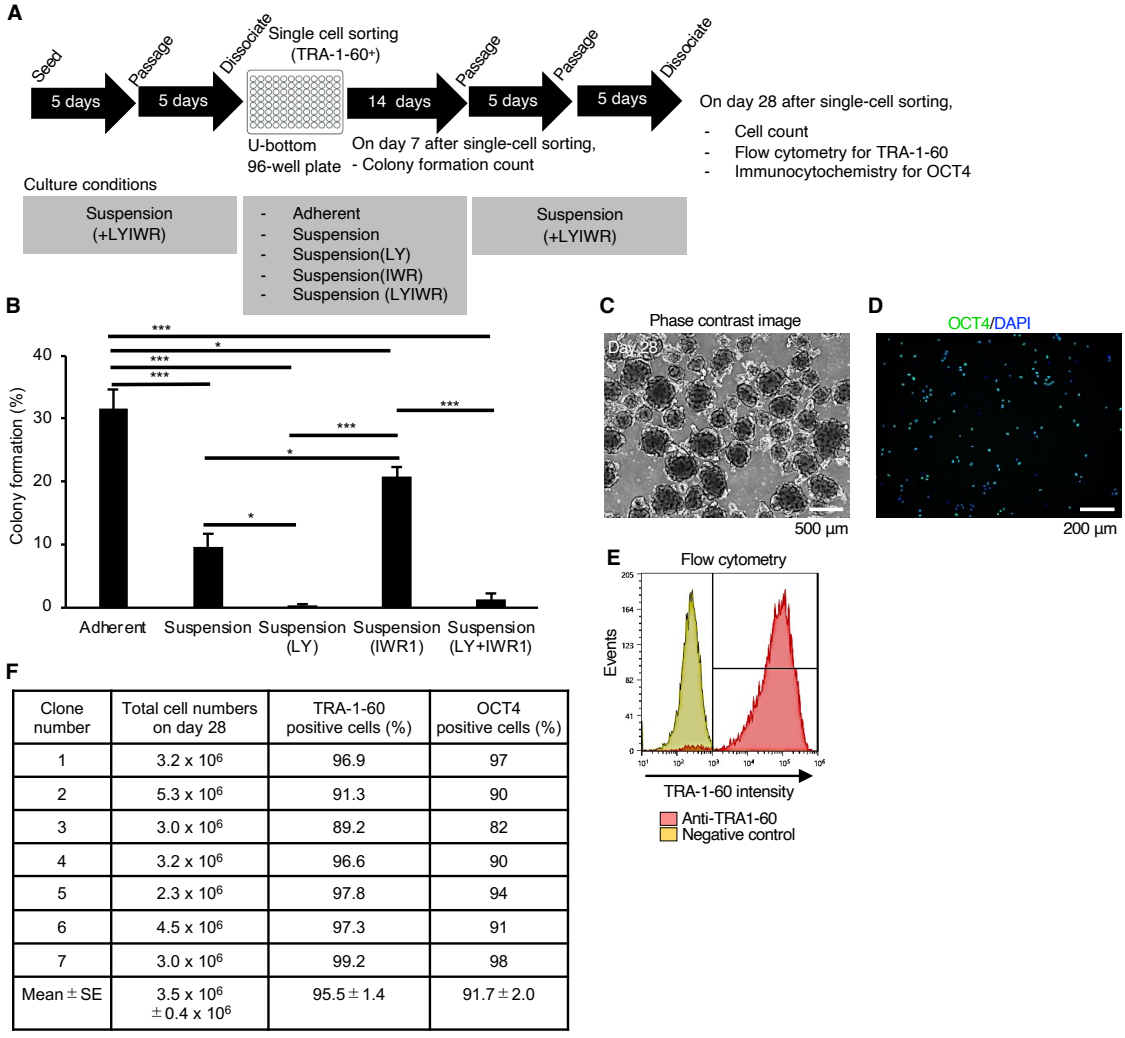

Clone number	Total cell numbers on day 28	TRA-1-60 positive cells (%)	OCT4 positive cells (%)
1	3.2 x 10^6	96.9	97
2	5.3 x 10^6	91.3	90
3	3.0 x 10^6	89.2	82
4	3.2 x 10^6	96.6	90
5	2.3 x 10^6	97.8	94
6	4.5 x 10^6	97.3	91
7	3.0 x 10^6	99.2	98
Mean ± SE	3.5 x 10^6 ± 0.4 x 10^6	95.5 ± 1.4	91.7 ± 2.0

Figure 7. Establishment of single-cell-sorted hiPSC subclones cultured in suspension conditions supplemented with IWR1-endo and LY3333531. (A) Schematics representing the establishment of single-cell-derived hiPSC subclones from 201B7 line. Single-cell-sorted cells were expanded in the culture medium supplemented with IWR-1-endo and LY333531. Formed colonies were picked on day 14, and expanded by repeating passage every 4-5 days under suspension conditions. Characteristic analysis was performed on day 28 after single-cell sorting. (B) On day 7 after single-cell sorting, formed colonies were counted per well in the 96-well plate. The ratio (%) of the colony formation is shown in a bar graph (mean ± SE) (n=3). Statistical analysis was performed using by one-way ANOVA and Tukey's tests for all graphs. P values < 0.05 were considered statistically significant. *, ** or *** in the graphs indicate P<0.05, P<0.01 or P<0.001, respectively. (C) Phase-contrast images of Clone #2 on day 28 after single-cell sorting. Scale bars: 500 µm. (D) Represented flow cytometry of TRA-1-60 (Clone #2). (E) Represented immunocytochemistry of OCT4 (Clone #2). Scale bars: 200 µm. (F) Summary table of the characterization of single cell-sorted clones. Total cell numbers on day 28, the ratio of

1248 TRA-1-60-positive cells (%), and the ratio of OCT4-positive cells (%) are shown (mean ± SE)
1249 (n=7).

1250

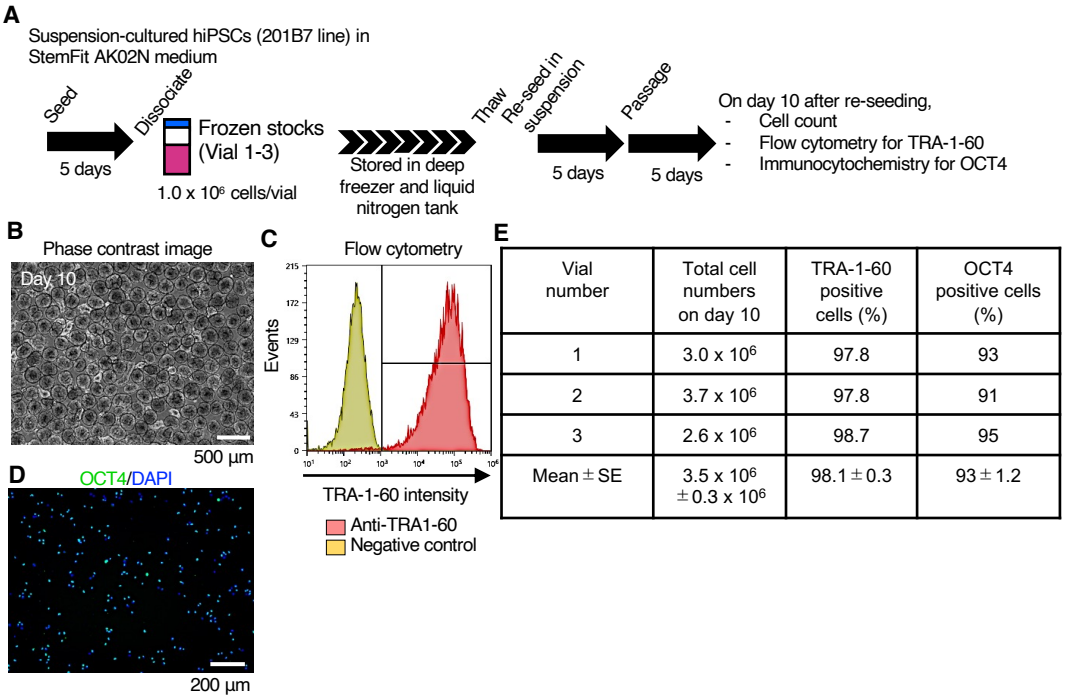

Vial number	Total cell numbers on day 10	TRA-1-60 positive cells (%)	OCT4 positive cells (%)
1	3.0×10^6	97.8	93
2	3.7×10^6	97.8	91
3	2.6×10^6	98.7	95
Mean ± SE	$3.5 \times 10^6 \pm 0.3 \times 10^6$	98.1 ± 0.3	93 ± 1.2

Figure 8. Re-suspension from frozen stocks of hiPSCs under suspension culture conditions supplemented with IWR-1-endo and LY333531. (A) Schematics of re-suspension culture of frozen stocks of single-cells-derived 201B7 clone (Vial 1-3). (B) Represented phase-contrast images on day 10 (Vial 3). Scale bars: 500 µm. (C) Represented flow cytometry of TRA-1-60 (Vial 3). (D) Represented immunocytochemistry of OCT4 (Vial 3). Scale bars: 200 µm. (E) Summary table of the characterization of re-suspension-cultured iPSCs from frozen stocks. Total cell numbers on day 10, the ratio of TRA-1-60-positive cells (%), and the ratio of OCT4-positive cells (%) are shown (mean ± SE) (n=3).

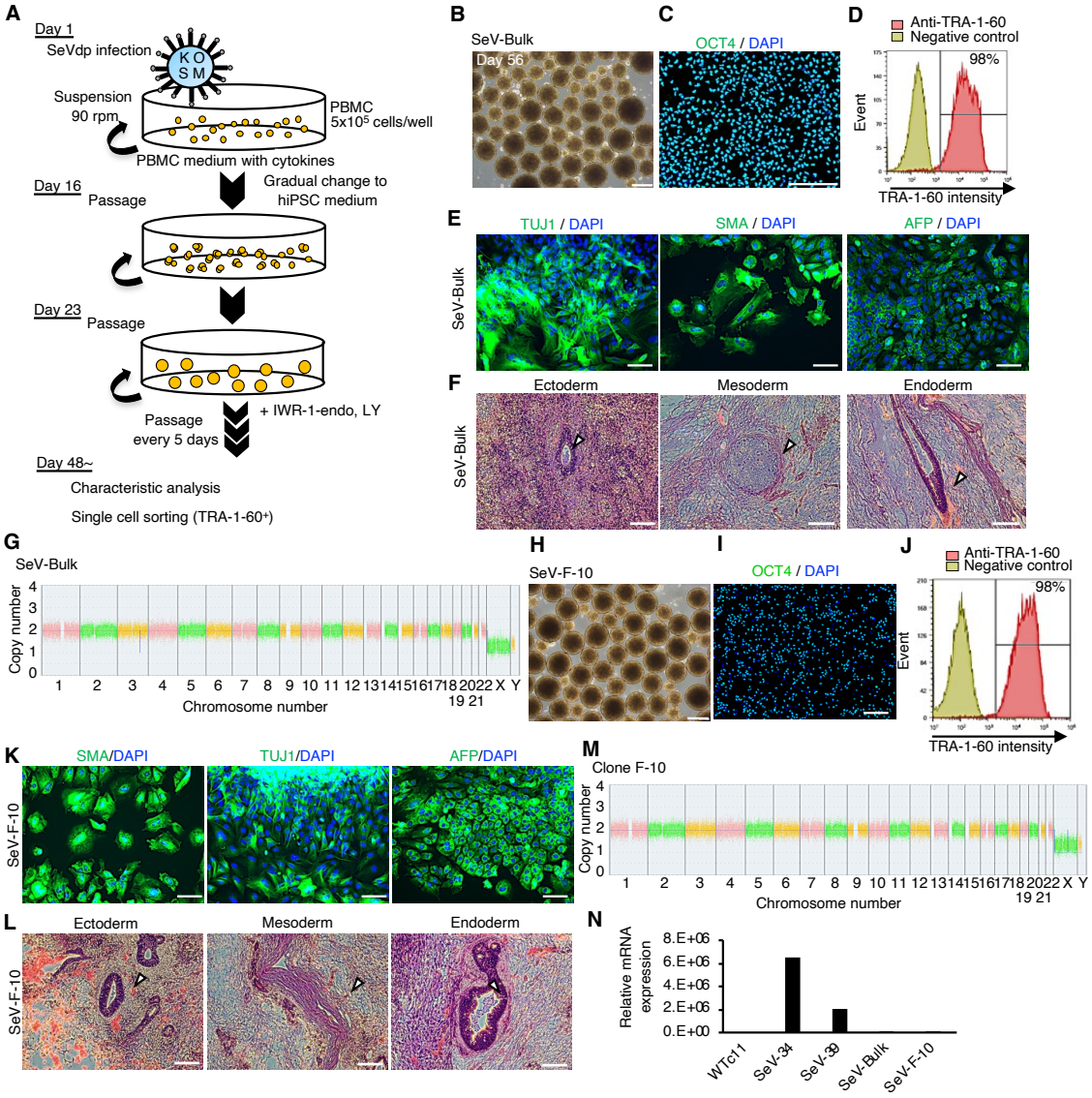

Figure 9. Establishment of hiPSCs in complete suspension conditions using SeVdp. (A) Schematics. (B) Phase-contrast images of PBMCs on day 56 after infection. Scale bars: 400 µm. (C) Immunocytochemistry of OCT4 on bulk-hiPSCs on day 56. Scale bars: 200 µm. (D) Flow cytometry of TRA-1-60 in bulk-hiPSCs on day 61. (E) Immunocytochemistry of TUJ1, SMA, and AFP on differentiated cells in EBs from bulk-hiPSCs on day 56. Scale bars: 100 µm. (F) HE staining of teratoma sections derived from bulk-hiPSCs. White arrowheads indicate representative tissue structures derived from ectoderm, mesoderm, and endoderm. Scale bars: 100 µm. (G) Chromosomal copy numbers detected with CNV array analysis on bulk-hiPSCs. (H) Phase-contrast image of an established hiPSC clone at passage 7. Scale bars: 400 µm. (I) Immunocytochemistry of established clone, F-10, with anti-OCT4 antibody. Scale bars: 200 µm.

1270 (J) The percentage of TRA-1-60-positive cells with flow cytometry on established clone F-10
1271 line. (K) HE staining of teratoma sections derived from F-10 clone line. The details are the same
1272 as in (F). (L) Immunocytochemistry in EBs from established F-10 clone. Scale bars: 100 μm. (M)
1273 Chromosomal copy numbers of F-10 clone line. (N) Residual SeVdp genomic RNA in
1274 established hiPSCs with RT-qPCR.
1275

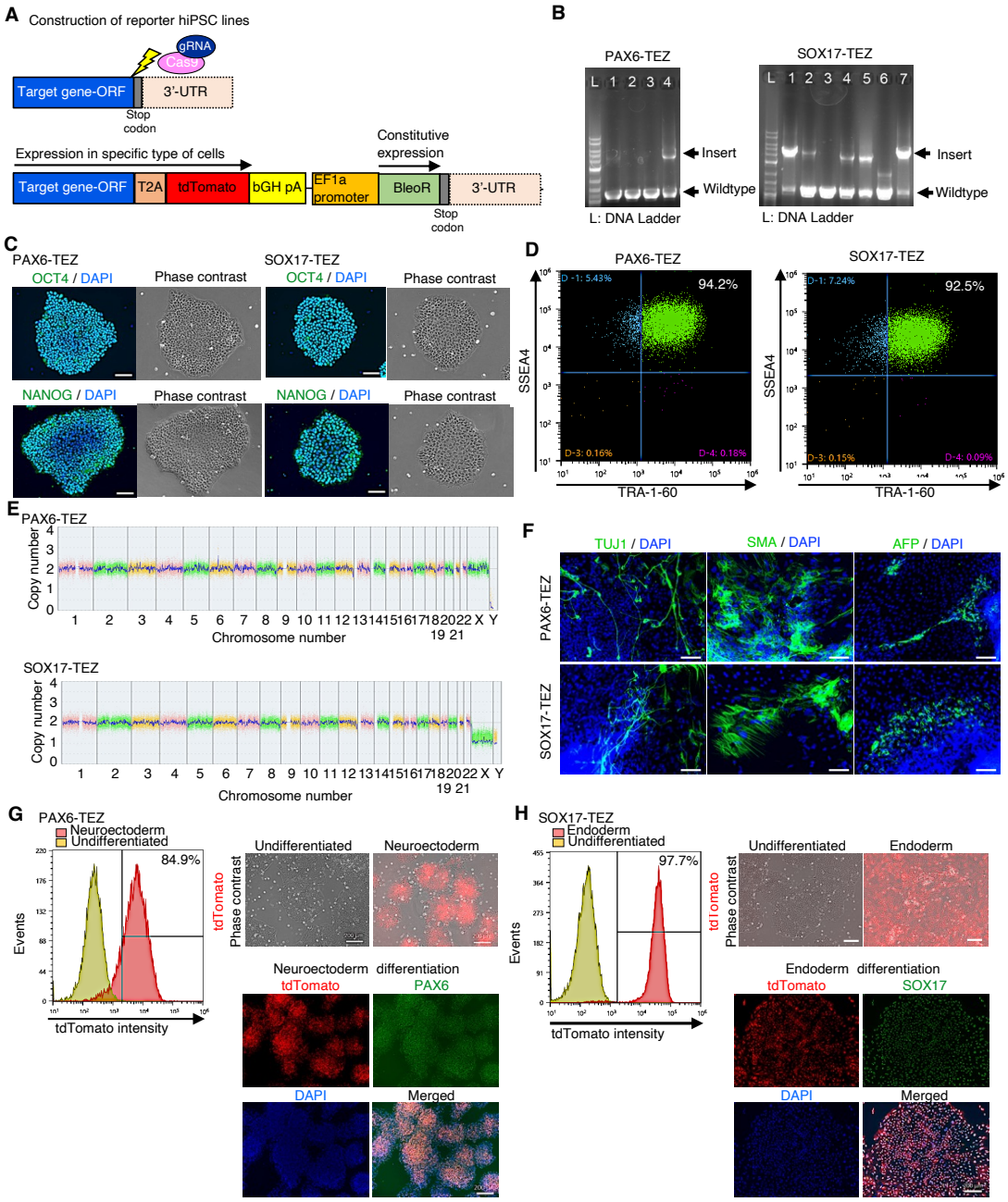

Figure 1−figure supplement 1. Characterization of PAX6-tdTomato and SOX17-tdTomato reporter lines. (**A**) Schematic of construction of reporter hiPSC lines. CRISPR/Cas9 was employed to knock-in the 2A-tdTomato gene and EF1a promoter-driven Zeocin (Bleomycin) resistance gene sequence (TEZ) to the 3' terminal of SOX17 or PAX6 open reading frame (ORF), respectively. (B) Genotyping of selected clones by genomic PCR. Arrows indicate alleles of wildtype or insertion in the PAX6 (left panel) or SOX17 (right panel) genes. (C) Phase-contrast images of representative colonies and immunocytochemistry of pluripotency markers: OCT4 and NANOG. Left panels: PAX6-TEZ. Right panels: SOX17-TEZ. (D) Flow cytometry of cell

1284 surface markers: TRA-1-60 and SSEA4. Left: PAX6-TEZ. Right: SOX17-TEZ. (E)
1285 Chromosomal copy numbers detected with CNV array analysis of PAX6-TEZ (top) and SOX17-
1286 TEZ (bottom). (F) Immunocytochemistry of differentiated cells in EBs from established bulk-
1287 hiPSCs on day 56. Anti-TUJ1, -SMA and -AFP antibodies were used. Scale bars: 100 µm. (G)
1288 Differentiation potency of PAX6-TEZ in the neural ectoderm. Left: Flow cytometry of tdTomato
1289 using PAX6-TEZ cultured in neuroectodermal differentiation medium for 7 days. Right upper:
1290 Overlay images of phase-contrast and tdTomato fluorescence of PAX6-TEZ cultured in
1291 neuroectodermal differentiation medium (upper) or maintenance medium (lower). Scale bars: 200
1292 µm. Right lower: Images of tdTomato fluorescence and endogenous PAX6 protein detected with
1293 immunocytochemistry with anti-PAX6 antibody. Nuclear staining was performed with DAPI.
1294 Scale bars: 200 µm. (H) Differentiation potency of SOX17-TEZ in the endoderm. Left: Flow
1295 cytometry of tdTomato using SOX17-TEZ cultured in endodermal differentiation medium for 7
1296 days. Right upper: Overlay images of phase-contrast and tdTomato fluorescence of SOX17-TEZ
1297 cultured in endoderm differentiation medium (upper) or maintenance medium (lower). Right
1298 lower: Images of tdTomato and endogenous SOX17 protein detected by immunocytochemistry
1299 with anti-SOX17 antibody. Nuclear staining was performed with DAPI. Scale bars: 200 µm.
1300

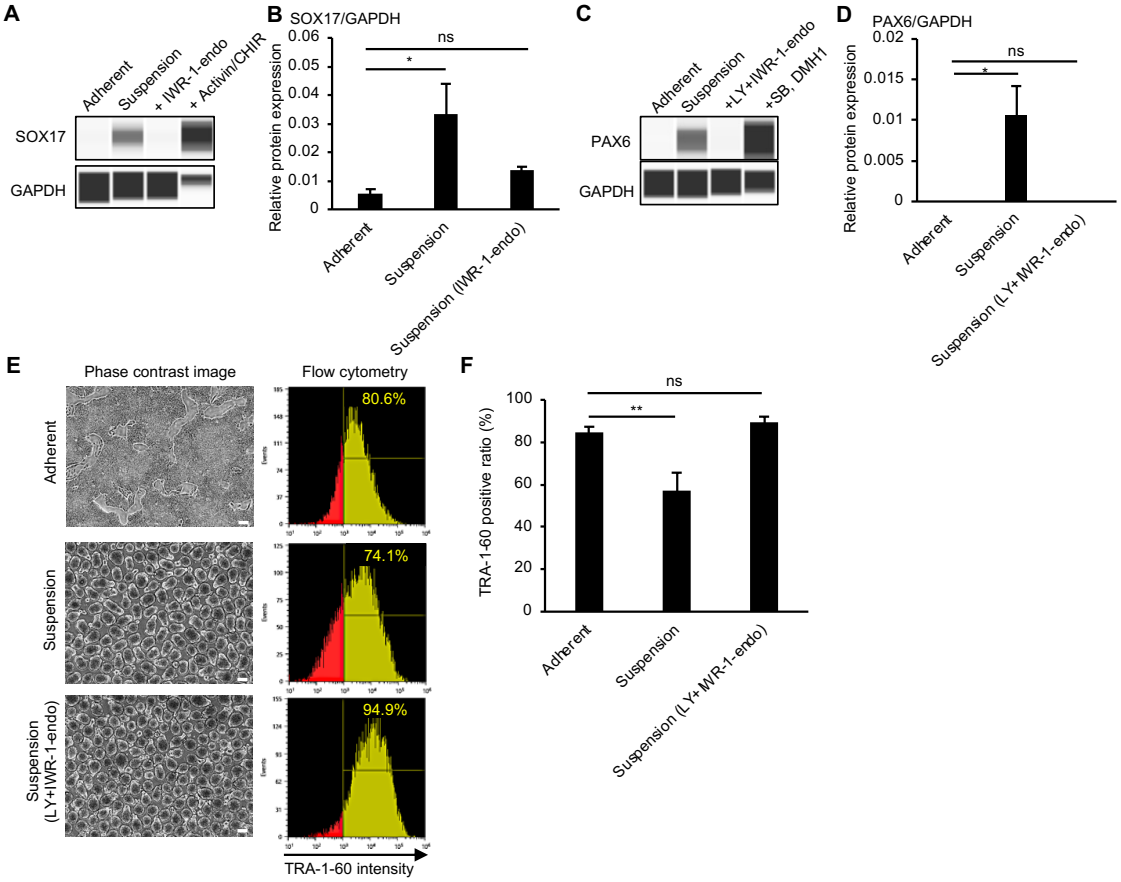

Figure 2−figure supplement 1. Effects of PKCβ and IWR-1-endo on suspension-cultured hiPSCs at the protein level. (A) Simple western blotting of adherent- or suspension-cultured hiPSCs (SOX17-TEZ) in the presence or absence of IWR-1-endo. SOX17-TEZ cultured in endoderm differentiation medium (Actinin A + CHIR) was used as a positive control for SOX17 expression. (B) Quantification of SOX17 expression. The protein expression was normalized to GAPDH. Data are presented as mean ± SE (n=3). (C) Simple western blotting of adherent- or suspension-cultured hiPSCs (PAX6-TEZ) in the presence or absence of IWR-1-endo and LY333531. PAX6-TEZ cultured in neurectoderm differentiation medium (SB431542+DMH1) was used as the positive control for PAX6 expression. (D) Quantification of expression of PAX6. The protein expression was normalized to GAPDH. Data are presented as mean ± SE (n=3). (E) Phase-contrast images and representative flow cytometry data of pluripotency marker, TRA-1-60, in adherent- or suspension-cultured hiPSCs (1383D6 line) on day10 (Passage 2). Suspension-culture was performed in the presence or absence of IWR-1-end and LY333531. The percentage of TRA-1-60 positive cells is shown in the right corner. (F) Quantified data for TRA-1-60 positive ratio (%). The percentage of TRA-1-60 positive cells is shown as mean ± SE (n=3).

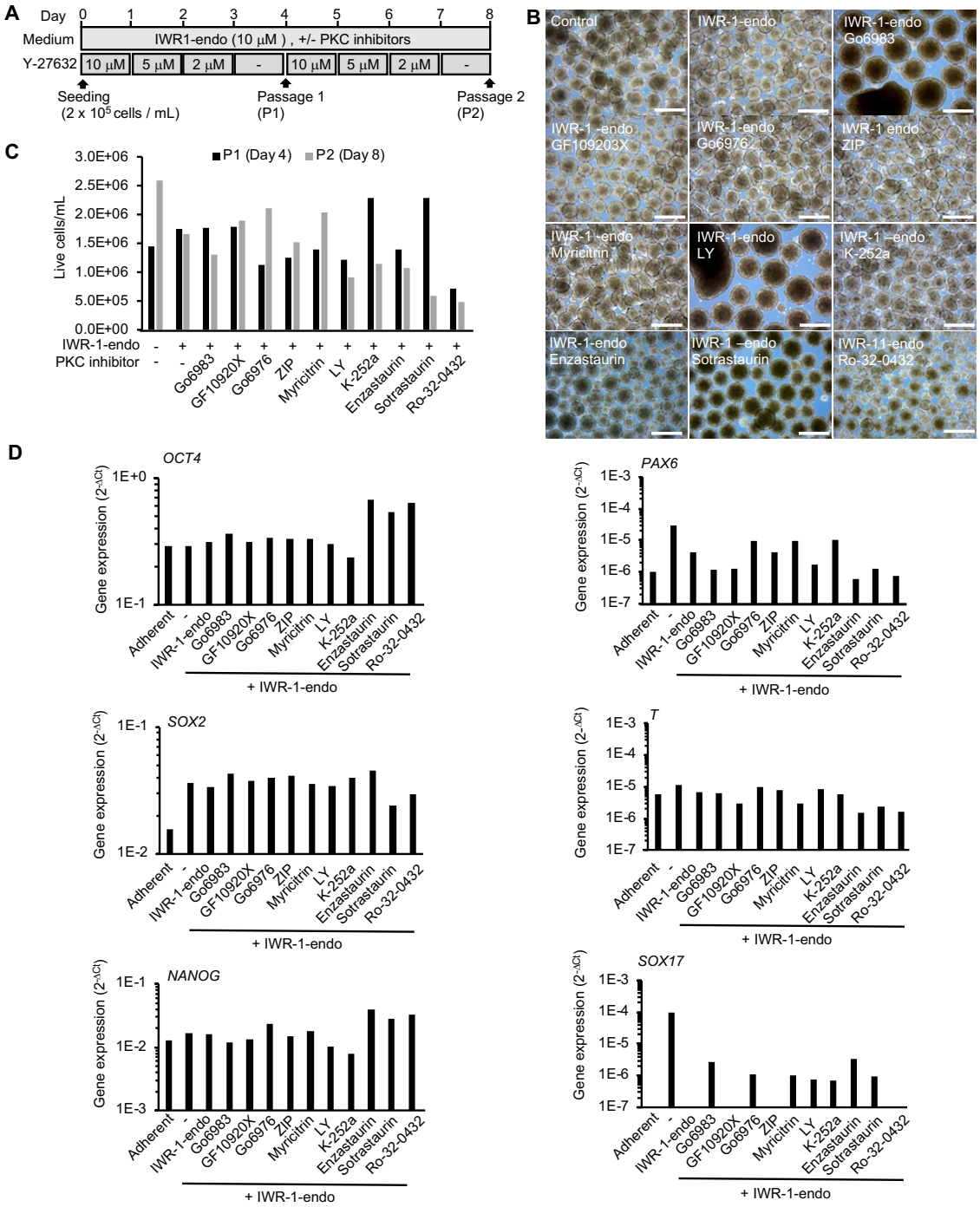

Figure 2–figure supplement 2. Activity of different type of PKC inhibitors on spontaneous differentiation of suspension-cultured hiPSCs. (A) Schematic representing suspension culture of hiPSCs supplemented with PKC inhibitors. Healthy donor-derived hiPSCs (201B7 line) were grown under continuous agitation in the presence of Y-27632, IWR-1-endo and PKC inhibitors. Passage was performed every four days. (B) Phase-contrast images of suspension cultured hiPSCs on day 8 (P2) in the absence or presence of IWR-1-endo and each PKC inhibitors. Scale

1323 bars, 500 µm. (C) Cell growth of hiPSCs (201B7). Graph shows live cell numbers counted on day
1324 4 and day 8 in suspension-culture (n=1). The PKC inhibitors added are labelled in the graphs. (D)
1325 Gene expression in hiPSCs cultured in adherent or suspension conditions with each PKC
1326 inhibitor. RT-qPCR was performed on cDNAs prepared from day 8 (passage 2) samples (n=1).
1327 qPCR was performed for pluripotency (OCT4, SOX2, NANOG) and early differentiation markers
1328 (PAX6, T, SOX17). Gene expression was normalized to beta-ACTIN.

1329

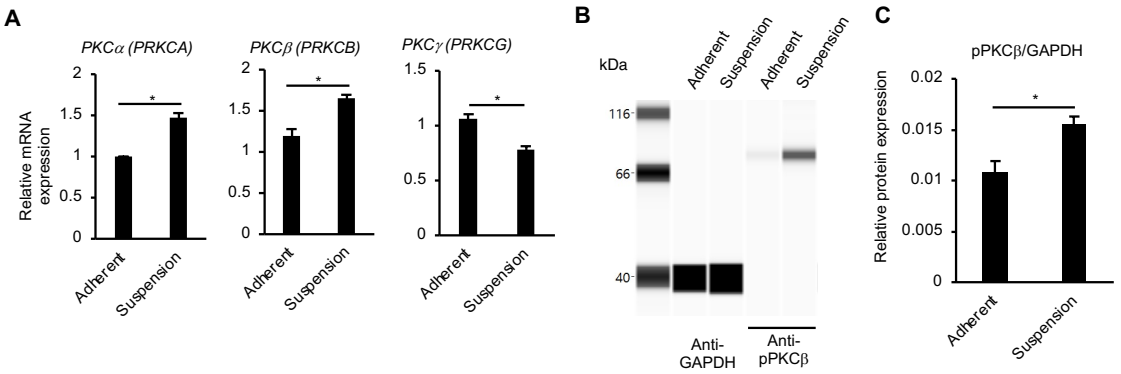

1330 **Figure 3—figure supplement 1. Up-regulation of PKC genes in suspension-cultured hiPSCs.**
1331 (A) RNA expression of conventional PKC isoform genes in hiPSCs as detected by RT-qPCR.
1332 cDNA was prepared from adherent- or suspension-cultured hiPSCs on day 5. The gene
1333 expression was normalized to GAPDH. Results are displayed as relative fold increase to
1334 adherent-culture. Data are presented as mean ± SE (n=3). P-values were statistically analyzed by
1335 Student's t-test. (B) Detection of phosphorylated PKCβ protein (pPKCβ) in suspension cultured
1336 hiPSCs on day 5 using an automated capillary western blot (Simple Western) assay. Adherent-
1337 cultured hiPSCs were used as a control. (C) Quantification of pPKCβ expression. The protein
1338 expression was normalized to GAPDH. Data are shown as mean ± SE (n=3). P-value was
1339 statistically analyzed using Student's t-test. Scale bars, 200 μm.

1340

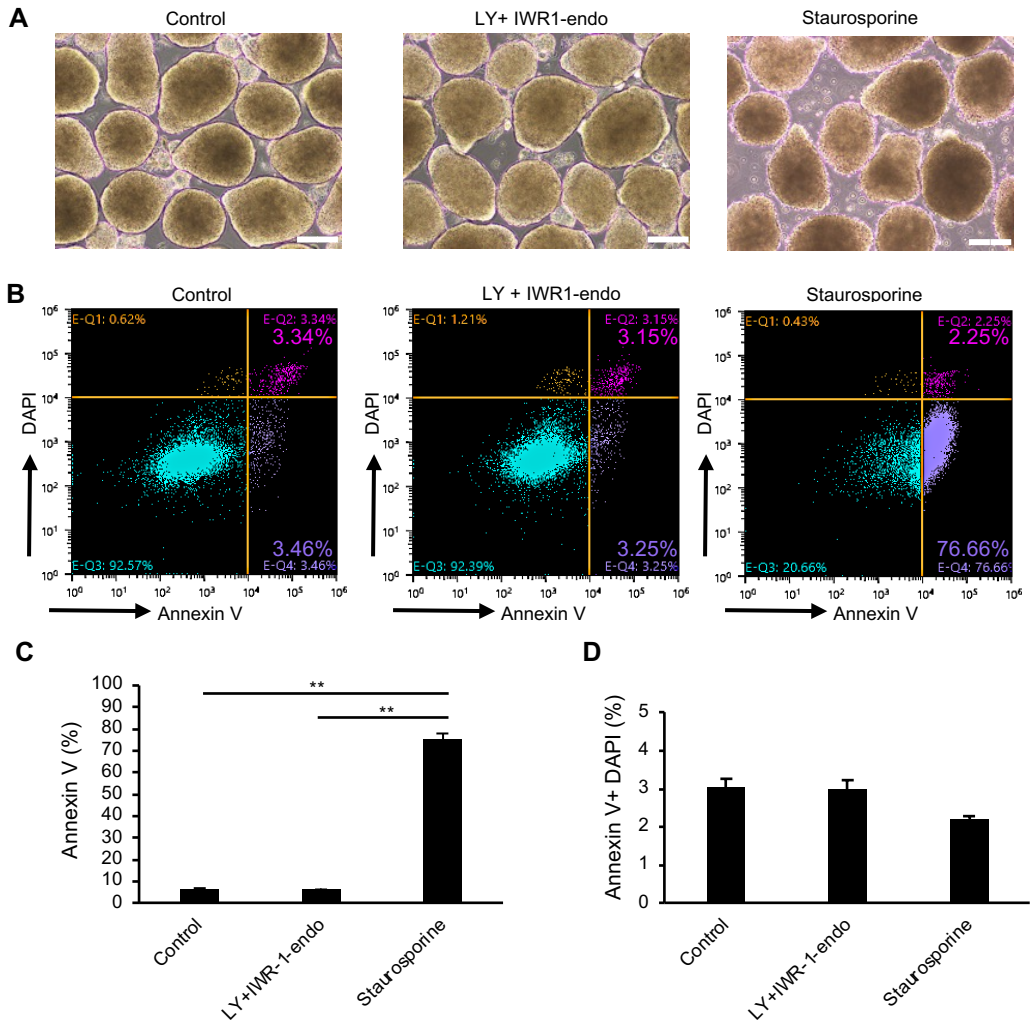

1341 **Figure 3—figure supplement 2. Cell death of suspension cultured iPSCs after the treatment**
1342 **with LY333531 and IWR-1-endo.** (A) Phase-contrast images of suspension-cultured hiPSCs
1343 (WTC11 line) on day 10 (Passage 2). Cells were culture in StemFit AK02N medium with no
1344 supplement (left), with LY333531 + IWR-1-endo (middle) for 10 days, with Staurosporine for 2
1345 hours. Scale bars: 200 µm. (B) Evaluation of apoptotic cells by flow cytometry using Annexin V
1346 (Alexa Fluor 680) conjugates. (C) Bar-graph indicating Annexin V-positive cells (%) in each
1347 culture conditions. (D) Bar-graph indicating double positive cells for Annexin V and DAPI (%) in
1348 each culture conditions. Data are presented as mean ± SE (n=3). Statistical analysis was
1349 performed using by one-way ANOVA and Tukey's tests for all graphs. P values < 0.05 were
1350 considered statistically significant. ** in the graphs indicate P<0.01.

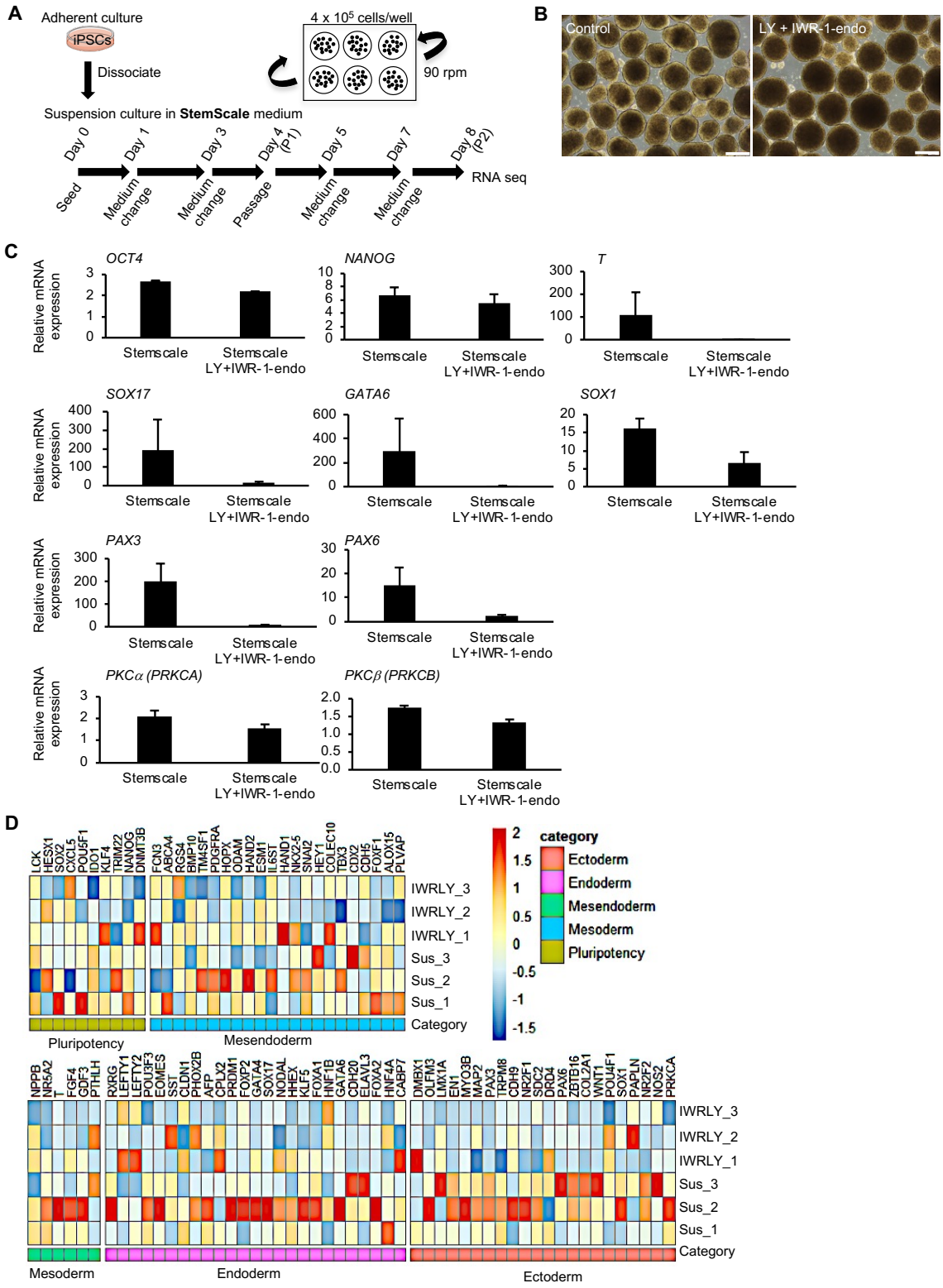

1351 **Figure 4—figure supplement 1. Generality of the inhibitory effects of IWR-1-end and**
1352 **LY333531 on spontaneous differentiation of hiPSCs cultured in suspension condition.** (A)

1353 Schematic representing suspension culture of hiPSCs using StemScale medium (Thermo Fisher
1354 Scientific) as the basic culture medium. hiPSCs were grown under continuous agitation (90 rpm)
1355 in the presence or absence of IWR-1-endo and LY333531. Passage was performed every four
1356 days according to the manufacture's protocol. cDNAs were prepared from day 8 (P2) and used
1357 for RNA seq. (B) Phase-contrast images of suspension cultured hiPSCs on day 8 in the presence
1358 or absence of IWR-1-endo and LY333531. Scale bars, 400 µm. (C) RNA expression of
1359 pluripotency and early differentiated genes in hiPSCs, as detected by RT-qPCR. cDNA was
1360 prepared from suspension-cultured hiPSCs on day 8 in the presence or absence of IWR-1-endo
1361 and LY33353. The gene expression was normalized to GAPDH. Data are presented as mean ± SE
1362 (n=3). (D) Heat map of marker genes for pluripotency and differentiation to three germ layers
1363 from RNA-seq data in suspension-cultured iPSCs without compounds (Sus_1, Sus_2 and Sus_3)
1364 or with IWR-1-endo and LY333531 (IWRLY_1, IWRLY_2 and IWRLY_3). The listed genes
1365 were classified as pluripotent, mesendoderm, mesoderm, endoderm, and ectoderm, as defined in
1366 the Scorecard Assay (Thermo Fisher Scientific).
1367

1368

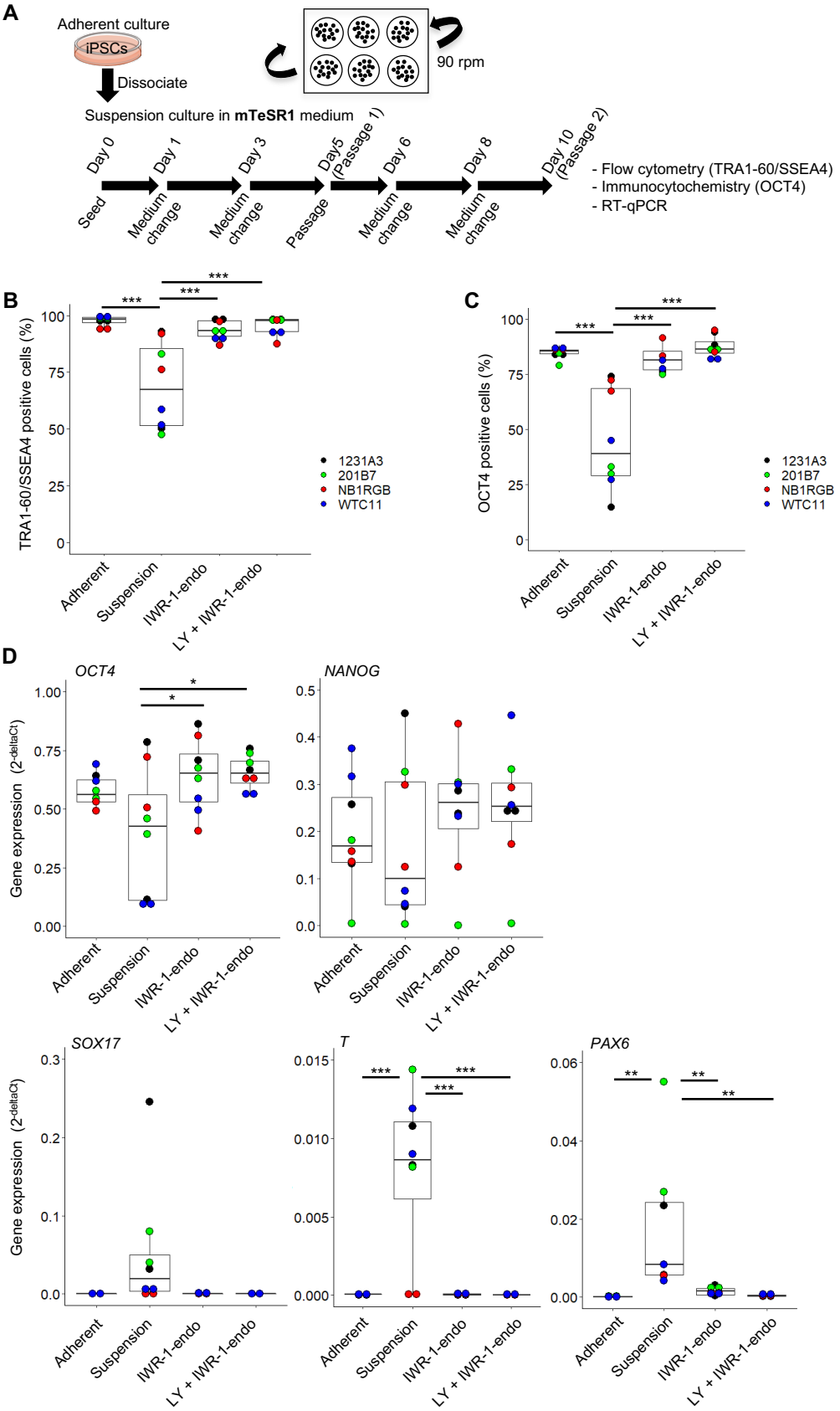
A
Adherent culture
iPSCs
Dissociate
90 rpm
Suspension culture in mTeSR1 medium
Day 0
Seed
Day 1
Medium change
Day 3
Medium change
Day5 (Passage 1)
Passage
Day 6
Medium change
Day 8
Medium change
Day 10 (Passage 2)
- Flow cytometry (TRA1-60/SSEA4)
- Immunocytochemistry (OCT4)
- RT-qPCR
B
TRA1-60/SSEA4 positive cells (%)
1231A3
201B7
NB1RGB
WTC11
Adherent
Suspension
IWR-1-endo
LY + IWR-1-endo
C
OCT4 positive cells (%)
D
OCT4
NANOG
SOX17
T
PAX6
Gene expression (2-deltaCt)

1369 **Figure 4—figure supplement 2. Suspension culture of multiple hiPSC lines in mTeSR1**
1370 **medium supplemented with or without IWR-1-endo and LY333531.** (A) Schematics of
1371 suspension culture of WTC11, 1231A3, HiPS-NB1RGB (NB1RGB) and 201B7 hiPSC lines.
1372 After suspension culture of these 4 hiPSC lines in mTeSR1 medium with or without IWR-1-endo
1373 and LY333531, characteristic analysis was performed on day10 (Passage 2). Suspension culture
1374 was performed twice in each cell lines (n=2 each from 4 cell lines). (B) Box plots of flow
1375 cytometry for TRA-1-60 and SSEA4 double positive cells (%). Used cell lines are indicated by
1376 the different colored circles shown on the right side of the graph. (C) Box plots of OCT4 positive
1377 cells (%). (D) Box plots of RT-qPCR. Differentiation markers (*SOX17, T,* and *PAX6*),
1378 undifferentiated markers (*OCT4* and *NANOG*), and naïve pluripotency markers (*KLF2* and *KLF5*)
1379 were assessed. Statistical analysis was performed using by one-way Anova and Tukey's test for
1380 all graphs. P values < 0.05 were considered statistically significant. *, ** or *** in the graphs
1381 indicate P<0.05, P<0.01 or P<0.001, respectively.

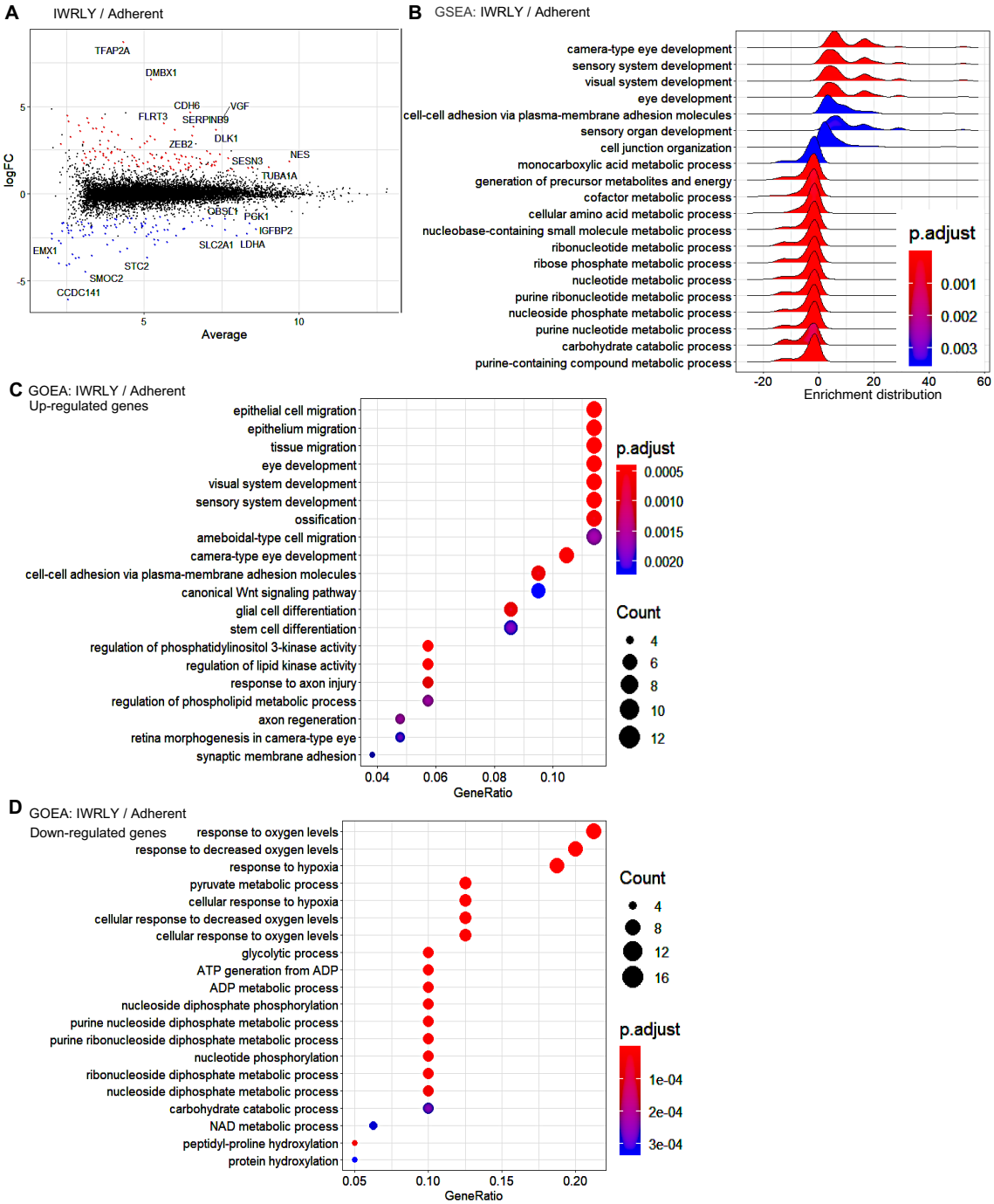

Figure 5—figure supplement 1. Global gene expression of suspension-cultured hiPSCs with IWR-1-endo and LY333531 in comparison to adherent-cultured hiPSCs. (A) MA plot (log2 fold change versus mean average expression) comparing the transcriptomes between adherent- and suspension-cultured hiPSCs treated with IWR-1-endo and LY33353 (IWRLY). Transcripts with log2 fold change ≧ 2 or ≦ -2 (FDR <0.01) are highlighted with red or blue dots, respectively. The names of the representative genes are shown in the plot. (B) GSEA of the gene

1388 sets of suspension-cultured hiPSCs with IWRLY compared to adherent-cultured hiPSCs.
1389 Analysis was performed on both up-regulated and down-regulated genes. Statistically significant
1390 enrichment is shown. Adjusted P-values are illustrated from blue to red as low to high. (C and D)
1391 GOEA of the gene sets of suspension-cultured hiPSCs with IWRLY compared to adherent-
1392 cultured hiPSCs. Analysis was performed on up-regulated genes in (C) and down-regulated genes
1393 in (D), respectively. Results are ranked by significance (adjusted P values) and/or counted gene
1394 numbers.
1395

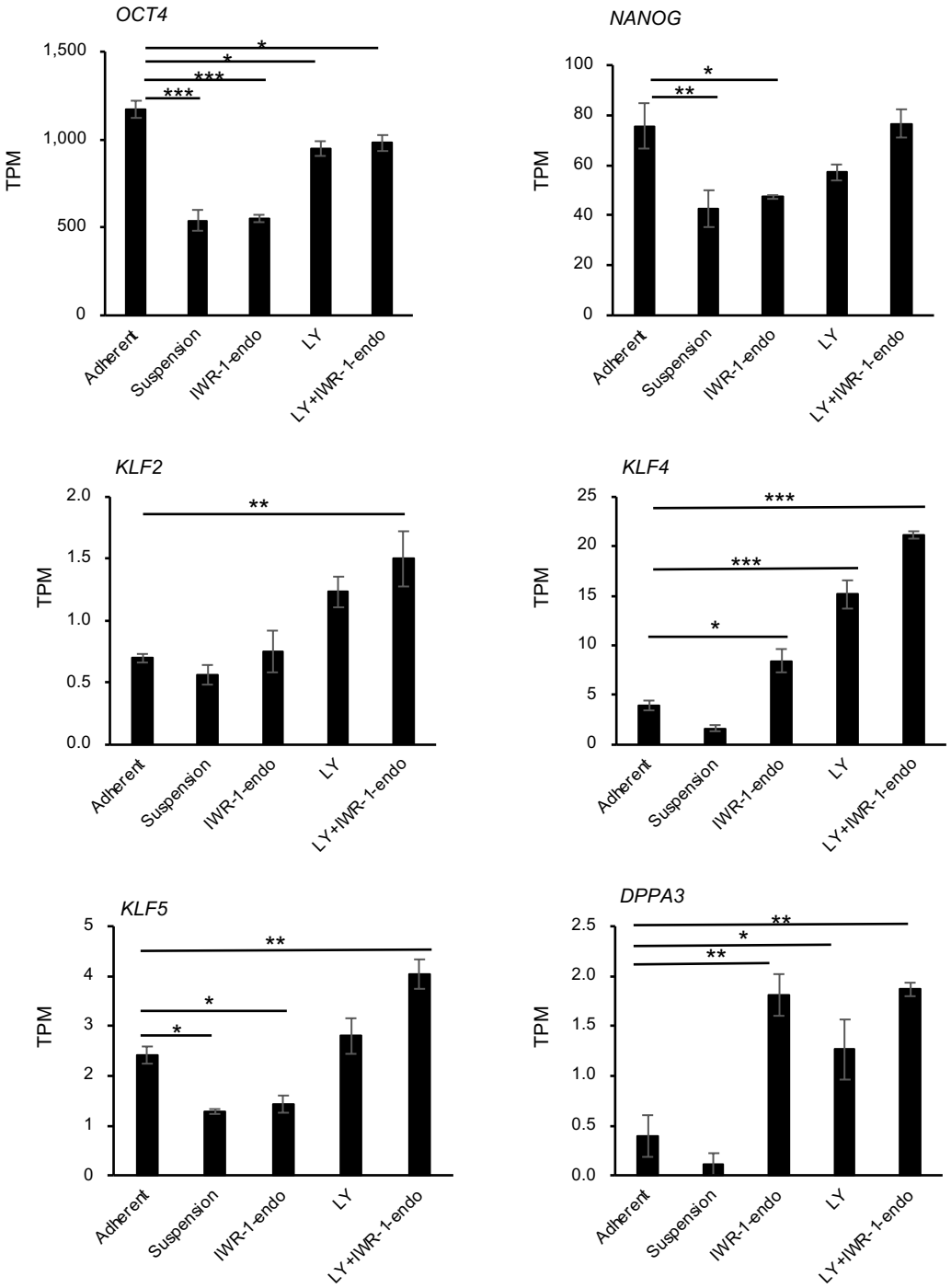

1396 **Figure 5-figure supplement 2. Comparison of expression on naïve markers between**
1397 **adherent and suspension-cultured hiPSCs.** HiPSCs (WTC11 line) were culture in continuous
1398 suspension culture in StemFitAK02N in the presence of IWR-1-endo, LY333531, or both. RNA-
1399 seq was performed using day 10 samples. The gene expression of naïve pluripotency markers
1400 (*OCT4, NANOG, KLF2, KLF4, KLF5,* and *DPPA3*) was extracted based on the TPM (Transcripts

1401 per million) values. Bar graphs show the mean ± SE (n=3). P-values were statistically analyzed
1402 with Dunnett's test to the samples of adherent conditions. P values < 0.05 were considered
1403 statistically significant. *, ** or *** in the graphs indicate P<0.05, P<0.01 or P<0.001,
1404 respectively.

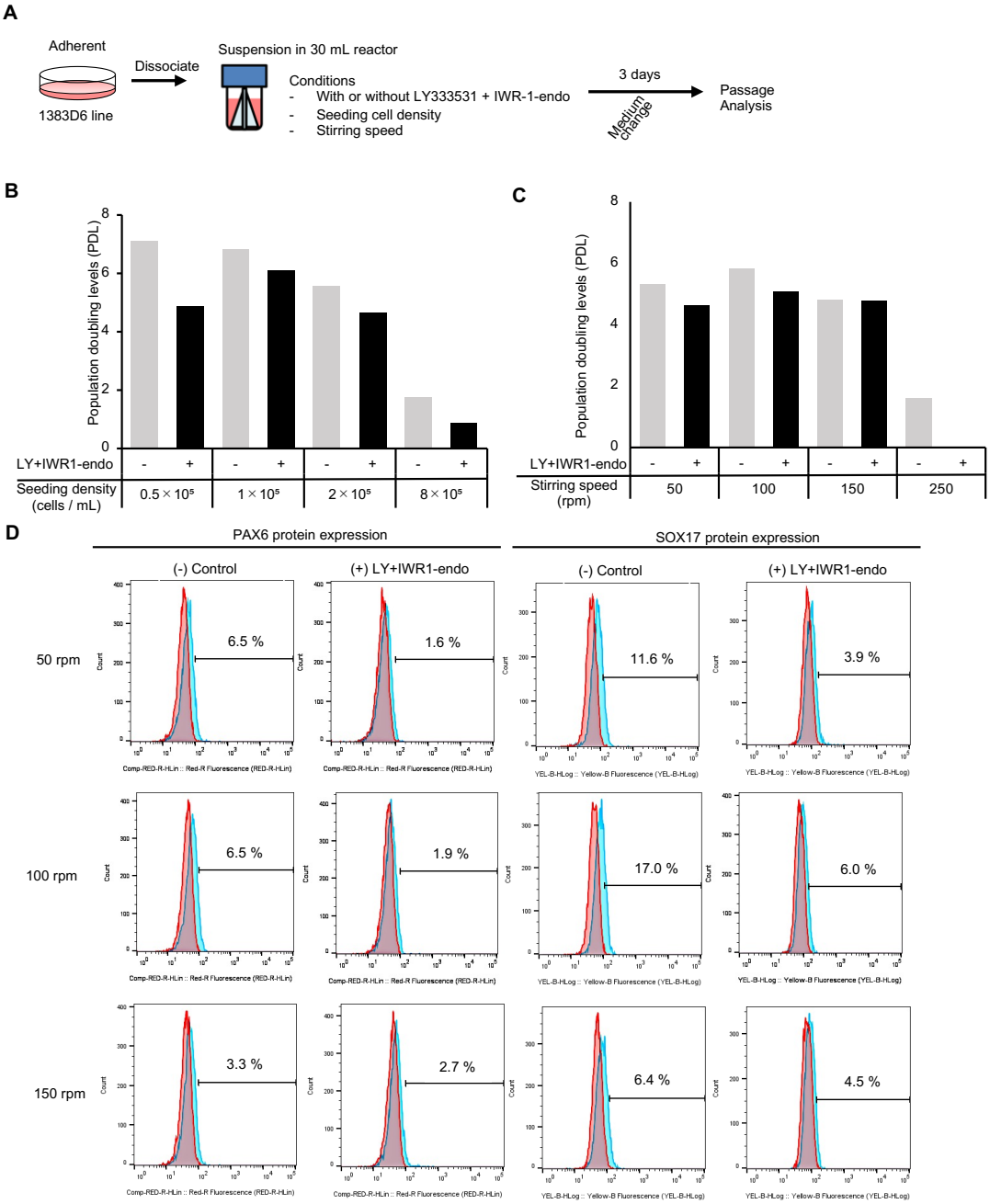

Figure 6−figure supplement 1. Suspension-culture of hiPSCs supplemented with IWR-1-endo and LY333531 using bioreactors with continuous agitation. (A) Schematic representing suspension culture of hiPSCs in a 30 mL bioreactor. Healthy donor-derived hiPSCs (1383D6 lines) were grown with continuous agitation in the presence or absence of IWR-1-endo and LY333531. Passages were performed every 3 - 4 days. (B) Graphs showing population doubling levels from the seeding cell numbers on day 3. (C) Flow cytometric analysis of of differentiation marker proteins, PAX6 and SOX17. Positive cells (%) are shown.

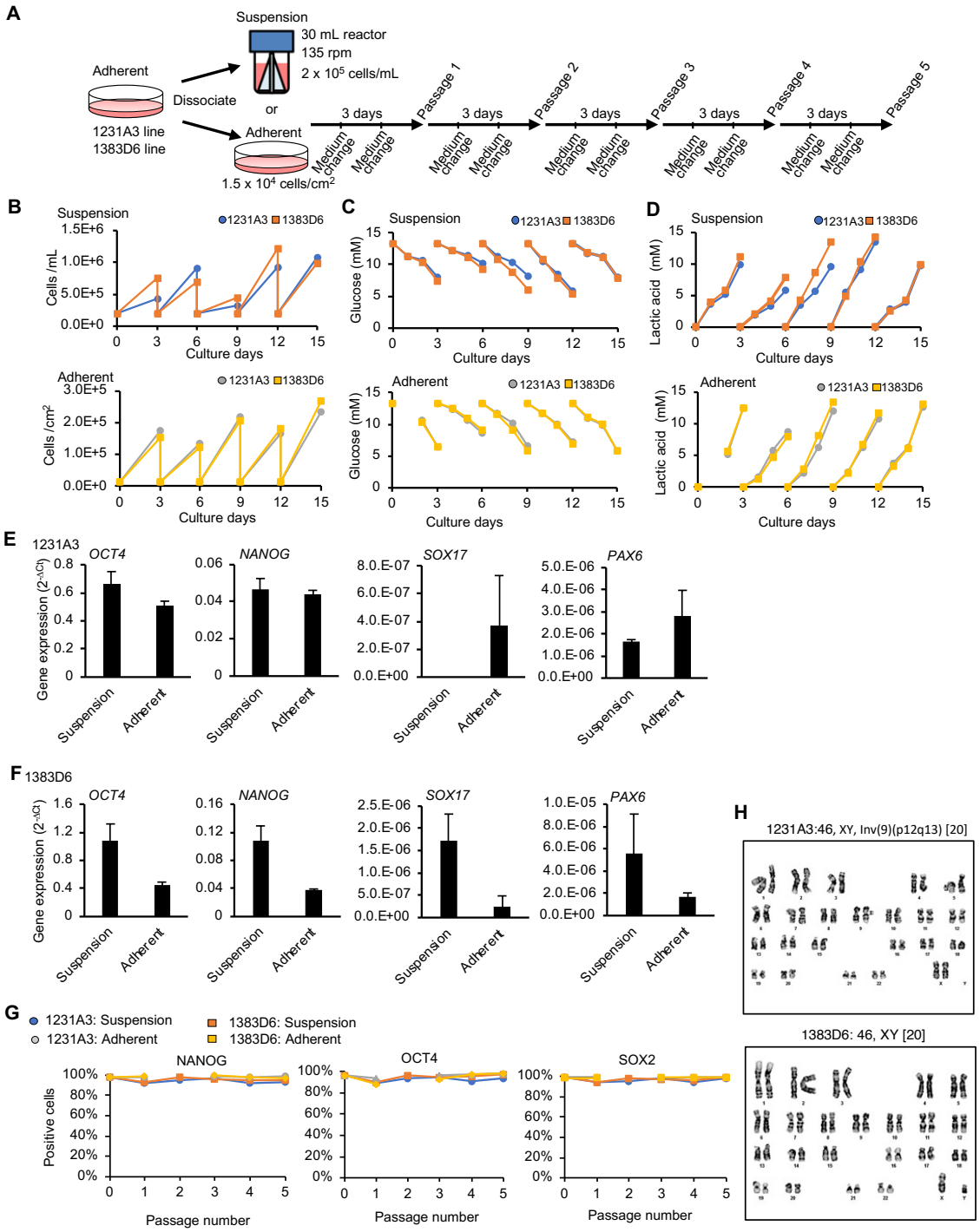

Figure 6—figure supplement 2. Suspension-culture of hiPSCs supplemented with IWR-1-endo and LY333531 using bioreactors with continuous agitation. (A) Schematic representing suspension culture of hiPSCs in a 30 mL bioreactor. Healthy donor-derived hiPSCs (1231A3 and 1383D6 lines) were grown with continuous agitation in the presence or absence of IWR-1-endo and LY333531. Passages were performed

1417 every three days. (B) Graphs showing cell numbers at each passage (n=1). Upper:
1418 suspension-culture of 1231A3 and 1383D6 lines. Lower: adherent-culture of 1231A3 and
1419 1383D6 lines. (C) Graphs showing glucose concentration in the culture medium at each
1420 culture day. Upper: suspension-culture of 1231A3 and 1383D6 lines. Lower: adherent-
1421 culture of 1231A3 and 1383D6 lines. (D) Graphs showing lactic acid concentration in the
1422 culture medium at each culture day. Upper: suspension-culture of 1231A3 and 1383D6
1423 lines. Lower: adherent-culture of 1231A3 and 1383D6 lines. (E and F) RT-qPCR analysis
1424 of hiPSCs cultured in 30 mL bioreactor or adherent conditions. cDNA samples were
1425 prepared from passage 3 and 5 of the 1231A3 in (E) and 1383D6 in (F). qPCR was
1426 performed for *OCT4* and *NANOG* (pluripotent), *CDX2* (mesoderm), *SOX17* (endoderm)
1427 and *PAX6* (neuroectoderm). The gene expression was normalized to *β-ACTIN*. Bar graph
1428 showing the average gene expressions of passage 3 and 5 (mean ± SE). (G) Flow
1429 cytometric analysis of suspension- or adherent-cultured 1231A3 and 1383D6 lines.
1430 Positive cells (%) of pluripotency marker proteins: NANOG, OCT4, and SOX2 are
1431 shown. (H) Karyotyping of hiPSCs cultured in 30 mL bioreactor. Cell samples were
1432 prepared on passage 5, and used for G-band karyotyping analysis. A short deletion on
1433 chromosome 9 of 1231A3 (indicated with arrow) was derived from the original line.

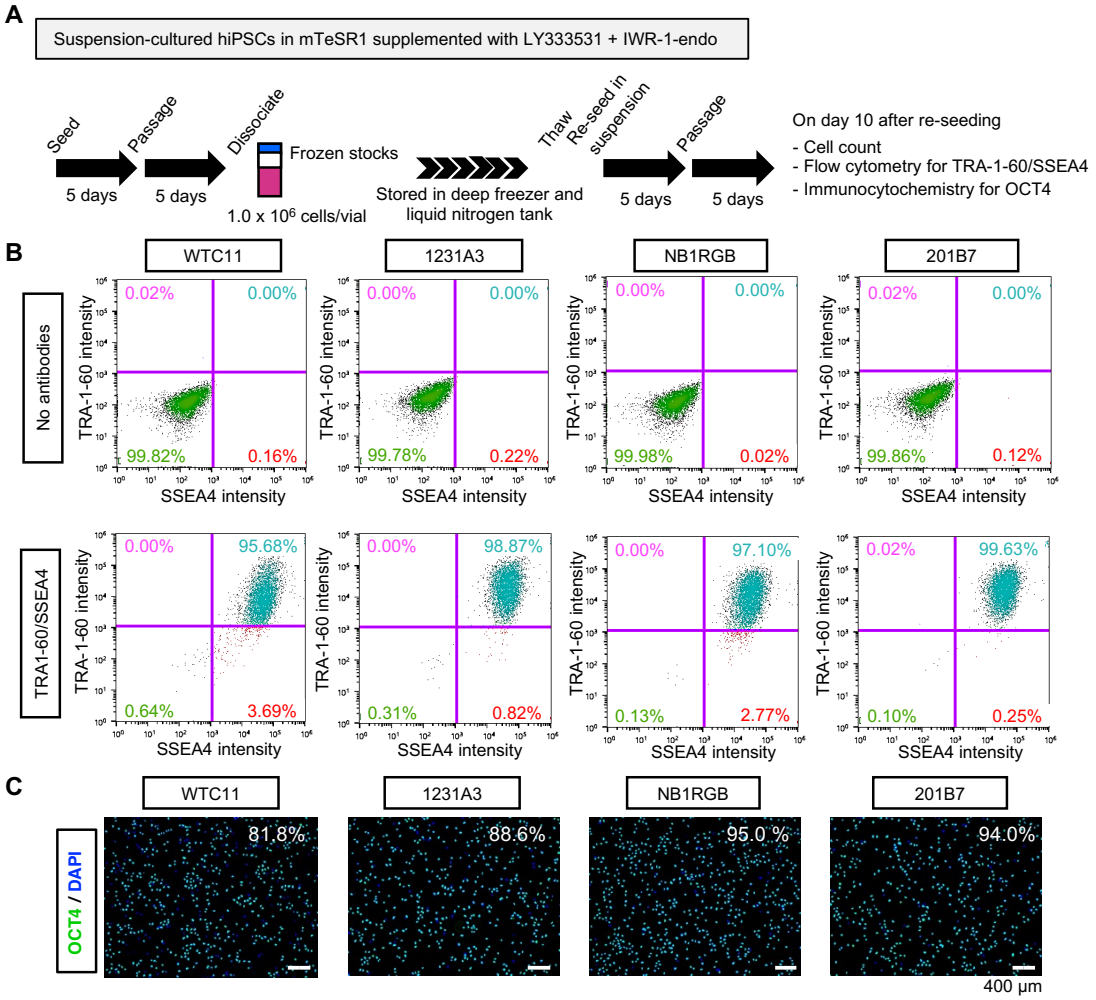

Frozen stock of hiPSCs	Total cell numbers on day 10	TRA-1-60/SSEA4 positive cells (%)	OCT4 positive cells (%)
WTC11	4.48 x 10^6	95.7	81.8
1231A3	4.17 x 10^6	98.9	88.6
NB1RGB	6.64 x 10^6	97.1	95.0
201B7	2.65 x 10^6	99.7	94.0
Mean ± SE	4.5 x 10^6 ± 0.4 x 10^6	97.9 ± 0.4	89.8 ± 1.5

Figure 8−figure supplement 1. Re-suspension from frozen stocks of hiPSCs under suspension culture conditions supplemented with IWR-1-endo and LY333531 in mTeSR1 medium. (A) Schematics of re-suspension culture of frozen stocks of WTC11, 1231A3, HiPS-NB1RGB (NB1RGB) and 201B7 hiPSC lines. After suspension culture in mTeSR1 medium supplemented with IWR-1-endo and LY333531, expanded iPS cells were cryopreserved. Each frozen stocks were expanded again in the mTeSR1 medium supplemented with IWR-1-endo and LY333531 by repeating passage every 5 days. Characteristic analysis was performed on day10.

1441 (B) Representative flow cytometry of TRA-1-60 and SSEA4. (C) Representative
1442 immunocytochemistry of OCT4. DAPI indicates nuclear staining. Scale bars: 400 μm. (D)
1443 Summary of the characterization of re-suspension-cultured hiPSCs from frozen stocks. Total cell
1444 numbers on day 10, the ratio of double positive cells for TRA-1-60 and SSEA4 (%), and the ratio
1445 of OCT4-positive cells (%) are shown (mean ± SE; n=4).

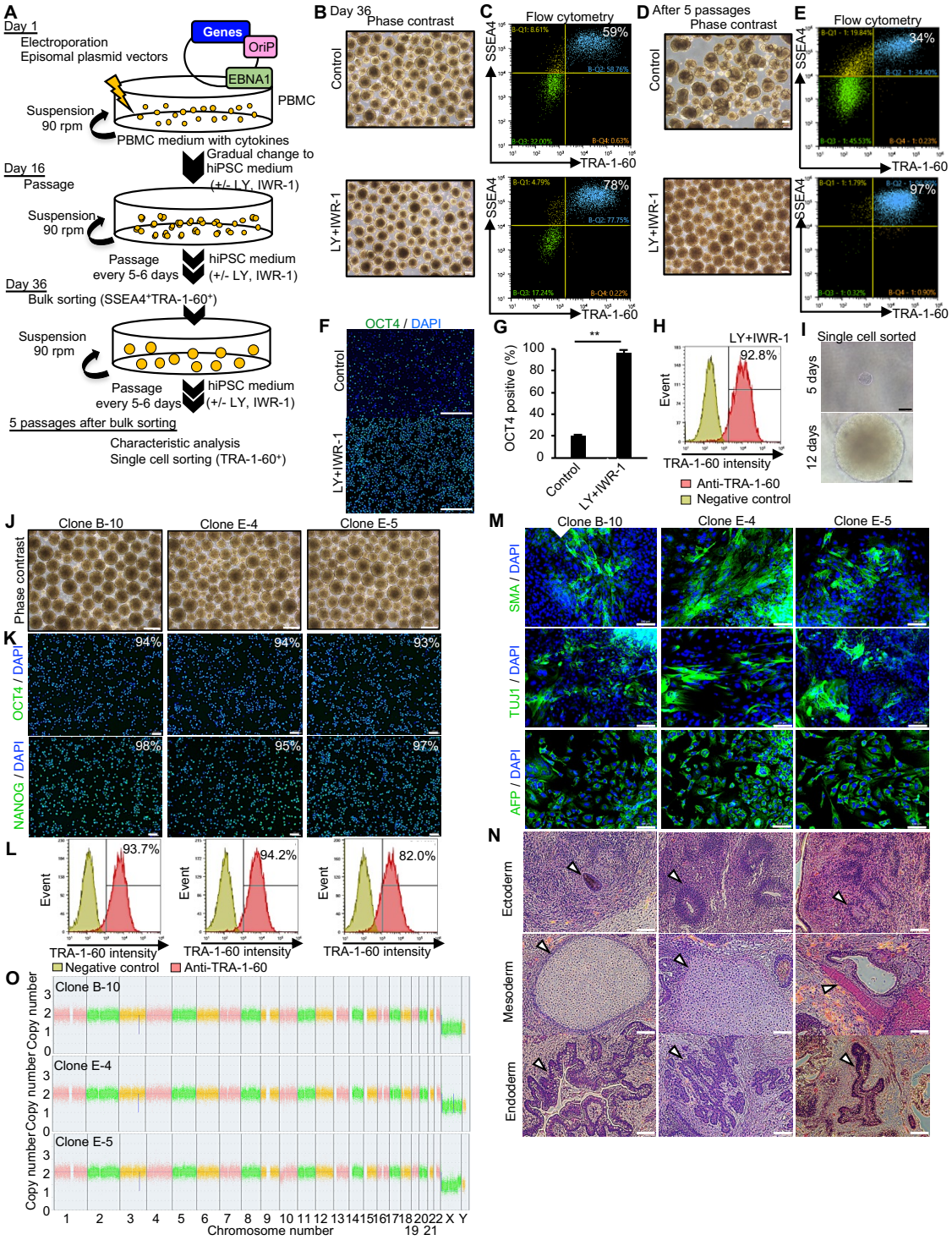

Figure 9—figure supplement 1. Establishment of hiPSCs in completed suspension conditions using episomal vectors. (A) Flow chart representing the establishment of hiPSCs from PBMCs by electroporation of episomal vectors. (B) Phase-contrast images of transfected cells on day 36 after electroporation of episomal vectors in the absence or presence of IWR-1-

1450 endo and LY333531. Scale bars: 400 µm. (C) Flow cytometry of TRA-1-60 and SSEA4. TRA-1-
1451 60 and SSEA4-psotive cells were sorted as the bulk fraction and further suspended in the absence
1452 or presence of IWR-1-endo and LY333531. The percentages of TRA-1-60 and SSEA4-psotive
1453 cells are shown in the right corner. (D) Phase-contrast images of suspension-cultured cell
1454 aggregates after bulk sorting on passage 5. Scale bars: 400 µm. (E) Flow cytometry of TRA-1-60
1455 and SSEA4. The percentage of TRA-1-60- and SSEA4-psotive cells are shown in the right
1456 corner. (F) Immunocytochemistry of OCT4 on sorted-cells cultured in the absence (top) or
1457 presence (bottom) of IWR-1-endo and LY333531 for 5 passages. Scale bars: 400 µm. (G)
1458 Quantified data for OCT4-positive cell percentage. Bar graph indicating average OCT4-positive
1459 cell percentages (mean ± SE) (n=3). P-value was statistically analyzed by Student's t-test. (H)
1460 Single-cell sorting and cloning of TRA-1-60 positive cells. Flow cytometry was performed for
1461 cell fraction that was cultured in the presence of IWR-1-endo and LY333531. TRA1-60-positive
1462 cells were collected as single cells in a 96-well plate and expanded in the culture medium
1463 supplemented with Y-27632, IWR-1-endo and LY333531. (I) Representative phase-contrast
1464 images of single-sorted cell aggregates on day 5 and 12. Scale bars, 400 µm. (J) Phase-contrast
1465 images of established clones (B-10, E-4, and E-5). Scale bars: 400 µm. (K)
1466 Immunocytochemistry of OCT4 and NANOG in these clones. The percentage of positive cell are
1467 shown. Scale bars: 100 µm. (L) Flow cytometry of TRA-1-60 in these clones. TRA-1-60 positive
1468 percentages are shown in the right corner. (M) Immunocytochemistry of differentiated cells in
1469 EBs from these clones. Anti-TUJ1, -SMA and -AFP antibodies were used. Scale bars: 100 µm.
1470 (N) Hematoxylin-Eosin staining of paraffin-embedded sections of teratoma derived from these
1471 clones. White arrowheads indicate representative tissue structures of the ectoderm, mesoderm, or
1472 endoderm. Scale bars, 100 µm. (O) Chromosomal copy numbers detected by CNV array analysis
1473 (Karyostat assay) of these clones.
1474

1475 **Table 1. The list of published study on scalable suspension culture without microcarriers**
1476 **for hPSCs.**

Article	Medium	Additives	Cell lines tested	Scalability	Transcriptome	Single cell cloning	Direct freeze and thaw	iPSC generation
Amit et al., 2010, 2011	DMEM/F12 + KSR	Y-27632, LIF, bFGF	hESC (I3, Ie, I5, H9.2, H9, H7, H14) hiPSC (iF4, J1.2.3, C3, C2, KTN7, KTN13)	~10^7	No	No	No	No
Krewetz et al., 2010	mTeSR1	Y-27632, Rapamycin	hESC (H9)	~10^8	No	No	No	No
Singh et al., 2010 Zweigerdt et al., 2011 Olmer et al., 2012	KnockOut DMEM + KSR, mTeSR1	Y-27632, bFGF	hESC (hES2, hES3, and ESI049) hiPSC (hCBiPS2, hiPSOCT4eGFP)	~10^8	No	No	No	No
Steiner et al., 2010	Neurobasal medium + KSR	Y-27632, bFGF, Activin A, Fibronectin, Gelatin, BDNF, NT3, NT4, Nutridoma-CS	hESC (HES1, HES2, H7)	~10^6	No	No	No	No (Of note, 3 hESC lines derivation)
Wang et al., 2013	TeSR-E8	Y-27632	hiPSC (BC1, TNC1)	~10^8	No	No	No	No
Hunt et al., 2014	mTeSR1	Y-27632	hESC (H1, H9)	~10^7	No	No	No	No
Elanzew et al., 2015	mTeSR1, TeSR-E8	Y-27632	hESC (H9) and hiPSC (iLB-C-31f-r1)	~10^7	No	No	No	No
Horiguchi et al., 2016; Ibuki et al., 2019	TeSR-E8, mTeSR1	Y-27632, KSR, Albumax, LPA, SIP,	hiPSC (TkDN4-M, TkDA3-4, 201B7)	~10^6	No	No	No	No
Nath et al., 2017	Dialyzed DMEM/F-12	Y-27632, bFGF, TGF-b1	hiPSC (Tic)	~10^8	No	No	No	No

Kwok et al, 2018	mTeSR1, StemMACS	Y-27632	hiPSC (AR1034ZIMA hiPSC clone1, FS hiPSC clone2)	~10^9	No	No	No	No
Lipsitz et al., 2018	Nutristem, DMEM/F12 + KSR	Y-27632, LIF, TGFβ1 FGF2, CHIR99021 SP600125 , BIRB796, Gö6983	hESC (H9, HES2, WIB) and hiPSC (C1.15)	~10^7	No	No	No	No
Rohani et al., 2020	mTeSR1, RSeT	Y-27632, Rapamycin	hESC (H1, H9)	~10^7	Yes	No	No	No
Matsuo-Takasaki et al. 2024 (This study)	AK02N, AK03N, StemScale, mTeSR1	Y-27632, IWR-1-endo, LY333531	hiPSC (WTC11, 201B7, 1383D6, 1231A3, HiPS-NB1RGB, Ff-I14s04)	~10^9	Yes	Yes	Yes	Yes

1477

1478 **Supplementary Table 1. The list of chemicals and cytokines used in the screening assay.**

Name	Effect	Manufacturer	Identifier	Concentration
CHIR99021	Wnt signal activator	Fujifilm Wako Pure Chemical	034-23103	3 μM
IWP-2	Wnt signaling inhibitor	Fujifilm Wako Pure Chemical	034-24301	5 μM
IWR-1-endo	Wnt signaling inhibitor	Fujifilm Wako Pure Chemical	037-25131	10 μM
Gö6976	PKC (α, β) inhibitor	Fujifilm Wako Pure Chemical	071-06551	5 μM
Gö6983	PKC (α, β, γ, δ) inhibitor	Fujifilm Wako Pure Chemical	078-06443	5 μM
GF109203X	PKC (α, β, γ) inhibitor	Tocris Bioscience	0741	5 μM
Enzastaurin	PKC (α, β, γ, ε) inhibitor	Sigma-Aldrich	SML0762	5 μM
K-252a	PKC (μ) inhibitor	Sigma-Aldrich	K1639	5 μM
LY333531 (Ruboxistaurin)	PKC (β) inhibitor	Sigma-Aldrich	SML0693	5 μM
Myricitrin	PKC (α, ε) inhibitor	Sigma-Aldrich	91255	5 μM
Sotrastaurin	PKC (α, β, δ, ε, η, θ) inhibitor	Cayman	16726	5 μM
ZIP	PKC (ζ) inhibitor	Tocris Bioscience	2549	5 μM
Ro-32-0432	PKC (α, β, γ, ε) inhibitor	Tocris Bioscience	1587	5 μM
FK506	Calcineurin inhibitor	Fujifilm Wako Pure Chemical	063-06071	100 ng/mL
Cyclosporine A (CsA)	Calcineurin inhibitor	Fujifilm Wako Pure Chemical	031-24931	1 mg/mL
DAPT	γ-secretase inhibitor	Fujifilm Wako Pure Chemical	043-33581	10 μM
BMP4 (Human, recombinant)	BMP-SMAD signaling activator	Fujifilm Wako Pure Chemical	020-18851	40 ng/mL
LIF (Human, recombinant)	LIF-STAT signaling activator	Nacalai Tesque	NU0013-1	2000 units/mL
Valproic acid (VPA)	Epigenetic modifier	Fujifilm Wako Pure Chemical	227-01071	0.5 mM
Ascorbic acid	Epigenetic modifier	Nacalai Tesque	13048-42	50 ng/mL

1479

1480 **Supplementary Table 2. The list of Taqman probes and primer sets used in this study.**

Target gene	Taqman Assay ID or sequence
ACTB	F: cctcatgaagatcctcaccga R: ttgccaatggtgatgacctgg
CDX2	F: cacccacagccatagacctac R: gtcagtccaggcaatgcttc
CXCR4	F: actgagaagcatgacggacaag R: aggtagcggtccagactgatg
GAPDH	Hs02786624_g1
GATA6	Hs00232018_m1
KLF2	Hs07291763_gH
KLF5	Hs00156145_m1
NANOG	Hs02387400_g1
OCT4 (POU5F1)	Hs04260367_gH
PAX3	Hs00240950_m1
PAX6	Hs01088114_m1
PDGFRa	F: gctgagcctaatcctctgcc R: actgctcacttccaagaccg
PKCα (PRKCA)	Hs00925200_m1
PKCβ (PRKCB)	Hs00176998_m1
PKCγ (PRKCG)	Hs00177010_m1
SOX1	Hs01057642_s1
SOX2	F: caccaatcccatccacactcac R: gcaaagctcctaccgtaccac
SOX17	Hs00751752_s1
T	Hs00610080_m1

SeV detection	F: accaacaggcggtggtgcaa R: tccaccccaacccctagcgt
PAX6 genotyping	F: ggaattccagtacttcacgtgaaggcatct R: tagaactgaagcggctctaacagccatttt
SOX17 genotyping	F: agaaaggggtgcctttagaggacgggtgtt R: aggaagtgtgtaacactgcttctggcctgc

1481

1482 **Supplementary Table 3. The list of primary antibodies used in this study.**

Name	Host species	Dilutions or Concentrations	SOURCE	IDENTIFIER
Alpha-Fetoprotein (AFP)	Mouse	1 µg/mL	R&D systems	Cat#MAB1368
Alpha-SMA	Mouse	1 µg/mL	R&D systems	Cat#MAB1420
Cardiac Troponin T	Mouse	10 µg/mL	Thermo Fisher Scientific	Cat#MA5-12960
CORIN	Mouse	10 µg/mL	Sigma-Aldrich	Cat#WH0010699M1
GAPDH	Mouse	1 µg/mL	R&D systems	Cat#MAB5718
NANOG	Rabbit	0.5 µg/mL	Reprocell	Cat#RCAB004P-F
OCT-3/4	Mouse	0.4 µg/mL	Santa Cruz	Cat#sc-5279
Oct-4A (C30A3) Rabbit mAb (Alexa Fluor 488 Conjugate)	Rabbit	1:30	Cell Signaling Technology	Cat# 5177S
PAX6	Rabbit	1:400 (Immunocytochemistry)	MBL	Cat#PD022
PAX6	Sheep	5 µg/mL (Wes)	R&D Systems	Cat#AF8150
Anti-PKC beta1 + PKC beta2 (phospho T641)	Rabbit	1:50	Abcam	Cat#ab194749
SOX17	Goat	0.4 µg/mL (Immunocytochemistry)	R&D systems	Cat#AF1924

		1 µg/mL (Wes)		
FITC Mouse anti-SSEA-4	Mouse	1:5	BD Bioscience	Cat#560126
APC anti-human SSEA4	Mouse	1:20	BioLegend	Cat#330418
Alexa Fluor 488 anti-human TRA1-60-R	Mouse	1:20	BioLegend	Cat#330614
Alexa Fluor 488 Mouse anti-Human TRA-1-60 Antigen	Mouse	1:10	BD Bioscience	Cat#560173
TUJ1	Mouse	1 µg/mL	R&D systems	Cat#MAB1195

1483

1484 **Supplementary Table 4. The list of secondary antibodies used in this study.**

Name	Host species	Dilutions	SOURCE	IDENTIFIER
Anti-Mouse IgG (H+L) Highly Cross-Adsorbed Secondary Antibody, Alexa Fluor Plus 488	Donkey	1:1000	Thermo Fisher Scientific	Cat#A-21202
DyLight 488 anti-rabbit IgG (minimal x-reactivity)	Donkey	1:1000	BioLegend	Cat#406404
Anti-Mouse IgG (H+L) Highly Cross-Adsorbed Secondary Antibody, Alexa Fluor Plus 555	Donkey	1:1000	Thermo Fisher Scientific	Cat#A-31570
Anti-Rabbit IgG (H+L) Cross-Adsorbed Secondary Antibody, Alexa Fluor 555	Goat	1:1000	Thermo Fisher Scientific	Cat#A-21428
Anti-Mouse IgG (H+L) Cross-Adsorbed Secondary Antibody, Alexa Fluor 488	Goat	1:1000	Thermo Fisher Scientific	Cat#A-11001
Donkey Anti-Sheep IgG HRP Affinity Purified PAb	Sheep	1:50	R&D systems	Cat# HAF016

1485

1486 **Supplementary Table 5. Software used in this study.**

Name	Source	URL
clusterProfiler (v3.16.1)	R package	https://bioconductor.org/packages/release/bioc/html/clusterProfiler.html
edgeR (v3.30.3)	R package	https://bioconductor.org/packages/release/bioc/html/edgeR.html
R (version4.1.0)	R package	https://www.r-project.org/
CLC Genomics Workbench (v20)	QIAGEN	https://digitalinsights.qiagen.com/products-overview/discovery-insights-portfolio/analysis-and-visualization/qiagen-clc-genomics-workbench/
SH800S cell sorter and flow cytometry software	Sony	https://www.sonybiotechnology.com/us/instruments/sh800s-cell-sorter/software/
Compass software for Simple Western	Protein Simple	https://www.bio-techne.com/resources/instrument-software-download-center/compass-software-simple-western
BZ-X800 microscope analysis software	Keyence	https://www.keyence.com/landing/microscope/lp_fluorescence.jsp
QuantStudio 3 and 5 Real-Time PCR System Software	Thermo Fisher Scientific	https://www.thermofisher.com/jp/ja/home/global/forms/life-science/quantstudio-3-5-software.html

Chromosome Analysis Suite (ChAS) and Affymetrix GeneChip Command Console software programs	Thermo Fisher Scientific	https://www.thermofisher.com/jp/ja/home/life-science/microarray-analysis/microarray-analysis-instruments-software-services/microarray-analysis-software/chromosome-analysis-suite.html
CellSens microscope software	Evident (Olympus)	https://www.olympus-lifescience.com/en/support/downloads/

1487